Electronic Supplementary Information for:

Switch the triplet excited state of the C_{60}-dimethylaminostyryl BODIPY dyads/triads

Ling Huang and Jianzhang Zhao*

State Key Laboratory of Fine Chemicals, School of Chemical Engineering, Dalian University of Technology, E-208 West Campus, 2 Ling-Gong Road, Dalian 116024, China

E-mail : zhaojzh@dlut.edu.cn Web : http://finechem2.dlut.edu.cn/photochem

Index

General information............ S2

Synthesis procedure and characterization data S3–18

Figure S1-S57. ^{1}H NMR, ^{13}C NMR and HRMS............S19–49

Figure S58-S62. UV/Vis absorption spectra and emission spectra of **B-5–8**............S49–51

Figure S63-S64.UV/vis absorption spectra and the fluorescence emission spectra **B-5–8**............S52–54

Figure S65-S69 Fluorescence excitation and absorption spectra of **B-5–8**. S53–55

Figure S70. Fluorescence of the dyad **B-2** and triad **B-3** and**B-4**............S56

Table S1. Photophysical parameters of **B-1—B-8**............ ....S57

Figure S71-S74. Cyclic voltammogram of **B-2—B-8** and ΔG^{o}_{cs} S58–S59

Figure S75–80. Switch singlet oxygen in presence of TFA of **B-3–4**............S61–64

Figure S81-83. Nanosecond time–resolved transient difference absorption **B-12** S65-S66

Figure S84-93. Reversibility of the spectral changes of **B-1–8** with acid/base............S66–S71

Figure S94. Switching of the singlet oxygen ($^1O_2$) photosensitizing ability of **B-3/B-3'**...S72

Scheme S5–S7. Jablonski diagram illustrating the photophysical processes of **B-3–4**.........S73–S75

General Information:

UV-Vis absorption spectra were taken on a HP8453 UV-visible spectrophotometer. Fluorescence spectra were recorded on a Shimadzu RF 5301PC spectrofluorometer. Luminescence lifetimes were measured on a OB920 fluorescence/phosphorescence lifetime spectrometer (Edinburgh Instruments, UK). The nanosecond time-resolved transient difference absorption spectra were detected by Edinburgh LP920 instruments (Edinburgh Instruments, UK). The signal was buffered on a Tektronix TDS 3012B oscilloscope and was analyzed by the LP900 software. All samples in flash photolysis experiments were deaerated with argon for ca. 15 min before measurement and the gas flow is kept during the measurement.

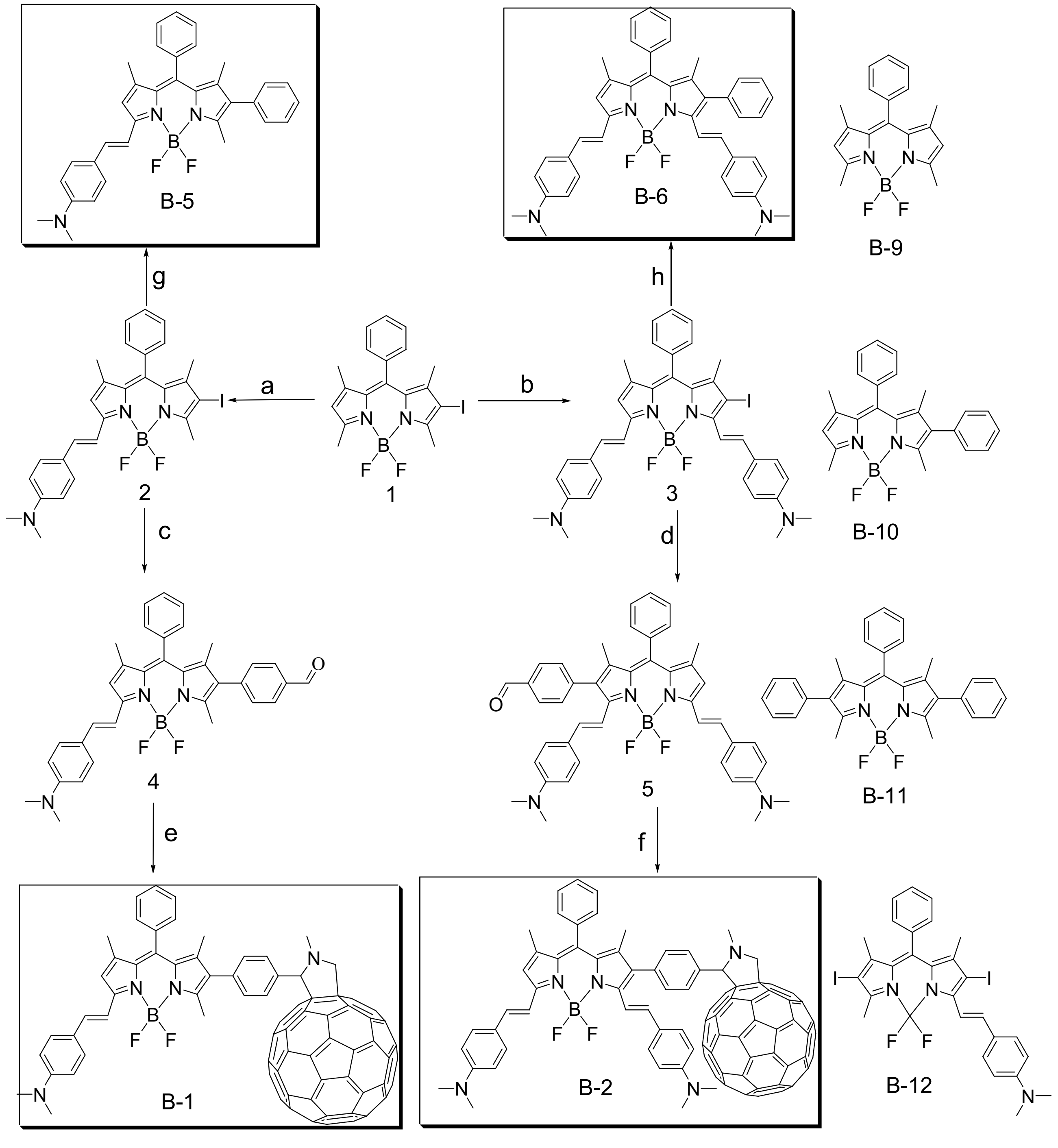

Scheme S1. The synthesis of **B-1**, **B-2**, **B-5** and **B-6**. (a) 4–*N,N*–dimethylbenzaldehyde, toluene, acetic acid, piperidine, refux, 4 h in Ar, 57 %; (b) the same step as (a), 63 %; (c) 4–formylphenylboronic acid, K_2CO_3, $Pd(PPh_3)_4$, 85%; (d) the same step as (c), 87 %; (e) sarcosine, fullerene, toluene, 62%; (f) the same steps to that of (e), 57%; (g) phenylboronic acid, K_2CO_3, $Pd(PPh_3)_4$, 92%; (h) the same as (g), 87%.

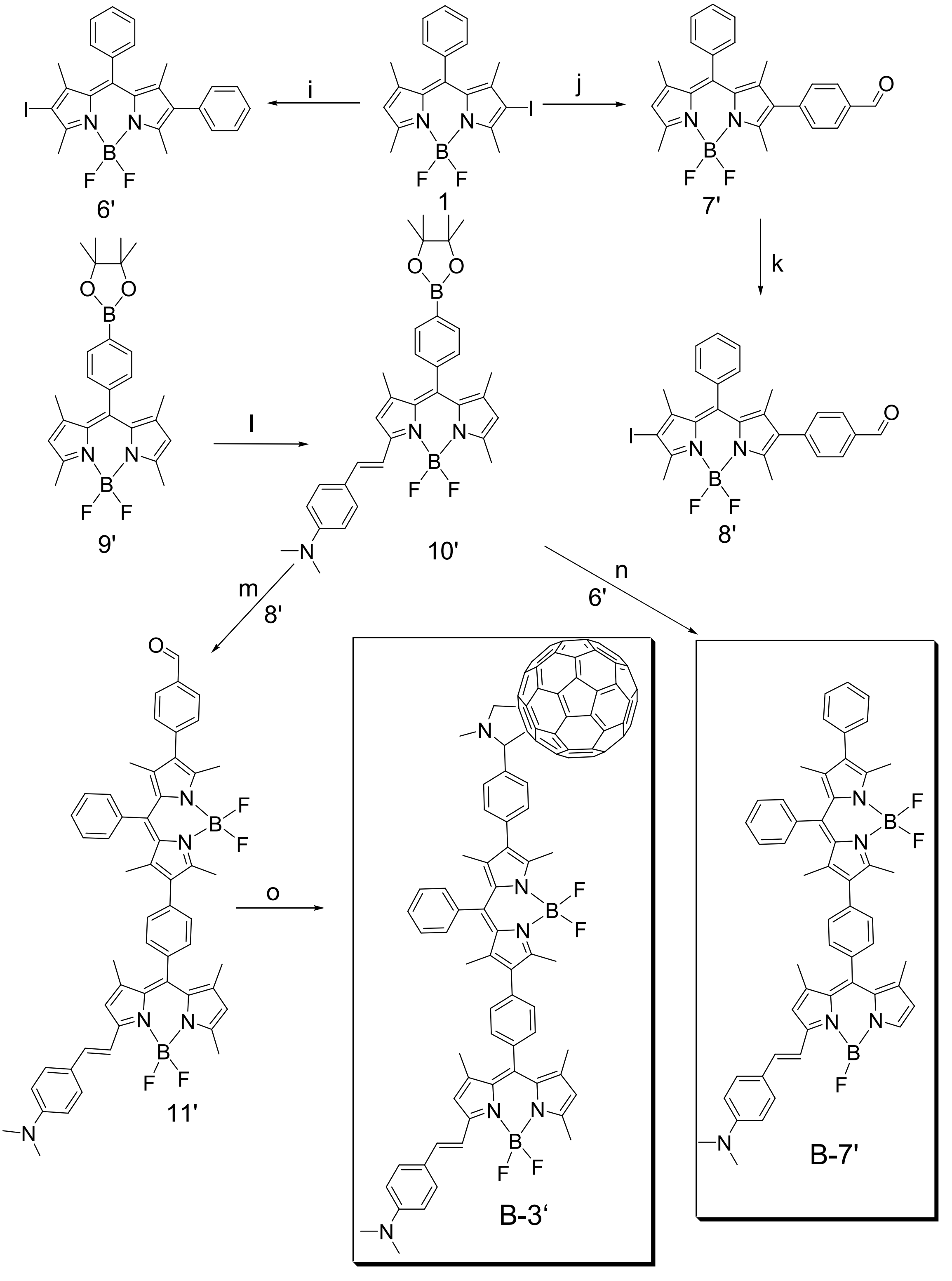

Scheme S2. The synthesis of B-3, B-7, B-3′ and B-7′. Key (i) phenylboronic acid, K_2CO_3, $Pd(PPh_3)_4$, 86%; (j) the same step i, 85 %; (k) NIS, CH_2Cl_2, 95%; (l) 4–*N,N*–dimethylbenzaldehyde, toluene, acetic acid, piperidine, refux, 8 h in Ar, 41 %; (m) K_2CO_3, $Pd(PPh_3)_4$, toluene/ethanol/water =2/2/1(v/v/v), 71%; (n) The same as (m), 67%; (o) sarcosine, fullerene, toluene, 49%.

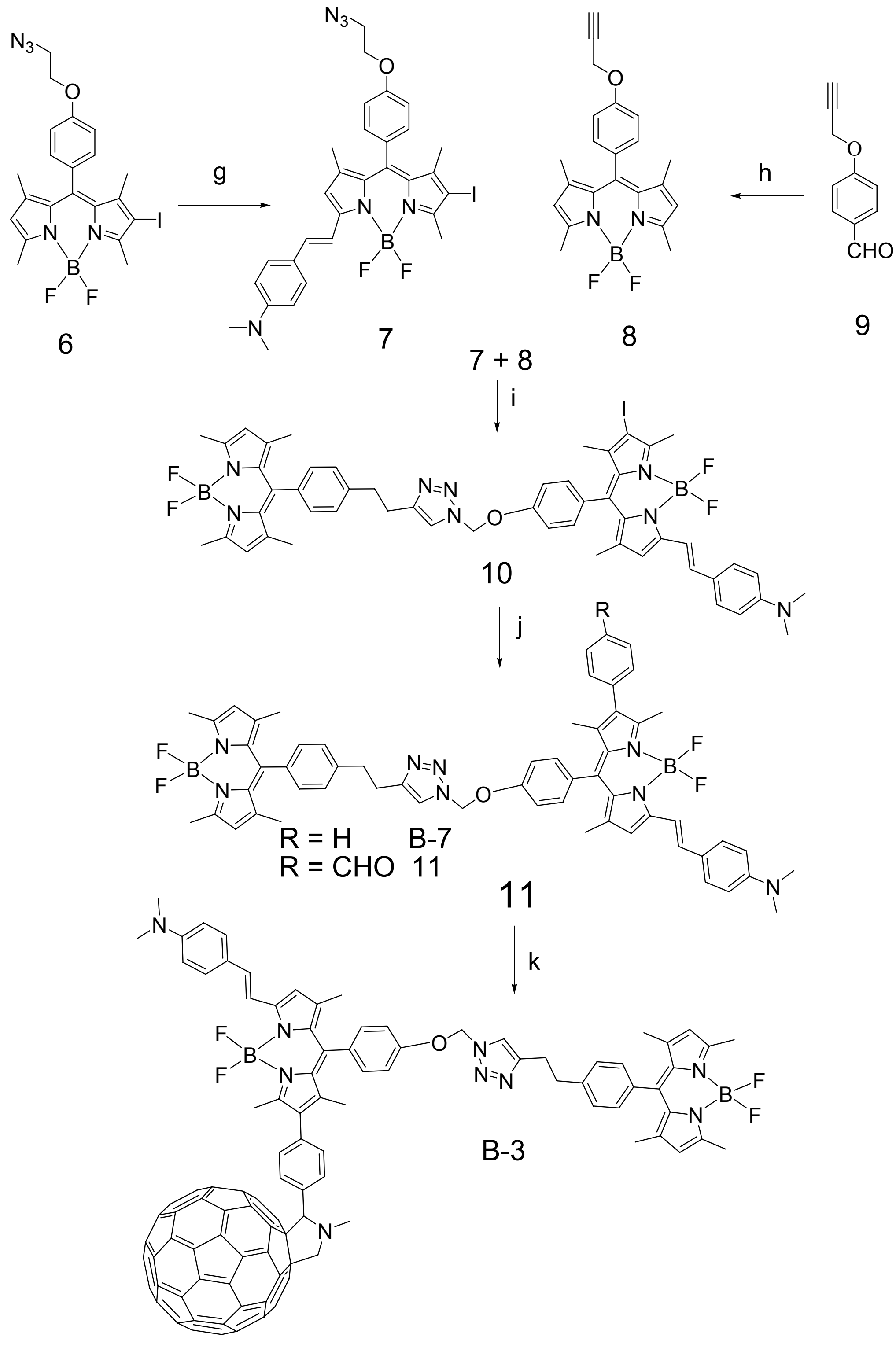

Scheme S3. Synthesis of B-3. (g') 4–*N,N*–dimethylbenzaldehyde, toluene, acetic acid, piperidine, reflux, 6 h in Ar, 61 %; (h')2,4-dimethylpyrrole, TEA, $BF_3·Et_2O$ in Ar, 11%; (i') $CuSO_4·5H_2O$, Sodium ascorbate, 90%; (j') K_2CO_3, $Pd(PPh_3)_4$, toluene/ethanol/water =2/2/1(v/v/v), for B-7 95%, for 11 89%. (k') Sarcosine, fullerenes, toluene, 49%.

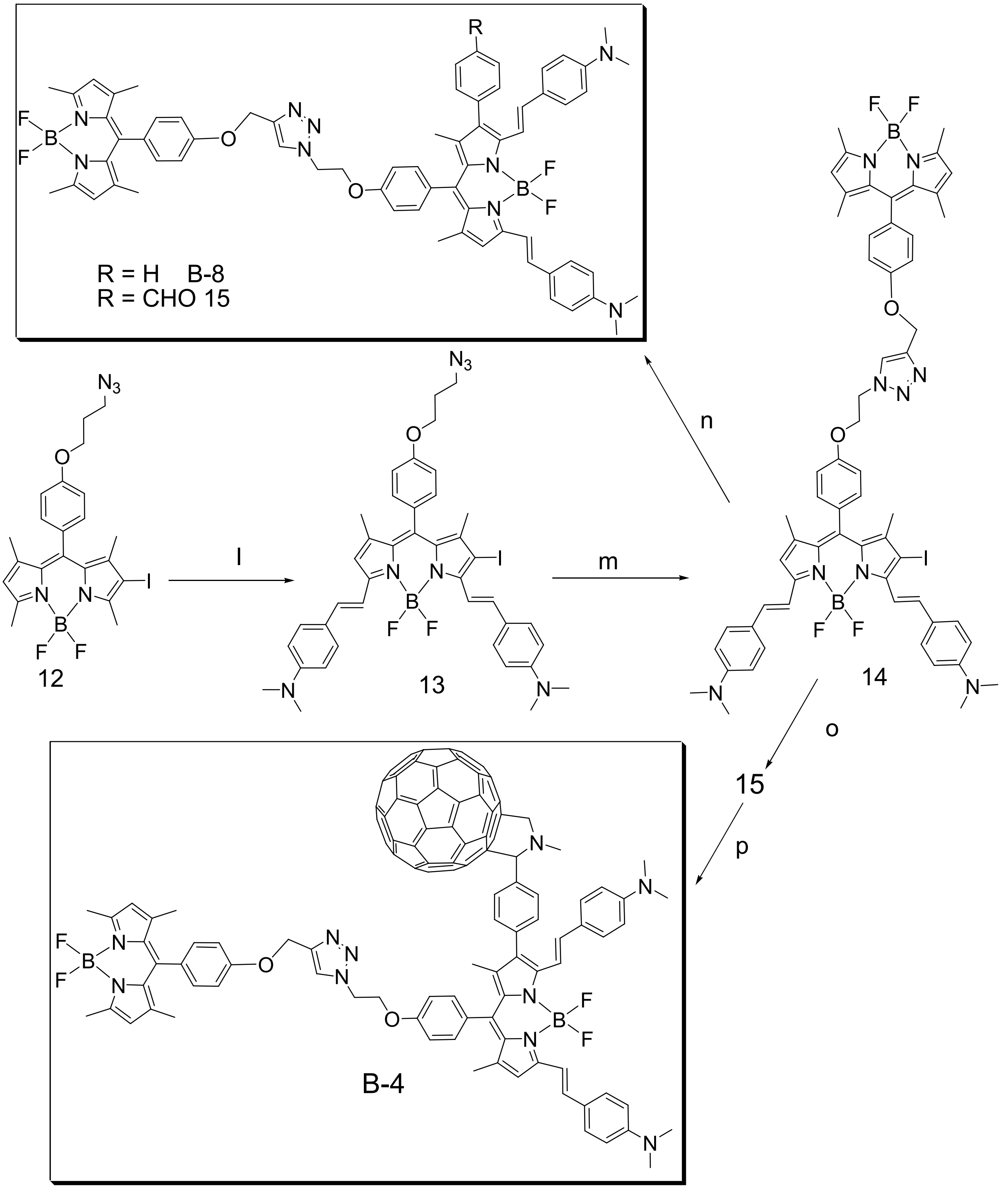

Scheme S4. Synthesis of B-4 and B-8. (p) 4–*N,N*–dimethylbenzaldehyde, toluene, acetic acid, piperidine, refux, 12 h in Ar, 61 %; (q) $CuSO_4$, Vitamin C sodium, $CHCl_3$/ethanol/H_2O = 12/1/1(v/v/v), 89%. (r) K_2CO_3, $Pd(PPh_3)_4$, toluene/ethanol/water =2/2/1(v/v/v), 76%, same procedures were used for preparation of **B-8** and **15**; (t) sarcosine, fullerenes, toluene, 38%.

Preparation of compound **2**

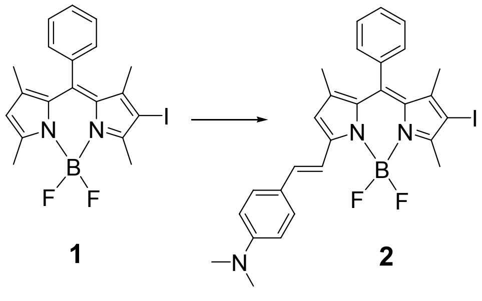

Compound 2: Under Ar atmosphere, a mixture of compound **1** (225.0 mg, 0.5 mmol) and 4-*N,N*-dimethylbenylaldehyde (160 mg ,1.0 mmol) was dissolved in dry toluene (50 mL), then 1.0 mL acetic acid and 1.0 mL piperidine was added. The mixture was refluxed for 3 h, and the reaction was monitored with TLC. After completion of the reaction, the mixture was cooled to room temperature (RT), water was added (50 mL), and the mixture was extracted with dichloromethane (3×60 mL). The organic layer was dried over Na_2SO_4. After removal of the solvent under reduced pressure, the crude product was purified by column chromatography (silica gel, DCM/ petroleum = 1:1, v/v) to give deep purple solid. Yield: 165.6 mg (57 %). M.p. 174.4–176.1°C. ^{1}H NMR (400 MHz, $CDCl_3$): 7.53–7.46 (m, 6H), 7.29 (s, 3H), 6.70 (d, 2H, J = 4.0 Hz), 6.65 (s, 1H), 3.04 (s, 6H), 2.67 (s, 3H), 1.42 (s, 3H), 1.37 ppm (s, 3H). HRMS (MALDI): m/z calcd for $[C_{28}H_{27}BIF_2N_3]^+$: 581.1311; found 581.1348.

Compound 3 :

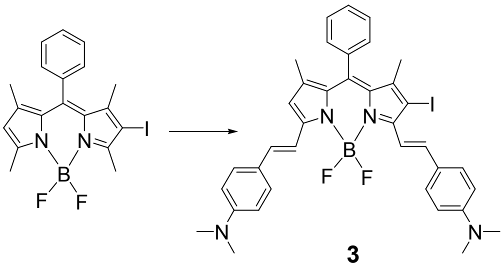

The method used for preparation of compound **3** is the same to that used for preparation of compound **2**. Crude compound **3** was purified by column chromatography (silica gel, DCM/ petroleum = 2:1, v/v) to give black solid. Yield: 89.7 mg (63 %). M.p > 250 °C. HRMS (MALDI): m/z calcd for $[C_{37}H_{36}BIF_2N_4]^+$: 712.2046; found 712.2057.

Compound 4 :

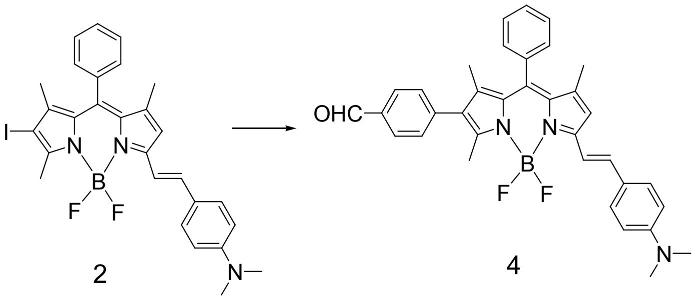

Under Ar atmosphere, a mixture of compound **2** (58.1 mg, 0.10 mmol), 4- formylphenyl boronic acid (75.0 mg, 0.5 mmol) and K_2CO_3 (41.7 mg, 0.30 mmol) was dissolved in toluene/Ethanol/water (15mL, 2/2/1, v/v/v), and the mixture was bubbled with Ar for 15 min. $Pd(PPh_3)_4$ (18 mg, 0.015 mmol) was added, and the mixture was refluxed for 3 h. After completion of the reaction, the mixture was cooled to RT, water was added (30 mL). The mixture was extracted with dichloromethane (3×30 mL). The combined organic layers was dried over Na_2SO_4. After removal of the solvent under reduced pressure, the crude product was purified by column chromatography (silica gel, DCM) to give deep purple solid. Yield: 47.5 mg (85 %). ^{1}H NMR (400 MHz, $CDCl_3$): δ = 10.02 (s, 1H), 7.90 (d, 2H, J = 8.4 Hz), 7.56–7.49 (m, 6 H), 7.35 (d, 4H, J = 7.6 Hz), 7.28 (d, 1H, J = 16.0 Hz), 6.85 (s, 2H), 6.66 (s, 1H), 3.06 (s, 6H), 2.58 (s, 3H), 1.45 (s, 3H), 1.32 ppm (s, 3H). HRMS (MALDI): m/z calcd for $[C_{35}H_{32}BF_2N_3O]^+$: 559.2606; found 559.2656.

Compound 5 :

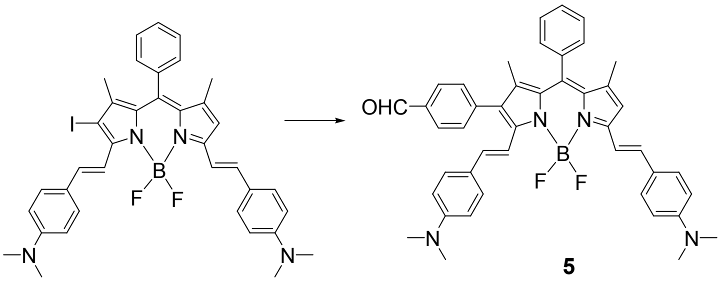

The preparation of compound **5** was carried out with method similar to that of compounds **4**. Compound **5** was purified by column chromatography (silica gel, DCM) to give black solid. Yield: 60.1 mg (87 %). M.p > 250 °C. ^{1}H NMR (400 MHz, $CDCl_3$): δ = 10.02 (s, 1H), 7.91 (d, 2H, J = 8.0 Hz), 7.69–7.65 (m, 1H), 7.57–7.55 (m, 4H), 7.48–7.44 (m, 6H), 7.36 (d, 2H, J = 8.0 Hz), 7.20 (d, 2H, J = 4.0

Hz), 6.74 (d, 4H, J = 7.6 Hz), 6.42 (s, 1H), 3.04–2.97 (m, 12H), 1.44 (s, 3H), 1.20 ppm (s, 3H). HRMS (MALDI): m/z calcd for $[C_{44}H_{31}BF_2N_4O]^+$: 690.3341; found 690.3333.

The preparation of compounds 1, 6, 7, 8 and 9 have been report.[1]

Compound 6 : M.p. 202.8–203.9°C. ^{1}H NMR (400 MHz, $CDCl_3$): δ = 7.51–7.50 (m, 3H), 7.40–7.37 (m, 2H), 7.33–7.30 (m, 3H), 7.15 (d, 2H, J = 7.8 Hz), 2.66 (s, 3 H), 2.53 (s, 3H), 1.40 (s, 3H), 1.29 ppm (s, 3H).

Compound 8 : M.p. 201.3–203.5°C. ^{1}H NMR (400 MHz, $CDCl_3$): δ = 10.03 (s, 1H), 7.92 (d, 2H, J = 8.0 Hz), 7.53 (d, 2H, J = 4.0 Hz), 7.34–7.30 (m, 4H), 2.69 (s, 3H), 2.54 (s, 3H), 1.41 (s, 3H), 1.31 ppm (s, 3H).

Compound 9 : ^{1}H NMR (400 MHz, $CDCl_3$): δ = 7.91 (d, 2H, J = 7.6 Hz), 7.30 (d, 2H, J = 8.0 Hz), 5.97 (s, 2H), 2.55 (s, 6H), 1.40 (s, 12H), 1.38 ppm (s, 6H).

---

1. L. Huang, X. Cui, B. Therrien and J. Zhao, *Chem. Eur. J.*, 2013, **19**, 17472–17482.

Compound 10:

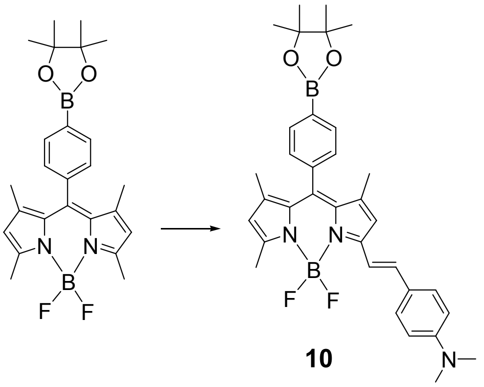

10

The method used for preparation of compound **10** is the same to that of compound **2**. Compound **10** was purified by column chromatography (silica gel, DCM/ petroleum = 2:1 v/v) to give purple solid. Yield: 47.6 mg (41 %). ^{1}H NMR (400 MHz, CDCl$_3$): δ = 7.91 (d, 2 H, J = 7.6 Hz), 7.52–7.48 (m, 3 H), 7.33–7.31 (m, 2H), 7.21 (d, 1H, J = 12.0 Hz), 6.74 (s, 2H), 6.59 (s, 1H), 5.96 (s, 1H), 3.03 (s, 6 H), 2.58 (s, 3H), 1.41 (s, 3H), 1.39 (s, 12H), 1.37 ppm (s, 3H). HRMS (MALDI): m/z calcd for $[C_{34}H_{39}B_2F_2N_3O_2]^+$: 581.3196; found 581.3186.

Compound 11:

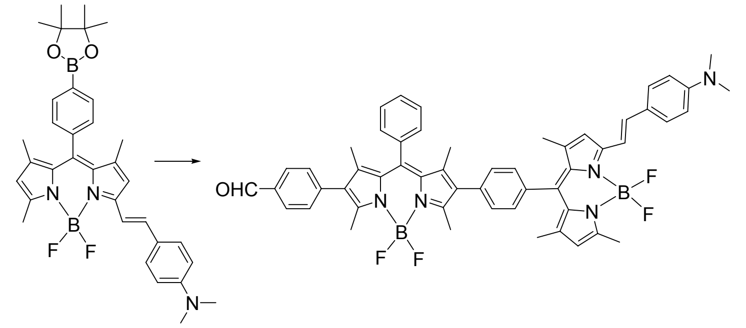

The same method was use for preparation of compound **11** as that used for compound **6**. Compound **11** was purified by column chromatography (silica gel, DCM) to give deep purple solid. Yield: (62.7 mg, 71 %). ^{1}H NMR (400 MHz, CDCl$_3$): δ = 10.04 (s, 1H), 7.93 (d, 2 H, J = 8.0 Hz), 7.55–7.50 (m, 6H), 7.40–7.34 (m, 6H), 7.30 (d, 2H, J = 8.0 Hz), 7.23 (d, 1H, J = 16.0 Hz), 6.87 (s, 2H), 6.61 (s, 1H), 5.99 (s, 1H), 3.06 (s, 6H), 2.58 (s, 9H), 1.45 (s, 3H), 1.41 (s, 12H), 1.35 ppm (s, 3H). HRMS (MALDI): m/z calcd for $[C_{54}H_{49}B_2F_4N_5O]^+$: 881.4059; found 881.4082.

Compound 12 :

The synthesis steps has been reported,[1] Compound **12** was purified by column chromatography (silica gel, DCM/ petroleum = 1:1 v/v) to give red solid. Yield: (163.2 mg, 61 %). M.p. 125.5–126.6°C ^{1}H NMR (400 MHz, CDCl$_3$): δ = 7.19 (d, 2H, J = 8.4 Hz), 7.06–7.18 (d, 2H, J = 8.8 Hz), 6.04 (s, 1 H), 4.23–4.21 (m , 2 H), 3.68–3.66 (m, 2 H), 2.63 (s, 3 H) , 2.56 (s, 3 H), 1.44 ppm (s, 6 H). HRMS (MALDI): m/z calcd for [$C_{21}H_{21}BF_2N_5OI$]$^+$: 535.0852; found 535.0865.

Compound 7':

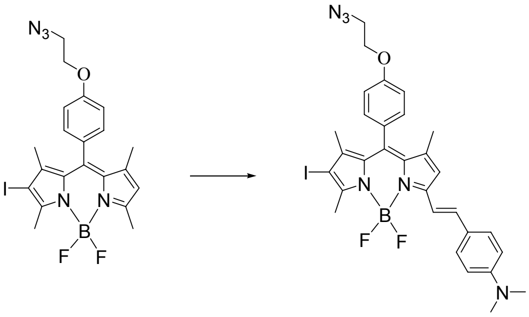

The same method was used for preparation of compound 7' as that use for compound 2. Compound 7' was purified by column chromatography (silica gel, DCM/PE = 2/1, v/v) to give deep purple solid. Yield: 60.4 mg (61 %). ^{1}H NMR (400 MHz, CDCl$_3$): δ = 7.56 (d, 3 H, J = 8.8 Hz), 7.28 (d, 1 H, J = 16.0 Hz), 7.21 (d, 2 H, J = 7.6 Hz), 7.05 (d, 2H, J = 8.4 Hz), 6.87 (s, 2H), 6.65 (s, 1H), 4.23–4.21 (m, 2H), 3.68–3.66 (m, 2H), 3.07 (s, 6H), 2.66 (s, 3H), 1.48 (s, 3H), 1.44 (s, 3H) ppm. HRMS (MALDI): m/z calcd for [$C_{30}H_{30}BF_2N_6O_3I$]$^+$: 666.1587; found 666.1544.

Compound 8:

The synthesis of compound 8 was reported.[2] ^{1}H NMR (400 MHz, CDCl$_3$): δ = 7.21 (d, 2 H, J = 7.8 Hz), 7.10 (d, 2 H, J = 8.4 Hz), 5.98 (s, 2 H), 4.76 (s, 2 H), 2.55 (s, 7 H), 1.42 ppm (s, 6 H).

---

[2] C. Zhang, J. Zhao, S. Wu, Z. Wang, W. Wu, J. Ma, S. Guo and L. Huang, *J. Am. Chem. Soc.*, 2013, **135**, 10566–10578.

Compound 10:

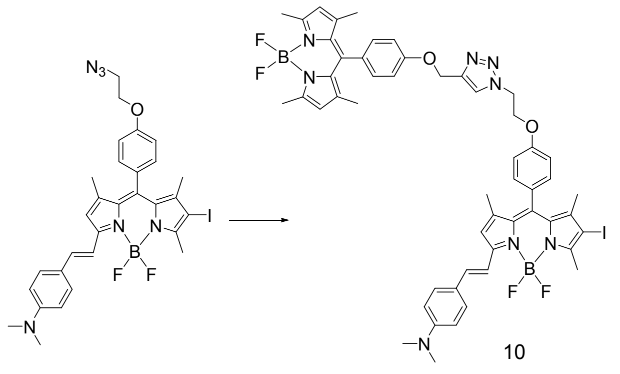

Under Ar atmosphere, a mixture of compound **8** (41.0 mg, 0.10 mmol), compound **7** (66.7 mg, 0.10 mmoL) were dissolved in $CHCl_3/EtOH/H_2O$ (14 mL, 12/1/1, v/v/v), then $CuSO_4 \cdot 5H_2O$ (2.5 mg, 0.10 mmoL) and sodium ascorbate (3.8 mg, 0.020 mmoL) were added. React in room temperature 24 h. After completion of the reaction, the mixture was washed in water (3×20mL). The organic layer was dried over Na_2SO_4. After removal of the solvent under reduced pressure, the mixture was purified by column chromatography (silica gel, DCM/methanol = 100/1, v/v) to give black solid. Yield: 93.9 mg (90 %). ^{1}H NMR (400 MHz, $CDCl_3$): δ = 7.92 (s, 1H), 7.52–7.45 (m, 3H), 7.28 (s, 1H), 7.24 (s, 1H), 7.21–7.17 (m, 4H), 7.13 (d, 2H, J = 8.4 Hz), 7.00 (d, 2H, J = 8.0 Hz), 6.72 (d, 2H, J = 5.2 Hz), 6.64 (s, 1H), 5.97 (s, 2 H), 5.27 (s, 2H), 4.85–4.83 (m, 2H), 4.47–4.44 (m, 2H), 3.04 (s, 6H), 2.65 (s, 3H), 2.55 (s, 6H), 1.42 (s, 9H), 1.40 ppm (s, 3H). HRMS (MALDI): m/z calcd for $[C_{52}H_{51}B_2F_4N_8O_2I]^+$: 1044.3302; found 1044.3279.

Compound 11':

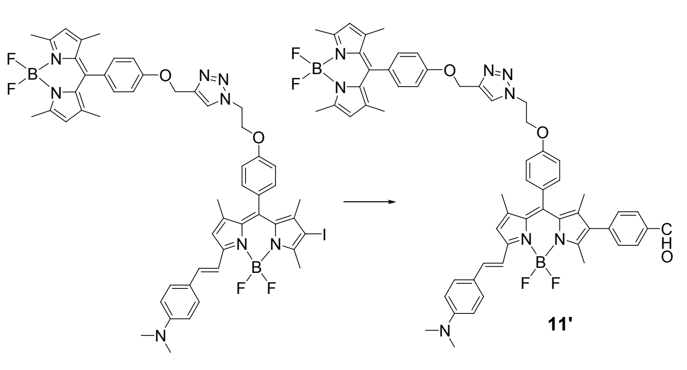

The same method was used for preparation of compound **11'** as that for compounds **4**. Compound **11'** was purified by column chromatography (silica gel, DCM / methanol = 80:1 v/v) to give black solid. Yield: 72.8 mg, 89 %. ^{1}H NMR (400 MHz, $CDCl_3$): δ = 10.07 (s, 1H), 7.92–7.88 (m, 3H), 7.54–7.50 (m, 3H), 7.34 (d, 2H, *J* = 8.0 Hz), 7.29 (s, 1 H), 7.25 (s, 2H), 7.20 (d, 2H, *J* = 8.4 Hz), 7.12 (d, 2H, *J* = 8.4 Hz), 7.02 (d, 2H, *J* = 7.6 Hz), 6.77 (s, 2H), 6.65 (s, 1H), 5.27 (s, 2H), 4.86–4.84 (m, 2H), 4.47–4.45 (m, 2H), 3.05 (s, 6H), 2.57 (s, 3H), 2.55 (s, 6H), 1.47 (s, 3H), 1.41 (s, 6H), 1.35 ppm (s, 3H). HRMS (MALDI): *m/z* calcd for $[C_{59}H_{56}B_2F_4N_8O_3]^+$: 1022.4598; found 1022.4576.

Compomd 13:

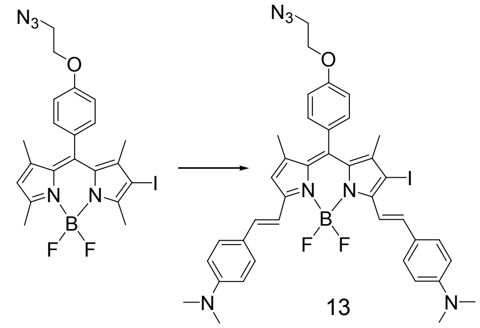
13

The same method was used for preparation of compounds **13** as that used for compound **2**. Compound **13** was purified by column chromatography (silica gel, DCM/ petroleum = 2:1 v/v) to give black solid. Yield: 97.2 mg (61 %). M.p. > 250°C. HRMS (MALDI): *m/z* calcd for $[C_{39}H_{39}BF_2N_7OI]^+$: 797.2322; found 797.2292.

Compound 14:

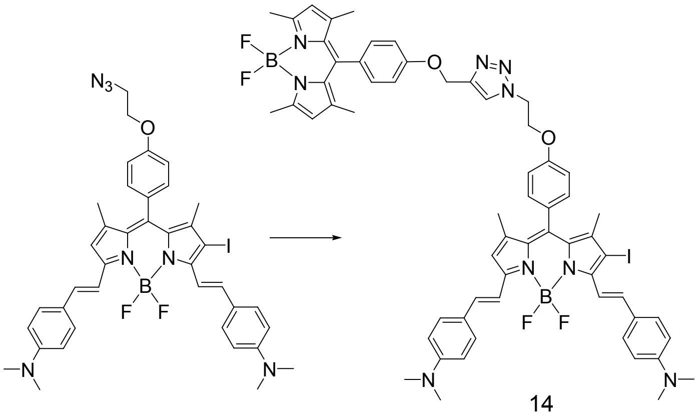
14

The same method was used for preparation of compounds **14** as that used for compound **10'**, compound **14** was purified by column chromatography (silica gel, DCM/methanol = 100/1, v/v) to give black solid. Yield: 97.2 mg (89 %). M.p. >250°C. ^{1}H NMR (400 MHz, CDCl$_3$): δ = 7.92 (s, 1 H), 7.59 (s, 4 H), 7.21 (d, 4H, *J* = 8.4 Hz), 7.13 (d, 3H, *J* = 8.8 Hz), 6.98–6.96 (m, 3H), 6.61 (s, 4H), 5.98 (s, 2H), 5.27 (s, 2 H), 4.85–4.82 (m, 2H), 4.46–4.44 (m, 2H), 2.55 (s, 6 H), 1.42 (s, 6H) ppm. HRMS (MALDI): *m/z* calcd for $[C_{61}H_{60}B_2F_4N_9O_2I]^+$: 1175.4047; found 1175.3943.

Compound 15:

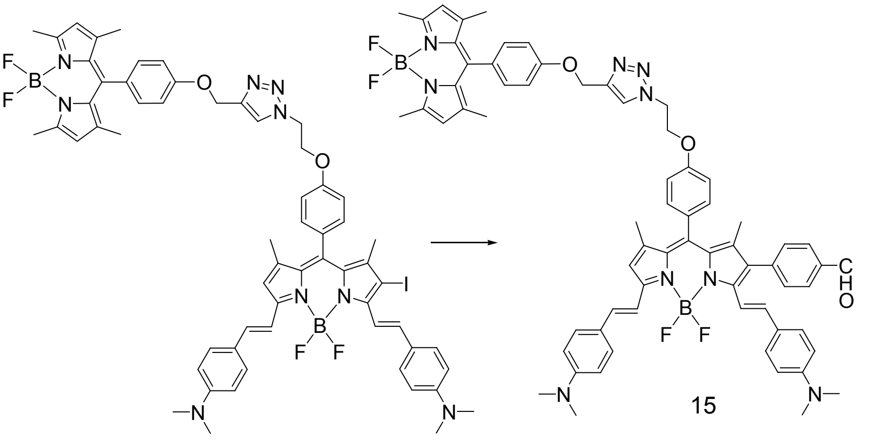
15

The same method was used for preparation of compound **15** as that used for compounds **4**. Compound **15** was purified by column chromatography (silica gel, DCM/ methanol = 80:1, v/v) to give black solid. Yield: 43.8 mg (76 %). M.p. 253.7–254.9°C. ^{1}H NMR (400 MHz, CDCl$_3$): δ = 10.07 (s, 1H), 7.99–7.94 (m, 2H), 7.90–7.88 (m, 1H), 7.80–7.74 (m, 2H), 7.69–7.65 (m, 4H), 7.60–7.53 (m, 4H), 7,48–7.41 (m, 4H), 7.23–7.21 (m, 1H), 7.19–7.15 (m, 3H), 7.11 (d, 1H, *J* = 8.8 Hz), 6.98 (d, 1H, *J* = 8.8 Hz), 6.71 (d, 1H, *J* = 8.8 Hz), 6.64–6.59 (m, 1H), 6.42 (d, 1H, *J* = 16.0 Hz), 5.97 (s, 2H), 5.24 (s, 2H), 4.79–4.77 (m, 2H), 4.41–4.39 (m, 2H), 3.03 (s, 6H), 2.96 (s, 6H), 2.35 (s, 6H), 1.41 (s, 6H), 1.26 (s, 3H), 1.22 ppm (s, 3 H). HRMS (MALDI): *m*/*z* calcd for $[C_{68}H_{65}B_2F_4N_9O_3]^+$: 1153.5333; found 1153.5328.

B-3′: **B-3’** was prepared with the same methods that used for **B-3** (see main text of the paper). **B-3′** was purified by column chromatography (silica gel, DCM) to give black solid. Yield: 23.9 mg (49 %). M.p. >250°C. ^{1}H NMR (400 MHz, CDCl$_3$): δ = 7.84–7.82 (m, 3H), 7.52–7.48 (m, 6H), 7.38–7.28 (m, 5H), 7.23–7.20 (m, 3H), 6.72 (s, 2H), 6.61 (s, 1H), 5.97 (s 1 H), 4.95 (s, 2H), 4.31 (s, 1H), 3.04 (s, 6H), 2.87 (s, 3H), 2.59 (s, 3H), 2.55 (s, 3H), 2.52 (s, 3H), 1.44 (s, 3H), 1.40 (s, 3H), 1.31 (s, 3H), 1.27 (s, 3H) ppm. ^{13}C NMR (100 MHz, CDCl$_3$): δ = 156.1, 156.0, 154.7, 154.0, 153.9, 153.3, 153.2, 153.1, 147.2, 146.6, 146.4, 146.3, 146.2, 146.1, 146.0, 145.9, 145.8, 143.1, 142.9, 142.8, 142.6, 142.3, 142.2, 142.1, 142.0, 141.8, 141.7, 141.6, 141.4, 140.7, 140.1, 139.7, 139.5, 139.1, 139.0, 138.5, 136.4, 135.8, 135.7, 135.2, 134.3, 134.1, 133.7, 133.5, 132.9, 132.8, 131.5, 131.2, 130.7, 129.1, 128.3, 127.9, 120.5, 117.8, 68.9, 67.9, 40.1, 31.5, 25.6, 14.6, `14.5, 14.1, 13.5, 13.2, 12.9, 12.8 ppm. HRMS (MALDI): *m*/*z* calcd for $[C_{116}H_{56}B_2F_4N_6]^-$: 1628.4532; found 1628.4485.

B-5:

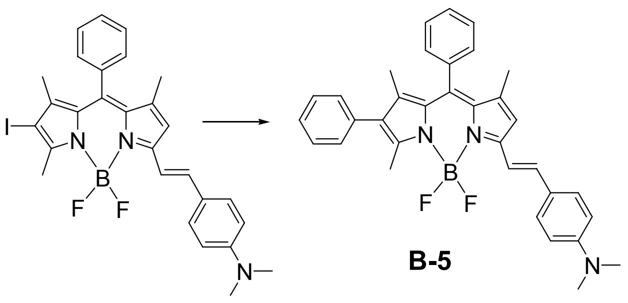

Under Ar atmosphere, a mixture of compound **2** (29.6 mg, 0.05 mmol), phenylboronic acid (24.2 mg, 0.25 mmol) and K_2CO_3 (20.7 mg ,0.15 mmol) were dissolved in toluene/Ethanol/water (10mL, 2/2/1, v/v), and bubbled with Ar for 15 min. $Pd(PPh_3)_4$ (12.0 mg, 0.001 mmol) was added. Then the mixture was refluxed for 3 h. After completion of the reaction, the mixture was cooled to RT, water (30 mL) was added, and the mixture was extracted with dichloromethane (3×50 mL). The organic layer was dried over Na_2SO_4. After removal of the solvent under reduced pressure, the mixture was purified by column chromatography (silica gel, DCM/petroleum = 1:1, v/v) to give deep purple solid. Yield: 24.4 mg (92 %). ^1H NMR (400 MHz, $CDCl_3$): δ = 7.55 (d, 3H, J = 8.4 Hz), 7.48 (d, 3H, J = 6.4 Hz), 7.30 (d, 1H, J = 8.0 Hz), 7.23 (d, 1H, J = 16.0 Hz), 7.16 (d, 2H, J = 7.6 Hz), 6.99 (s, 2H), 6.61 (s, 1H), 3.05 (s, 6H), 2.55 (s, 3H), 1.42 (s, 3H), 1.29 ppm (s, 3 H). ^{13}C NMR (100 MHz, $CDCl_3$): 154.9, 151.7, 143.0, 139.3, 137.8, 137.3, 135.7, 134.3, 133.5, 133.1, 131.0, 130.6, 130.4, 129.9, 129.4, 129.2, 129.0, 128.6, 128.4, 126.2, 118.1, 114.9, 112.5, 40.7, 29.9, 14.9, 12.7 ppm. HRMS (MALDI): m/z calcd for $[C_{34}H_{32}BF_2N_3]^+$: 531.2657; found 531.2694.

B-6:

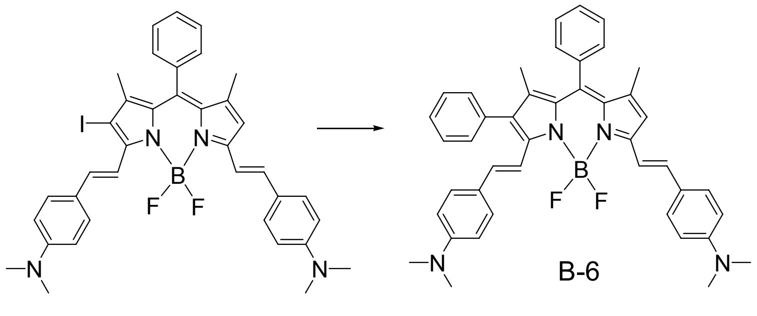

The method used for preparation for **B-6** is the same at that used for **B-5**. **B-6** was purified by column chromatography (silica gel, DCM/ petroleum = 2:1, v/v) to give black solid. Yield: 28.8 mg (87 %). M.p. > 250°C. ^{1}H NMR (400 MHz, $CDCl_3$): δ = 7.71–7.53 (m, 5H), 7.46–7.44 (m, 4H), 7.39–7.32 (m, 6H), 6.74 (d, 4H, J = 12.0 H), 6.44 (s, 1H), 3.02 (s, 12H), 1.42 (s, 3H), 1.19 ppm (s, 3H). ^{13}C NMR (100 MHz, $CDCl_3$): 154.8, 153.6, 150.9, 150.0, 149.9, 141.4, 138.5, 138.2, 136.9, 136.0, 133.2, 132.5, 131.1, 130.8, 129.4, 129.3, 129.1, 129.0, 128.9, 128.7, 127.3, 125.3, 117.8, 115.3, 112.4, 40.5, 29.9, 14.7, 12.4 ppm. HRMS (MALDI): m/z calcd for $[C_{43}H_{41}BF_2N_4]^+$: 662.3392; found 662.3375.

B-7′:

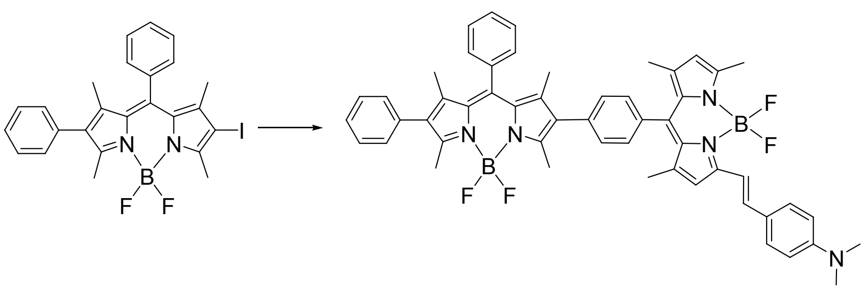

The same ways of preparation for **B-5** and **B-7**. **B-7** was purified by column chromatography (silica gel, DCM/ petroleum = 2:1, v/v) to give purple solid. Yield: 28.6 mg (67 %).^{1}H NMR (400 MHz, $CDCl_3$): δ = 7.58–7.54 (m, 4 H), 7.52 (d, 2 H, J = 8.0 Hz), 7.41–7.38 (m, 4 H), 7.35–7.20 (m, 5 H), 7.28 (d, 1 H, J = 8.4 Hz), 7.16 (d, 2H, J = 7.6 Hz), 7.02 (s, 2 H), 6.61 (s, 1H), 6.00 (s, 1H), 3.08 (s, 6H), 2.60 (s, 3H), 2.56 (s, 6H), 1.46 (s, 3H), 1.42 (s, 3H), 1.33 ppm (s, 6H). ^{13}C NMR (100 MHz, $CDCl_3$): δ = 155.3, 153.0, 142.3, 135.3, 134.8, 134.2, 133.8, 133.5, 131.6, 131.2, 131.1, 131.0, 130.1, 129.3, 129.2, 129.1, 129.0, 128.5, 128.4, 128.2, 128.0, 127.8, 127.2, 121.6, 121.5, 117.7, 117.6, 29.7, 14.8, 14.5, 14.3, 14.1, 13.5, 12.8 ppm. HRMS (MALDI): m/z calcd for $[C_{53}H_{49}B_2F_4N_5]^+$: 853.4110; found 853.4075.

B-7:

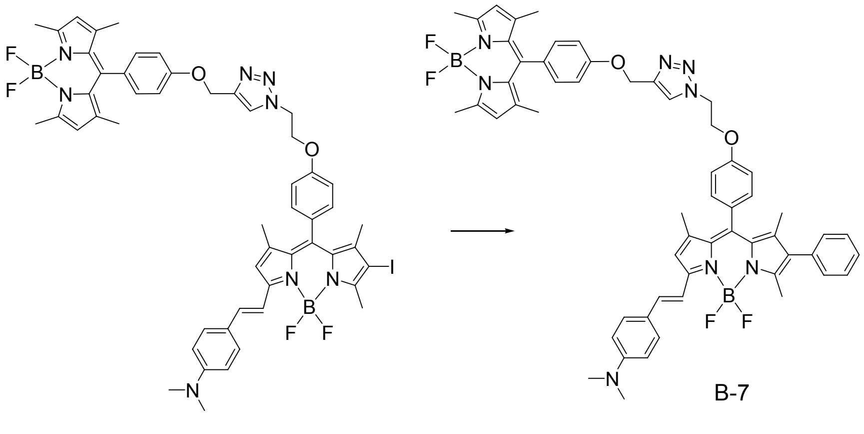

The method used for preparation of **B-7** is the same as that used for **B-5**. **B-7** was purified by column chromatography (silica gel, DCM) to give purple solid. Yield: 28.3 mg (95 %). ^{1}H NMR (400 MHz, CDCl$_3$): δ = 7.90 (s, 1H), 7.54–7.50 (m, 3H), 7.39–7.35 (m, 2H), 7.30 (d, 1H, J = 7.6 Hz), 7.25–7.23 (m, 2 H), 7.20–7.14 (m, 5H), 7.11 (d, 2H, J = 7.6 Hz), 7.00 (d, 2H, J = 8.0 Hz), 6.73 (s, 2H), 6.61 (s, 1H), 5.97 (s, 2H), 5.26 (s, 2H), 4.84–4.82 (m, 2H), 4.45–4.43 (m, 2H), 3.03 (s, 6H), 2.55 (s, 9H), 1.45 (s, 6H), 1.41 (s, 3 H), 1.33 ppm (s, 3 H). ^{13}C NMR (100 MHz, CDCl$_3$): δ = 158.9, 158.2, 155.4, 143.7, 143.1, 141.6, 131.8, 130.5, 130.2, 129.3, 129.2, 128.7, 128.6, 127.7, 127.3, 124.1, 121.2, 117.8, 115.4, 114.9, 112.6, 66.3, 62.0, 49.9, 40.9, 29.7, 14.9, 14.6, 14.1, 12.5 ppm. HRMS (MALDI): m/z calcd for $[C_{58}H_{56}B_2F_4N_8O_2]^+$: 994.4648; found 994.4630.

B-8:

The method used for preparation of **B-8** is the same as that used for **B-5**. **B-8** was purified by column chromatography (silica gel, DCM) to give purple solid. Yield: 25.7 mg, 76 %.^{1}H NMR (400 MHz, CDCl$_3$): ^{1}H NMR (400 MHz, CDCl$_3$): δ = 7.89 (s, 1H), 7.64–7.54 (m, 4H), 7.40–7.31 (m, 4H), 7.27 (s, 1H), 7.25 (s, 1 H), 7.22–7.17 (m, 8H), 7.11 (d, 2H, J = 8.4 Hz), 6.99 (d, 2H, J = 8.8 Hz), 6.70 (d, 4H, J = 7.6 Hz), 6.45 (s, 1H), 5.97 (s, 2H), 5.25 (s, 2H), 4.83–4.81 (m, 2H), 4.45–4.43 (m, 2H), 3.04–2.98 (m, 12H), 2.55 (s, 6H), 1.56 (s, 3H), 1.45 (s, 3H), 1.42 ppm (s, 6H). ^{13}C NMR (100 MHz, CDCl$_3$): δ = 158.9, 158.2, 155.4, 154.9, 151.5, 143.8, 143.1, 142.8, 141.5, 138.4, 137.9, 136.8, 134.1, 133.7, 132.9, 131.8, 131.1, 130.2, 130.0, 129.3, 128.8, 128.2, 127.7, 126.8, 124.1, 121.2, 117.9, 115.5, 115.0, 114.5, 112.2, 66.3, 62.0, 49.9, 40.4, 29.7, 15.0, 14.6, 14.1, 13.3, 12.8 ppm. HRMS (MALDI): m/z calcd for $[C_{67}H_{65}B_2F_4N_9O_2]^+$: 1125.5383; found 1125.5464.

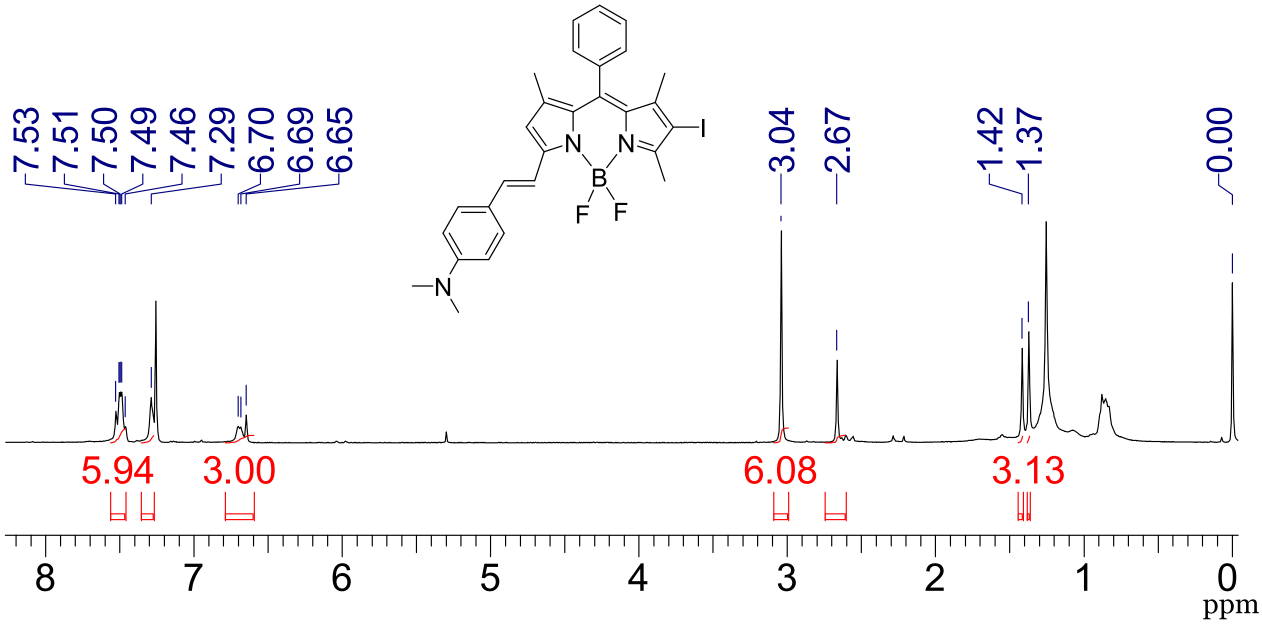

Figure S1. ^{1}H NMR of **Compound 2** (400 MHz, $CDCl_3$)

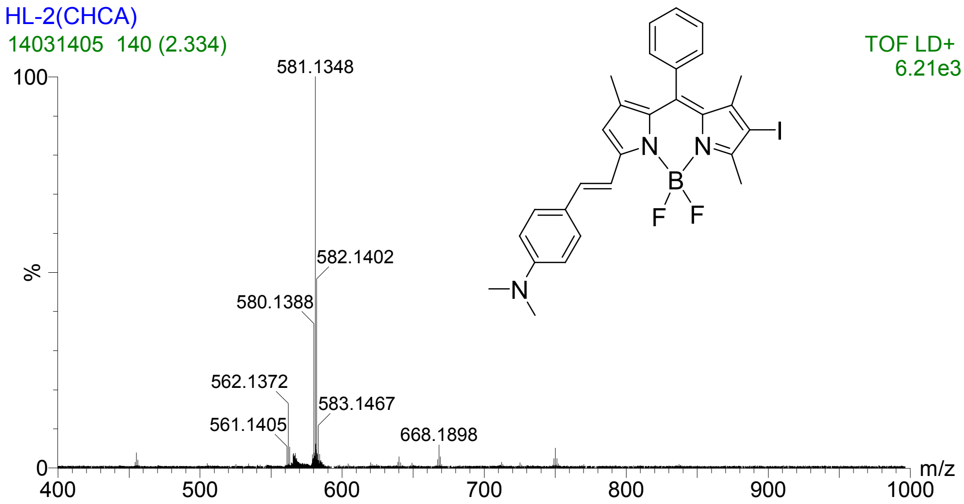

Figure S2. TOF HRMS MALDI of **Compound 2**.

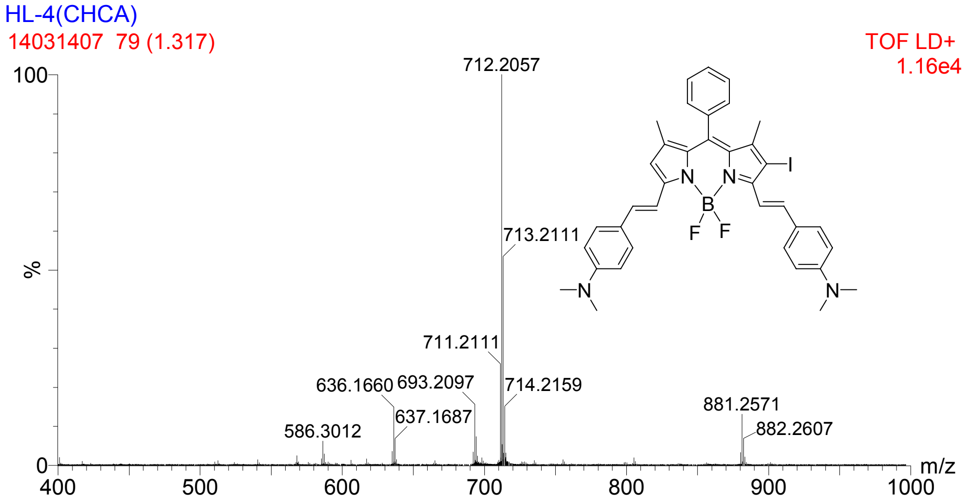

Figure S3. TOF HRMS MALDI of **Compound 3**.

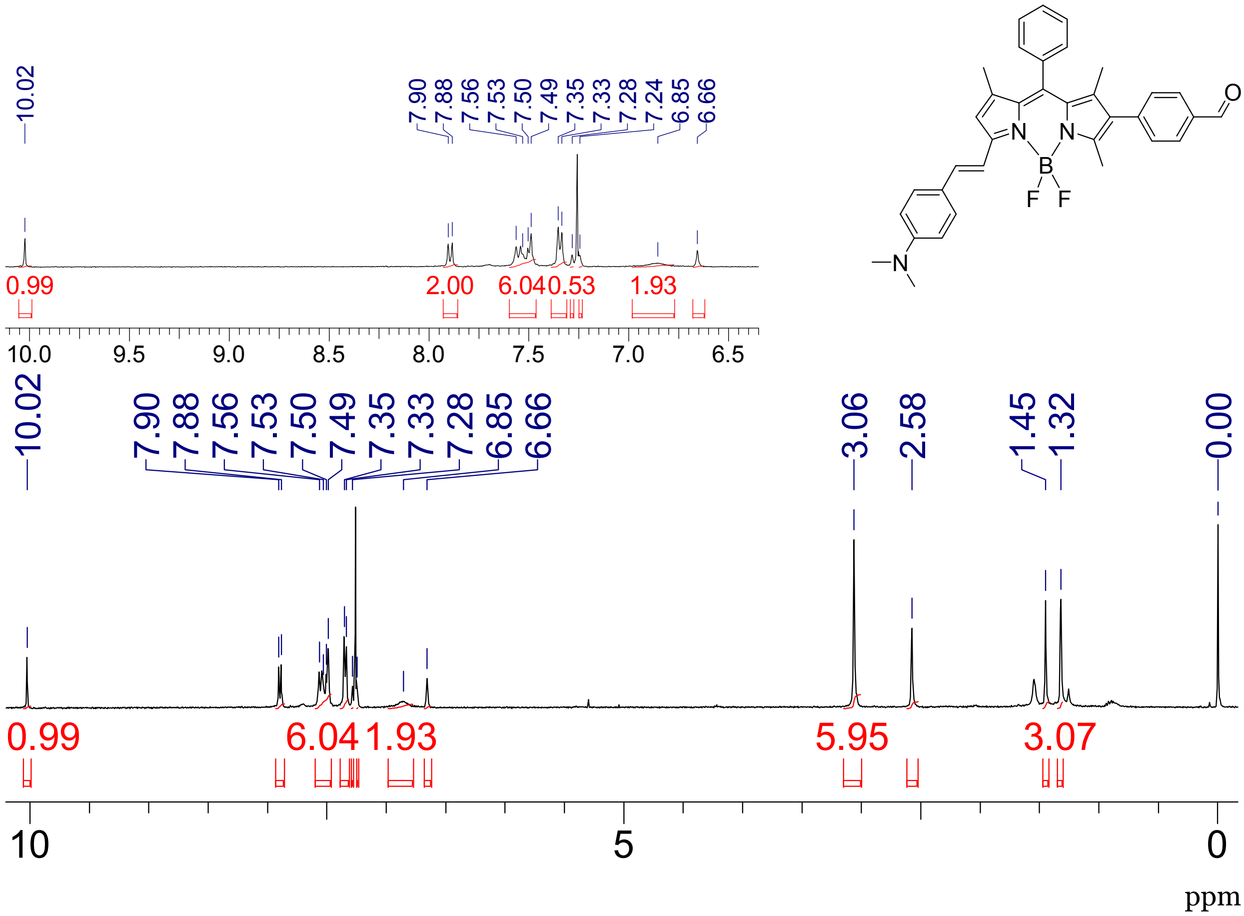

Figure S4. ^{1}H NMR of **Compound 4** (400 MHz, $CDCl_3$)

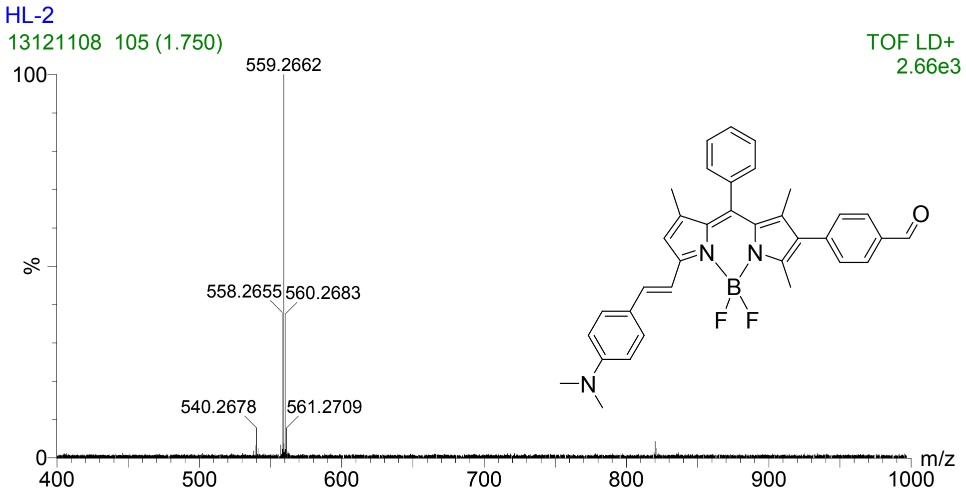

Figure S5. TOF HRMS MALDI of compound **4**.

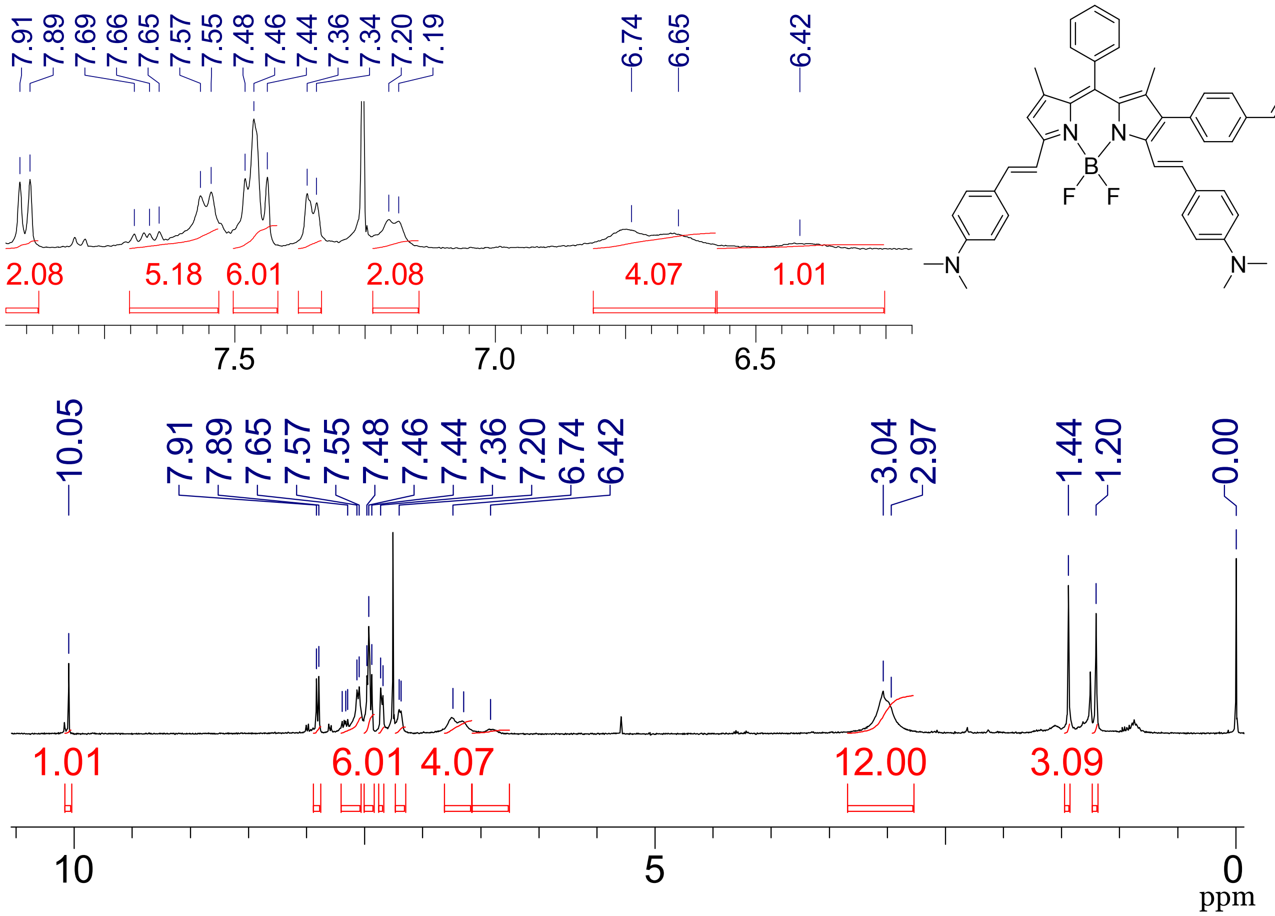

Figure S6. ^{1}H NMR spectrum of compound **5** (400 MHz, $CDCl_3$).

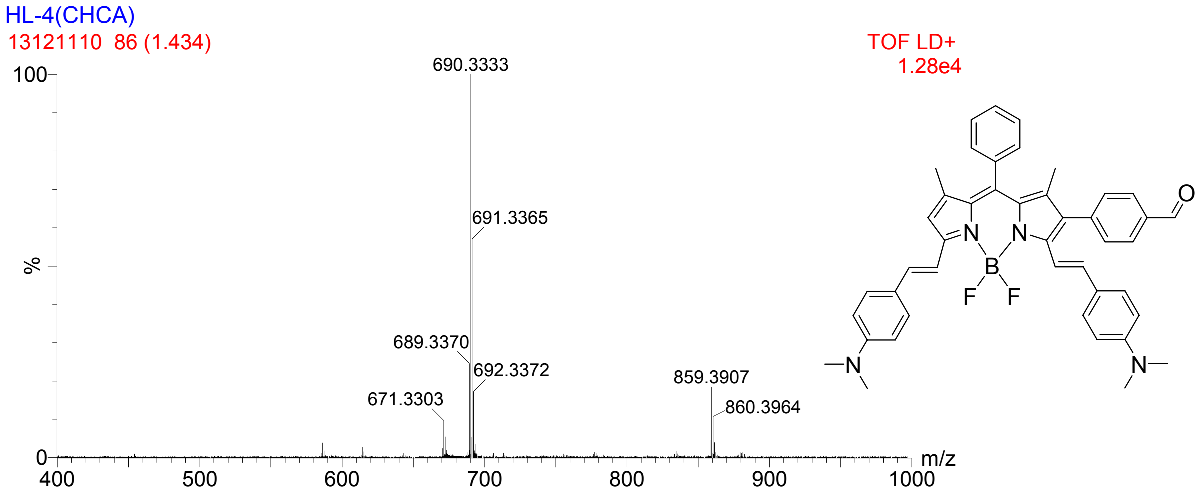

Figure S7. TOF HRMS MALDI spectrum of compound **5**.

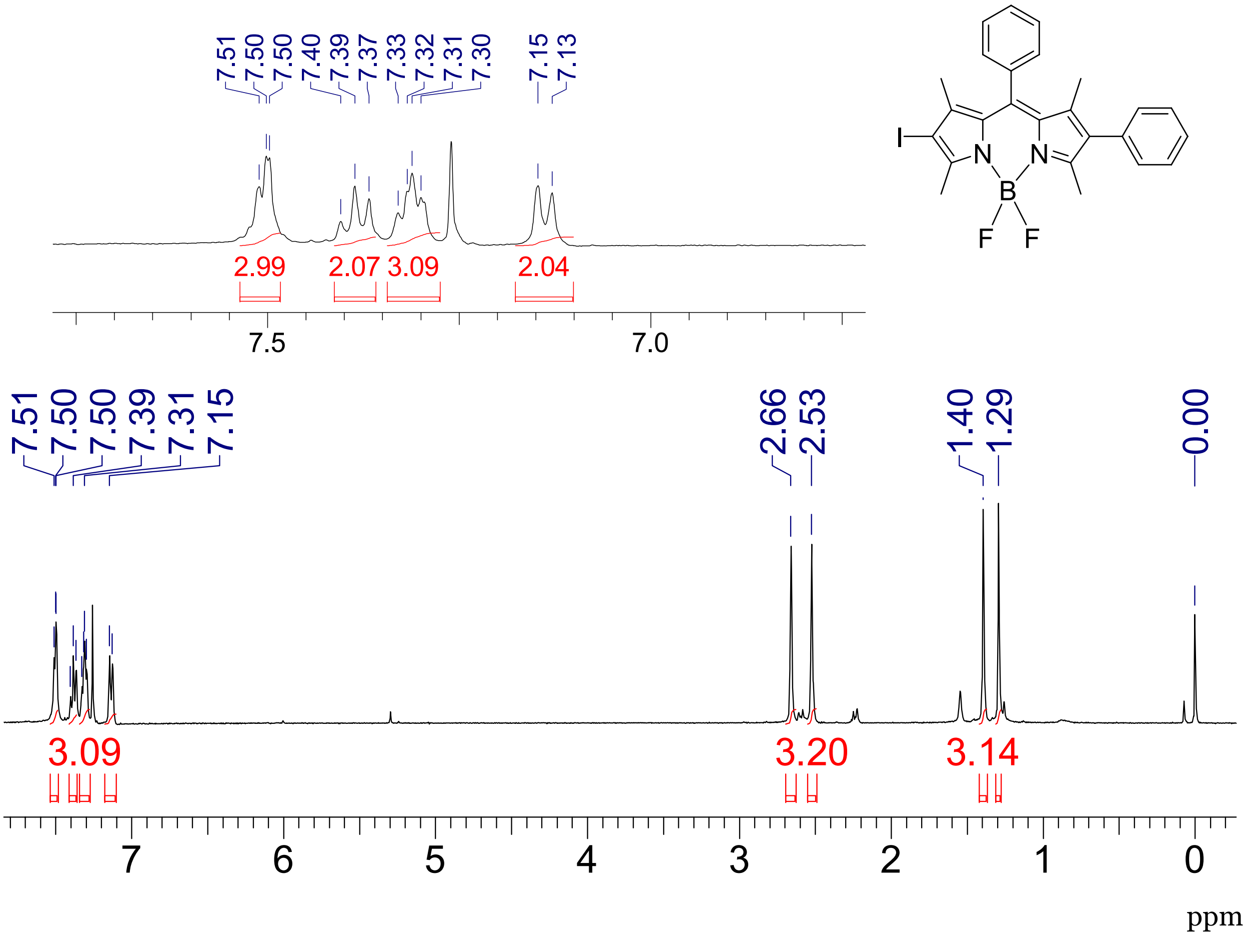

Figure S8. ^{1}H NMR spectrum of Compound **6** (400 MHz, $CDCl_3$).

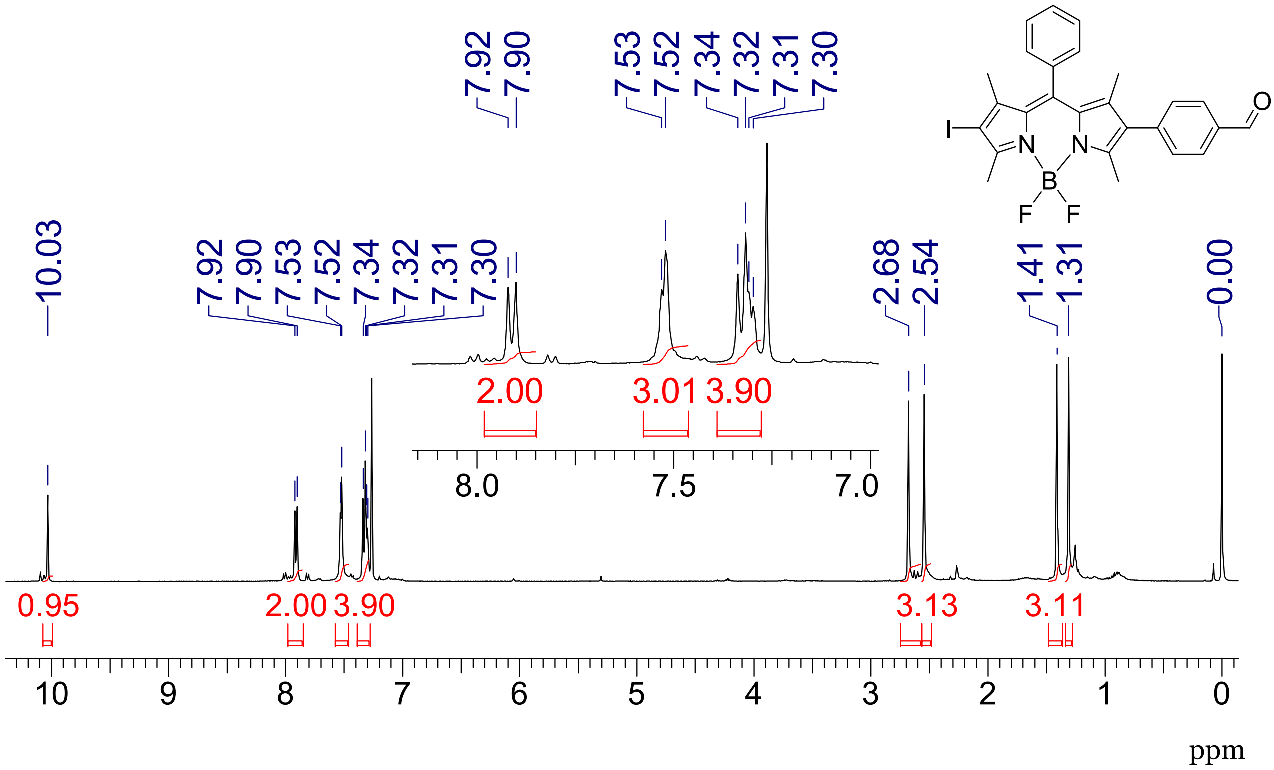

Figure S9. ^{1}H NMR of compound **8** (400 MHz, CDCl$_3$)

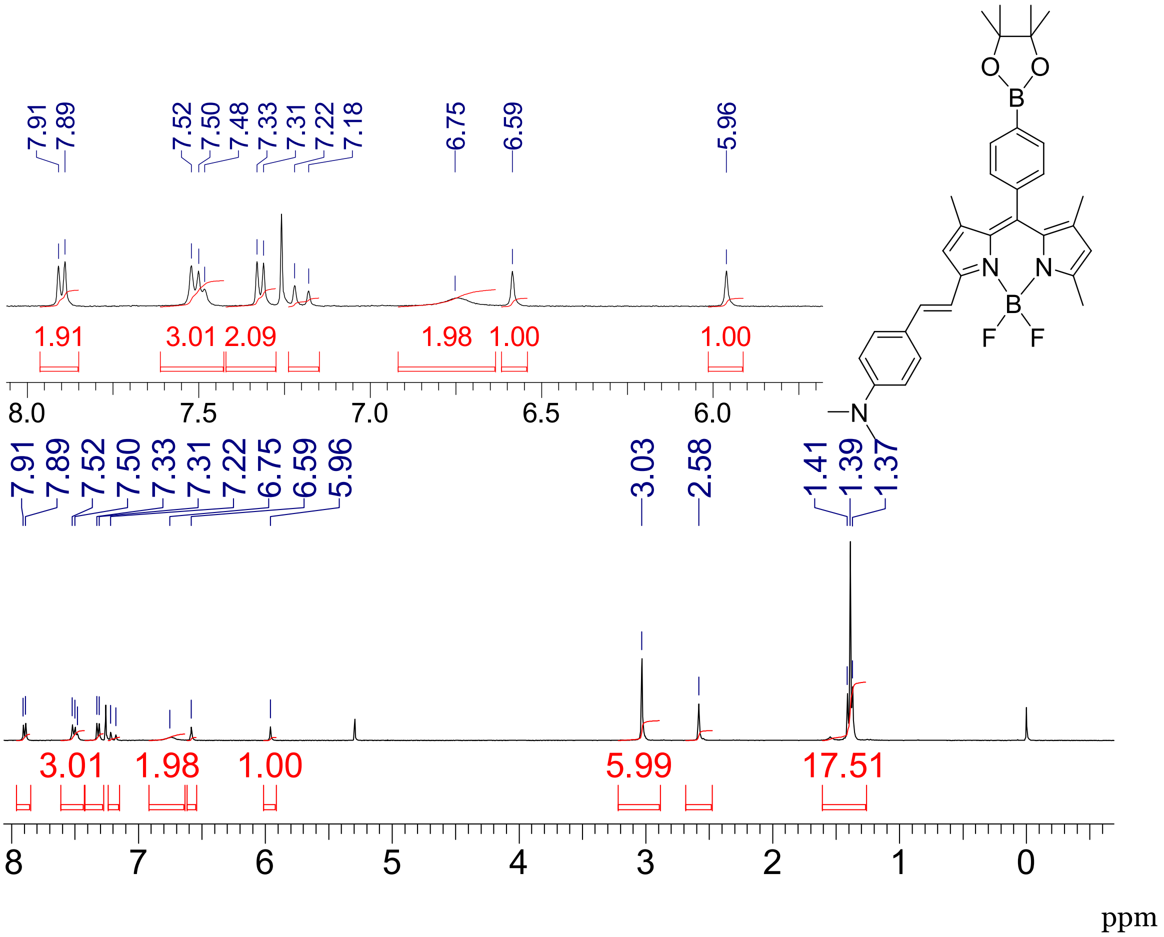

Figure S10. ^{1}H NMR spectrum of compound **10** (400 MHz, CDCl$_3$).

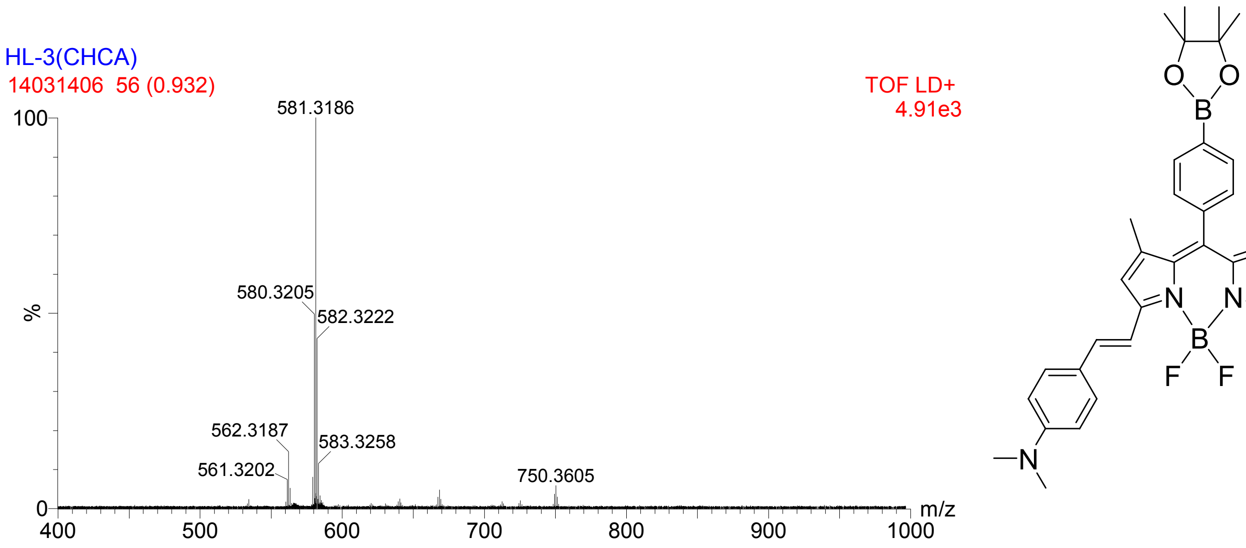

Figure S11 TOF HRMS MALDI of compound **10**.

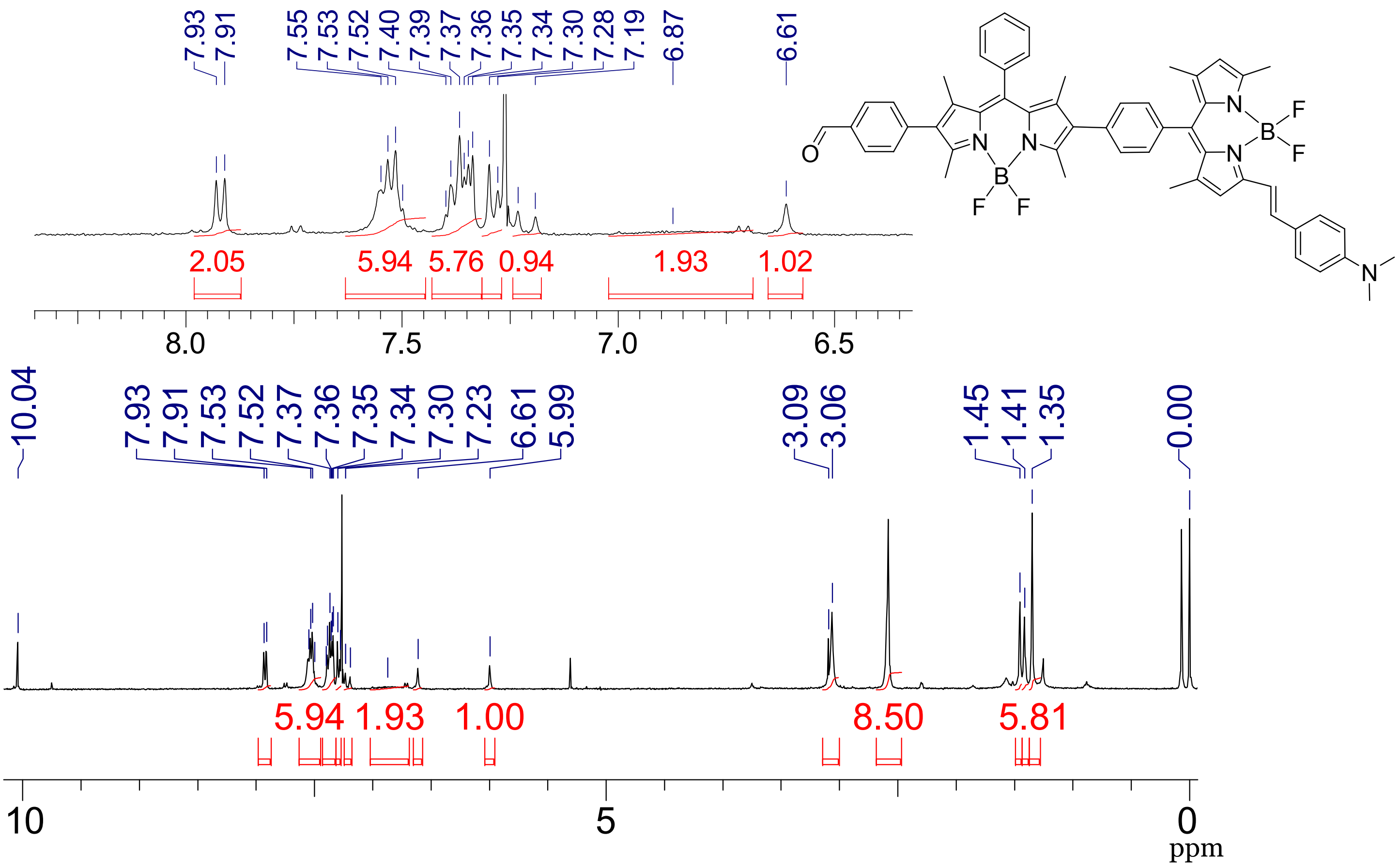

Figure S12. ^{1}H NMR of compound **11** (400 MHz, CDCl$_3$)

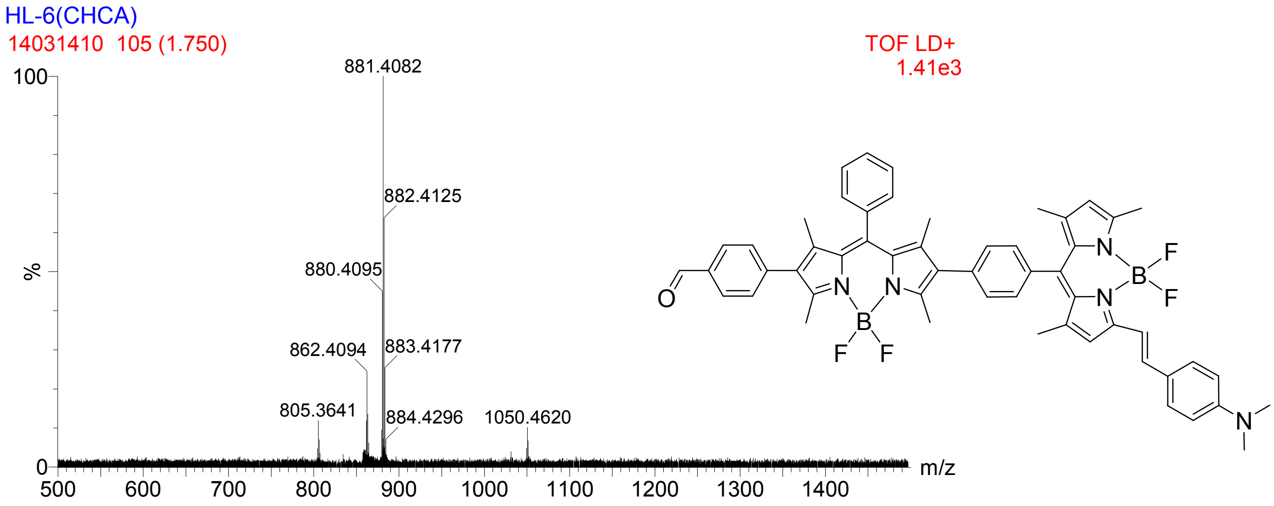

Figure S13 TOF HRMS MALDI of compound **11**.

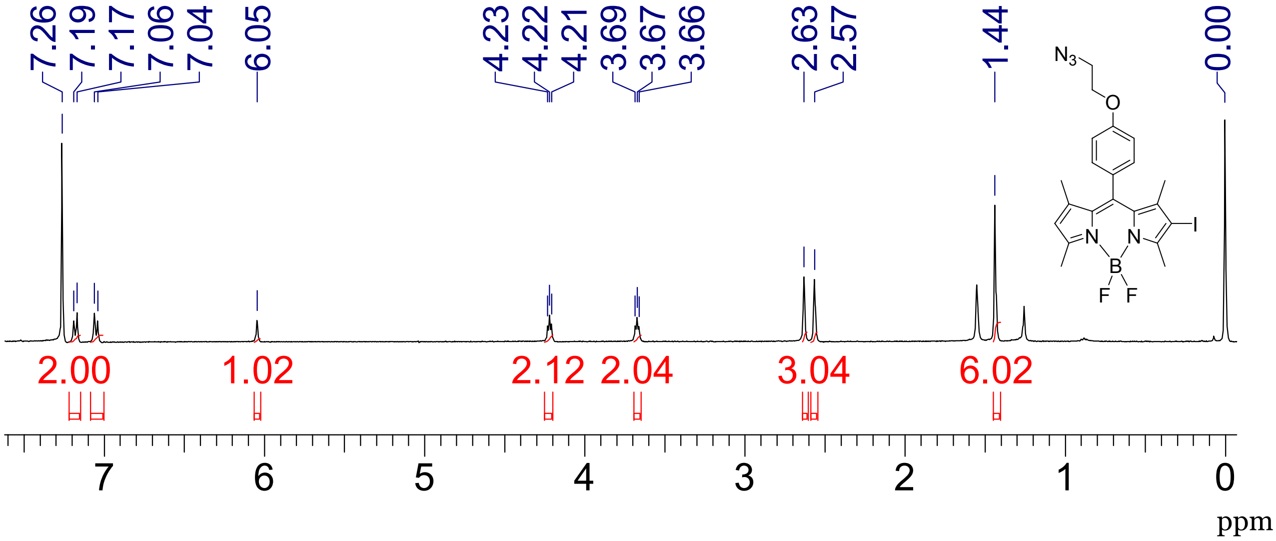

Figure S14. ^{1}H NMR of compound **12** (400 MHz, $CDCl_3$).

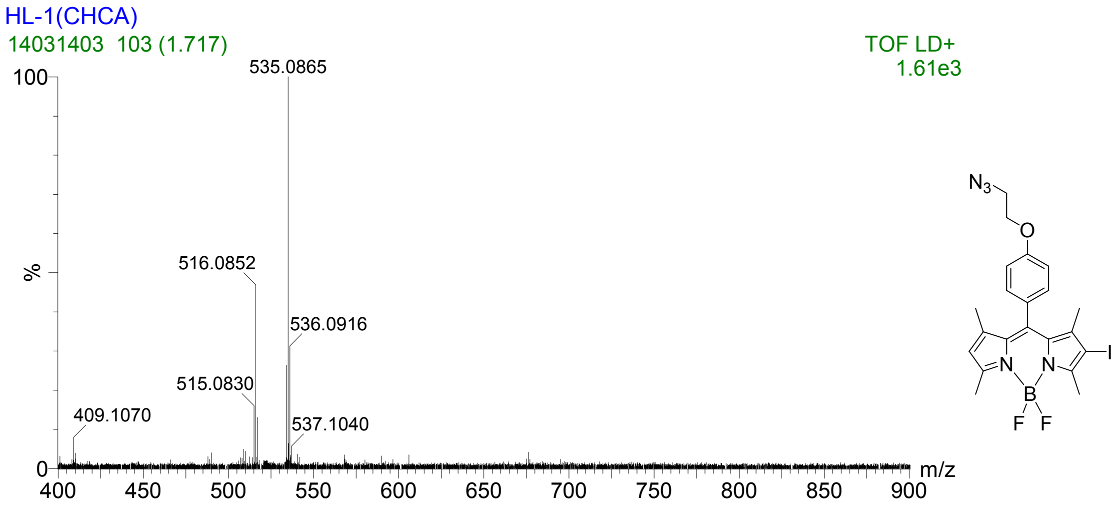

Figure S15. TOF HRMS MALDI of compound **12**.

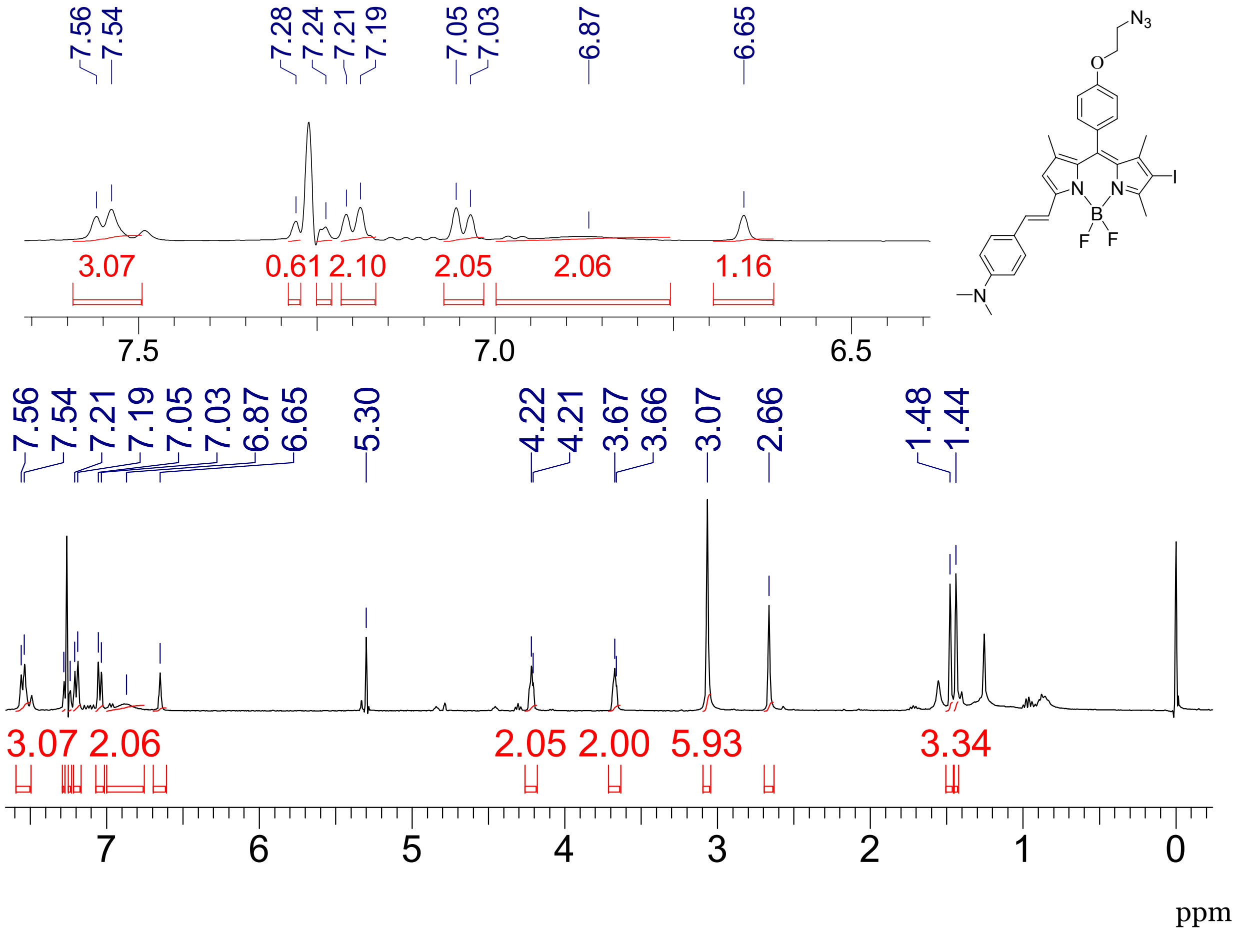

Figure S16. ¹H NMR of compound **7** (400 MHz, $CDCl_3$).

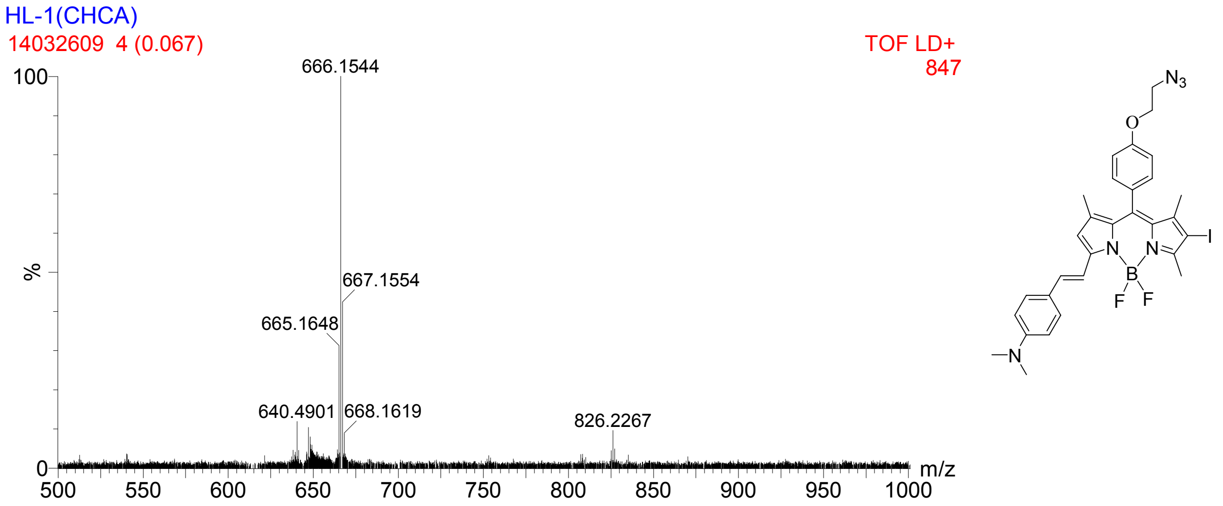

Figure S17. TOF HRMS MALDI of Compound **7'**.

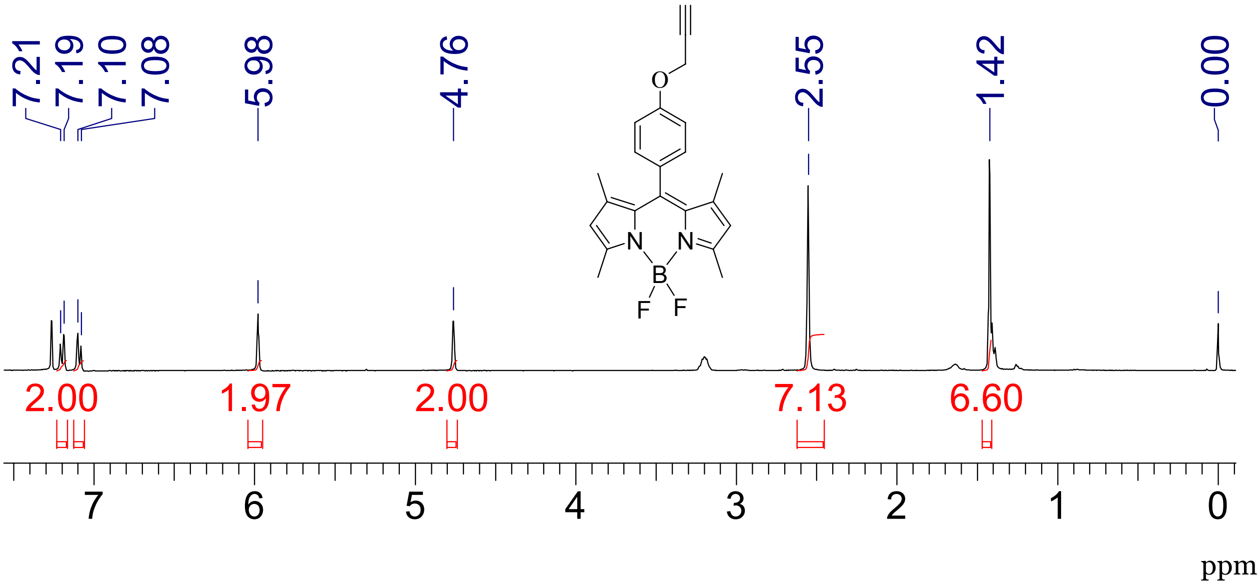

Figure S18. ^{1}H NMR of Compound **8** (400 MHz, $CDCl_3$).

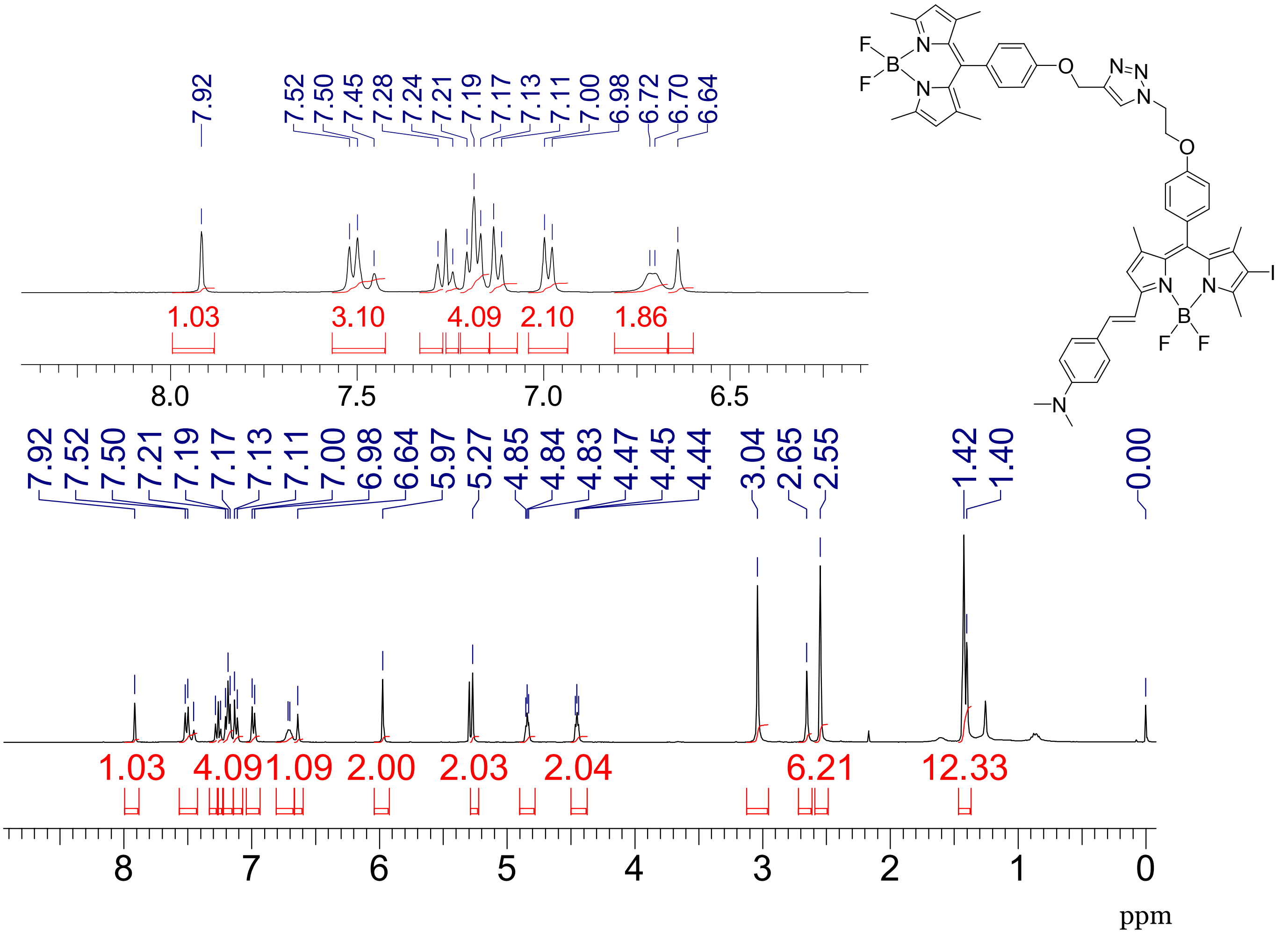

Figure S19. ^{1}H NMR of Compound **10** (400 MHz, CDCl$_3$).

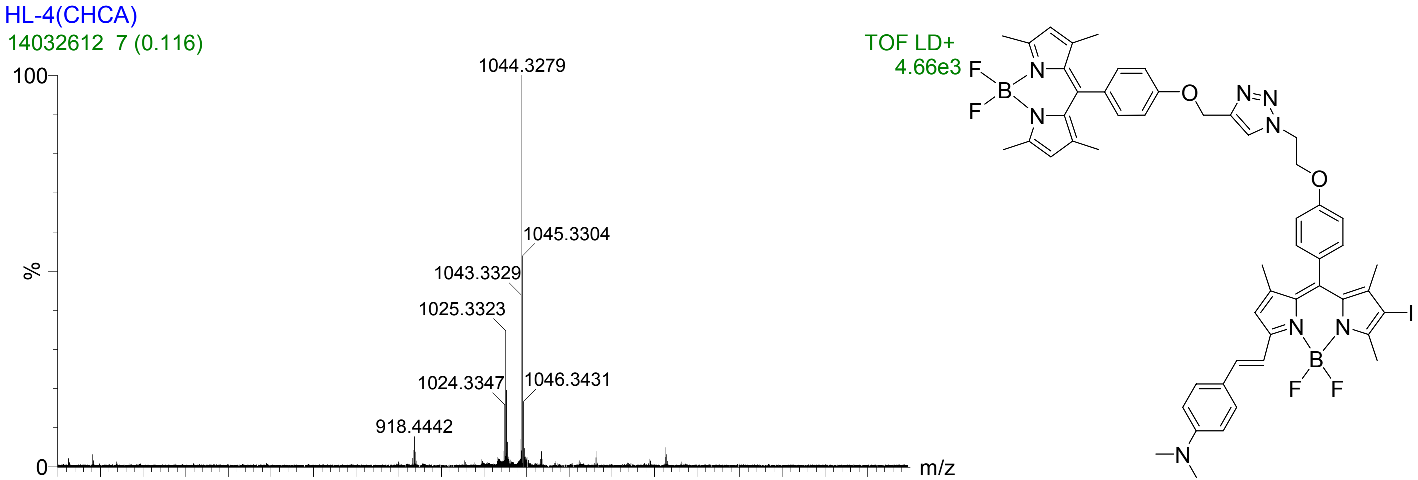

Figure S20. TOF HRMS MALDI of Compound **10**.

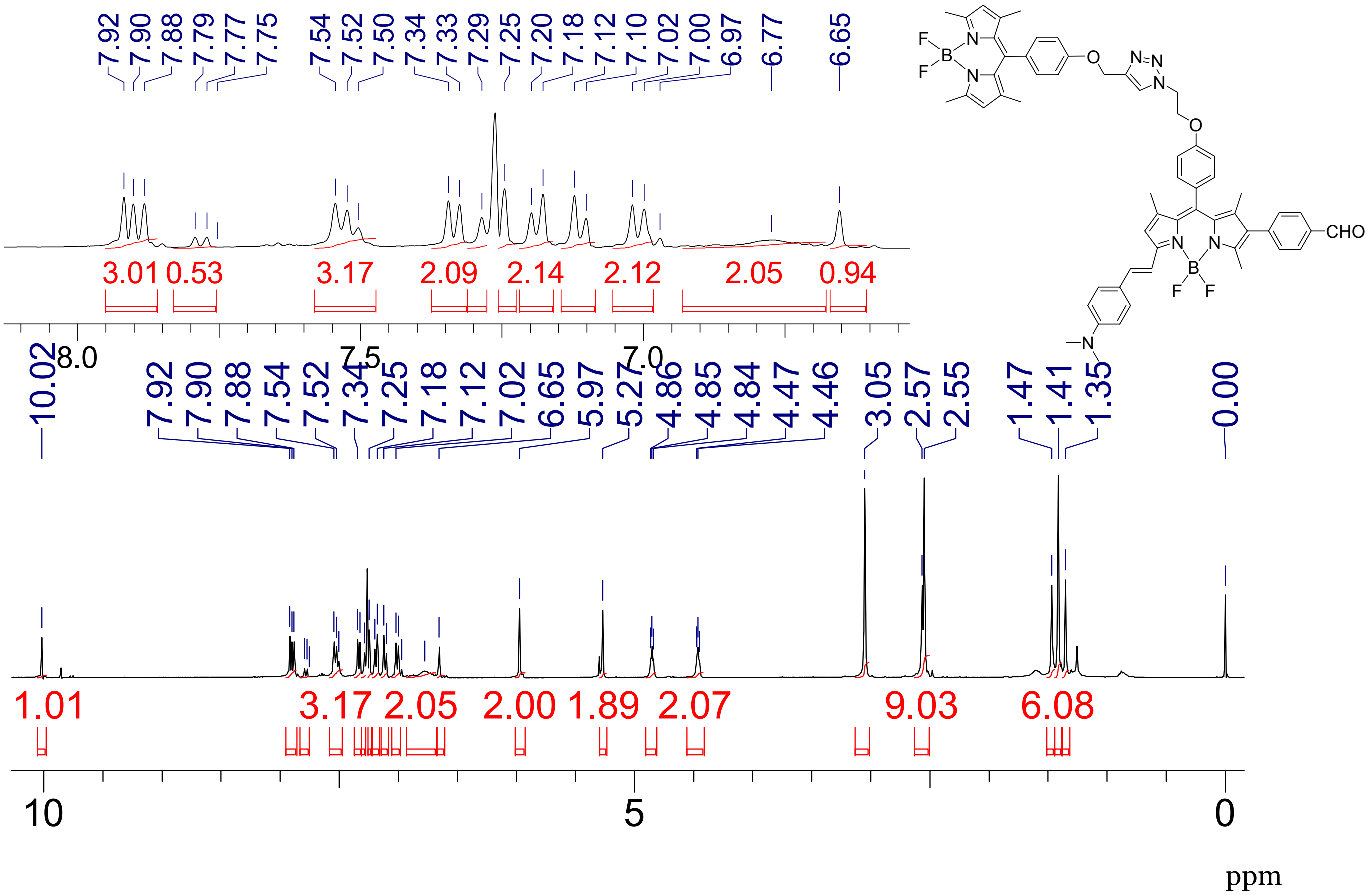

Figure S21. ^{1}H NMR of Compound **11** (400 MHz, $CDCl_3$).

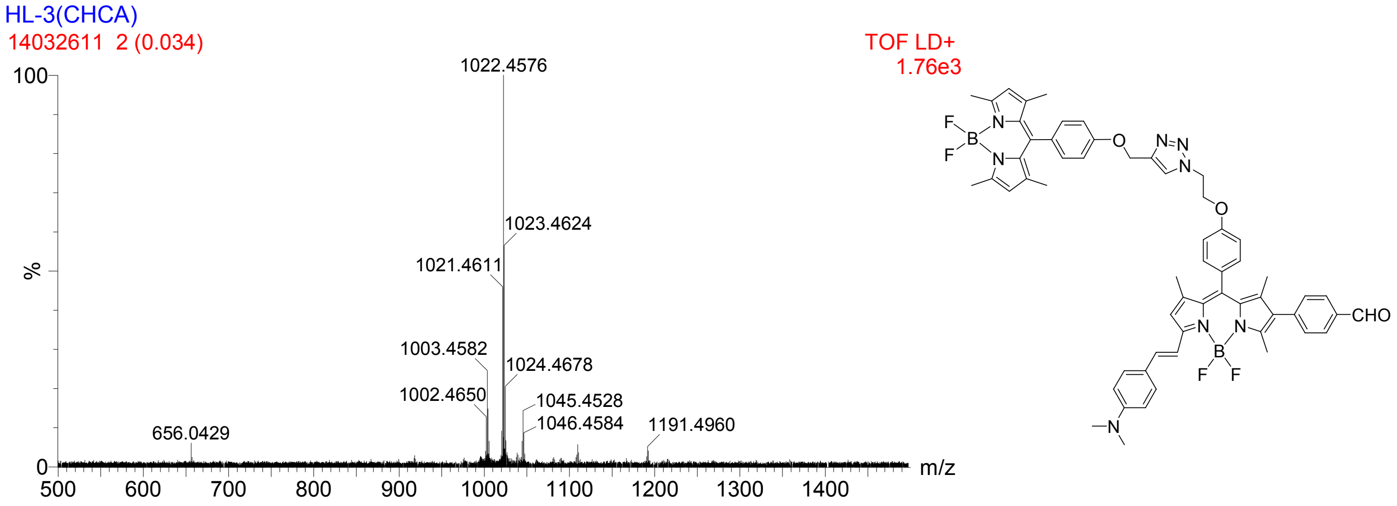

Figure S22. TOF HRMS MALDI of Compound **11**.

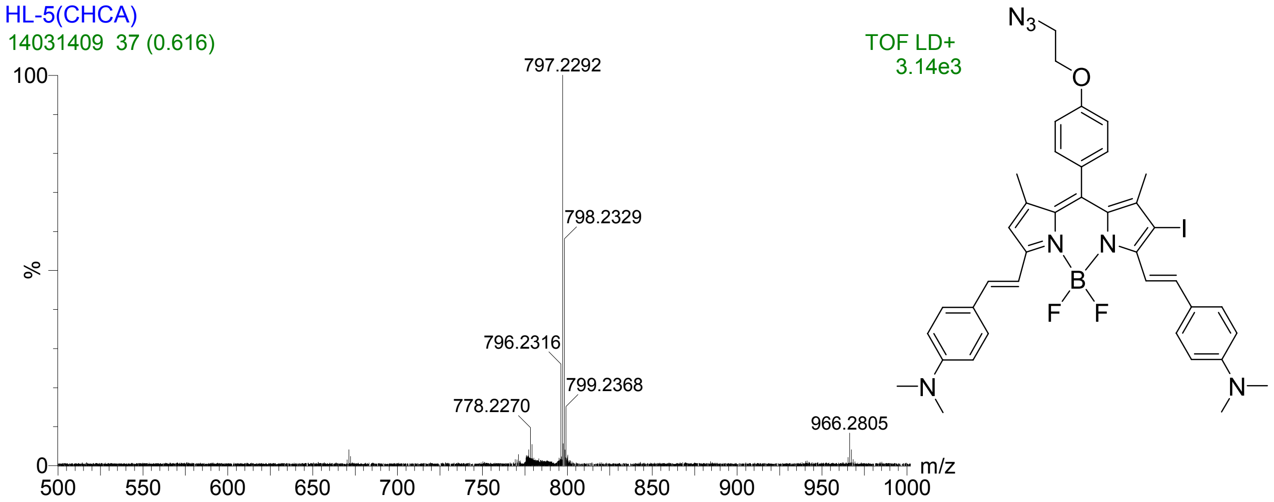

Figure S23. TOF HRMS MALDI of Compound **13**.

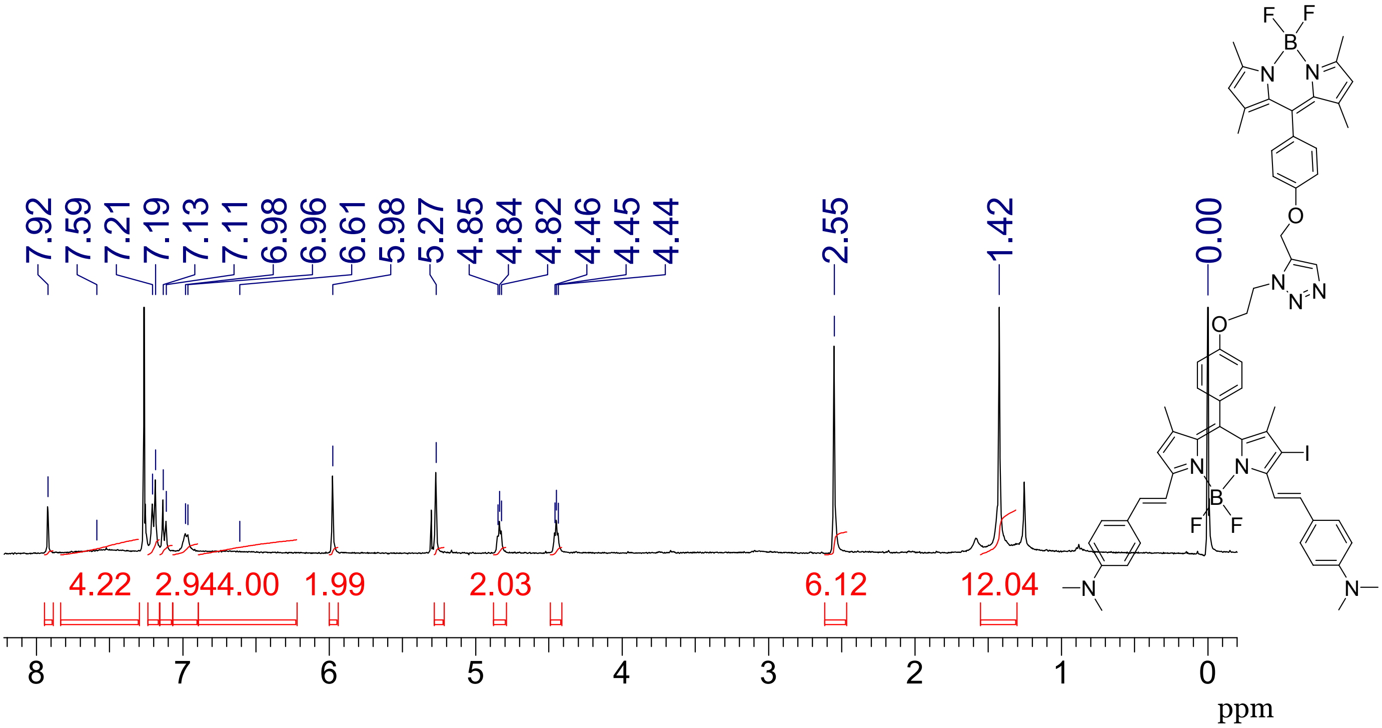

Figure S24. ^{1}H NMR of compound **14** (400 MHz, $CDCl_3$).

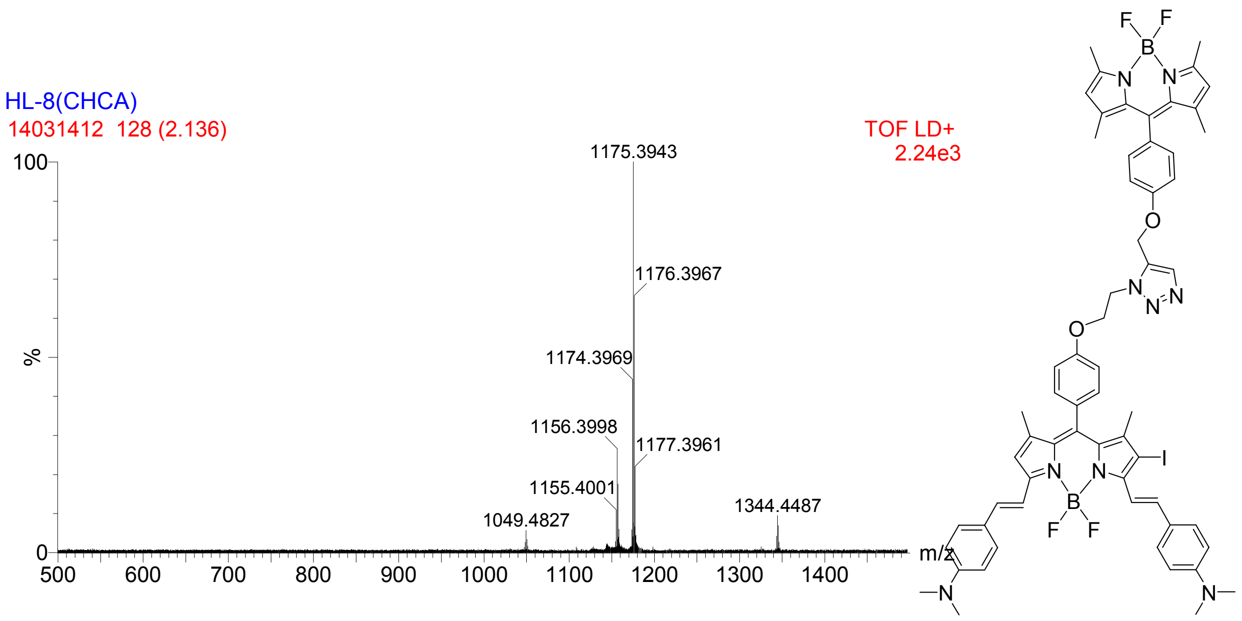

Figure S25. TOF HRMS MALDI of compound **14**.

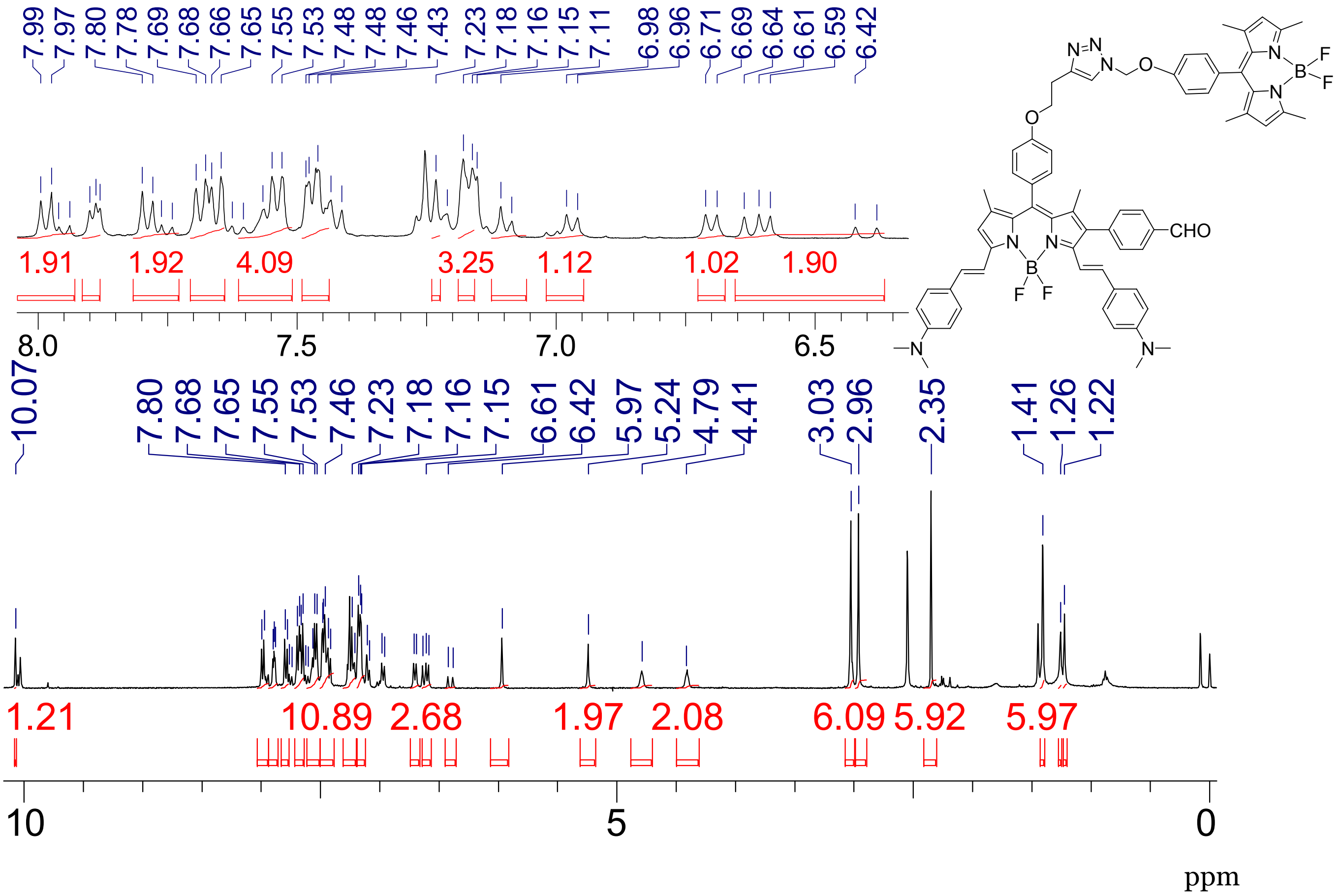

Figure S26. ^{1}H NMR of Compound **15** (400 MHz, $CDCl_3$).

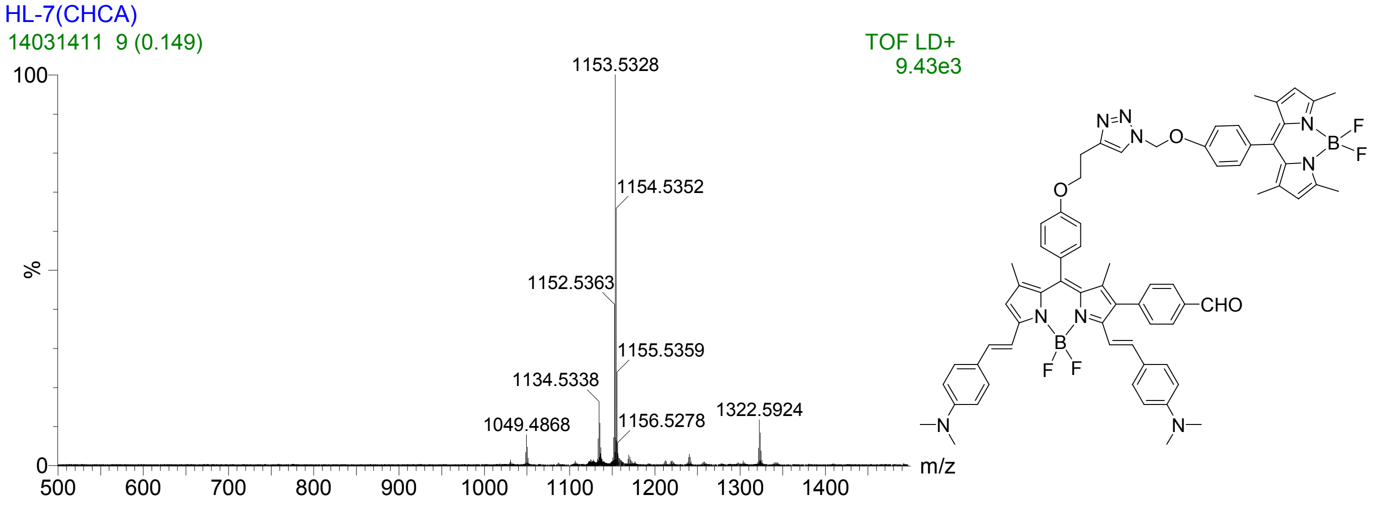

Figure S27. TOF HRMS MALDI of Compound **15.**

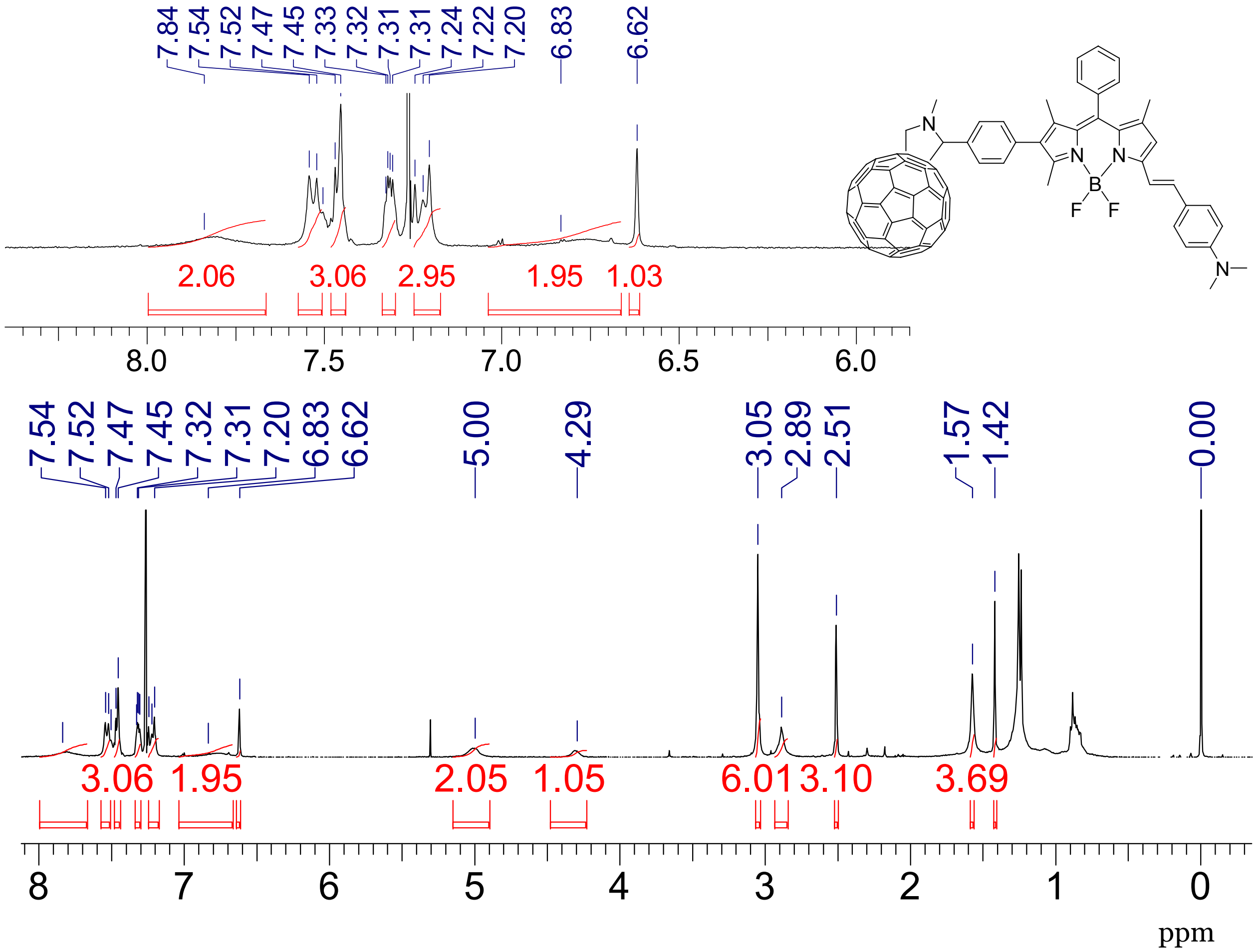

Figure S28. ^{1}H NMR of **B-1** (400 MHz, $CDCl_3$).

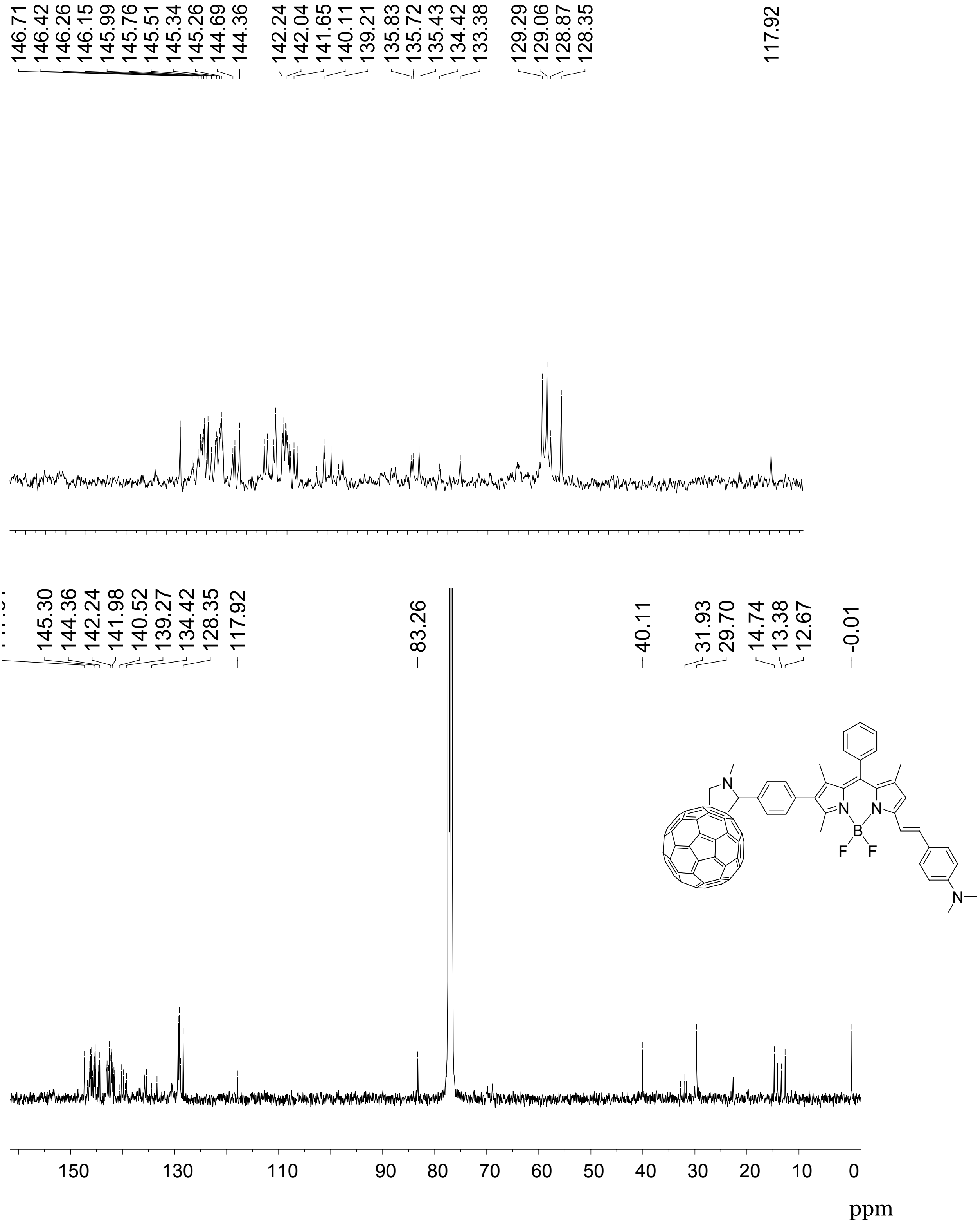

Figure S29. ^{13}C NMR of **B-1** (100 MHz, $CDCl_3$).

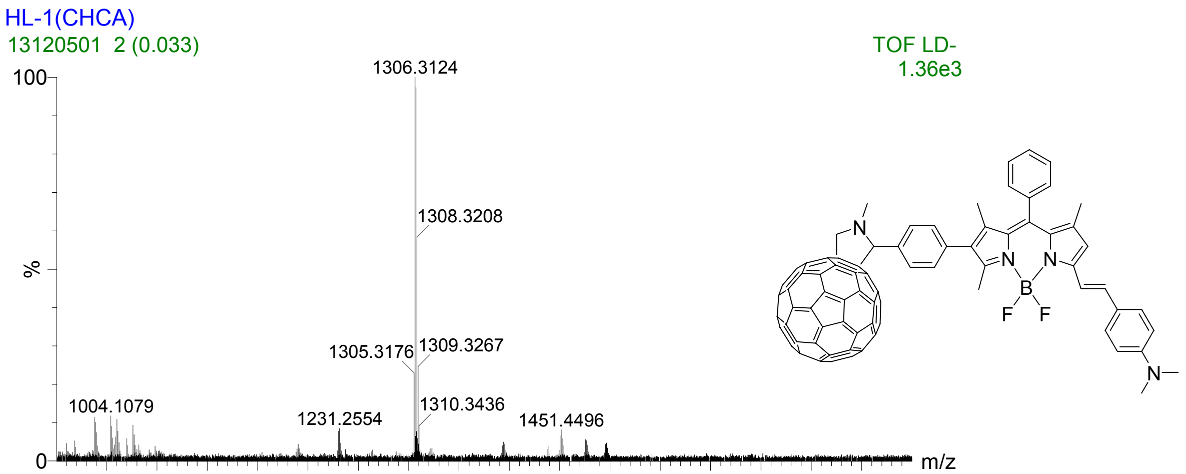

Figure S30. TOF HRMS MALDI of **B-1**

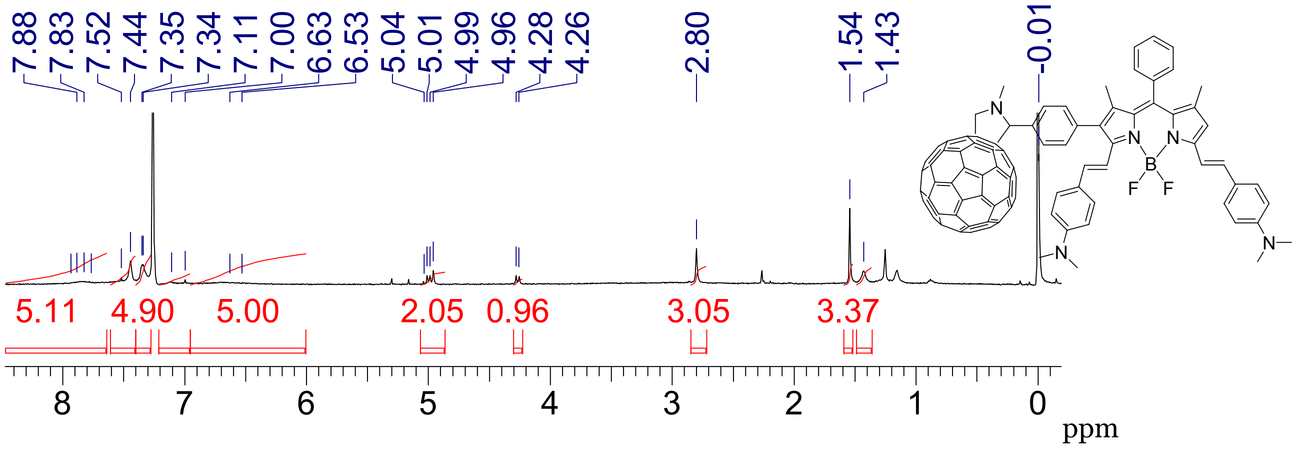

Figure S31. ^{1}H NMR of **B-2** (400 MHz, CDCl$_3$)

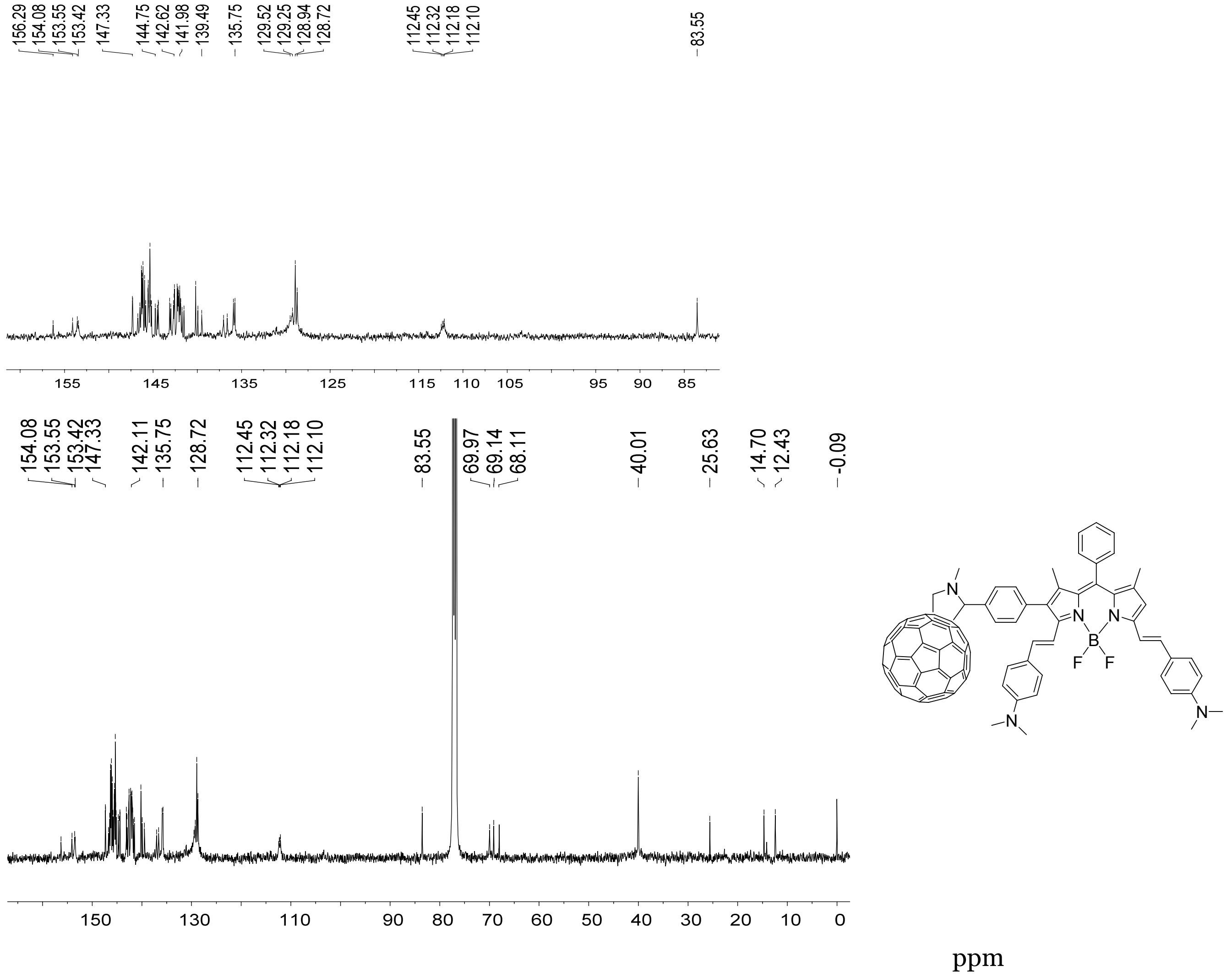

Figure S32. ^{13}C NMR of **B-2** (100 MHz, CDCl$_3$)

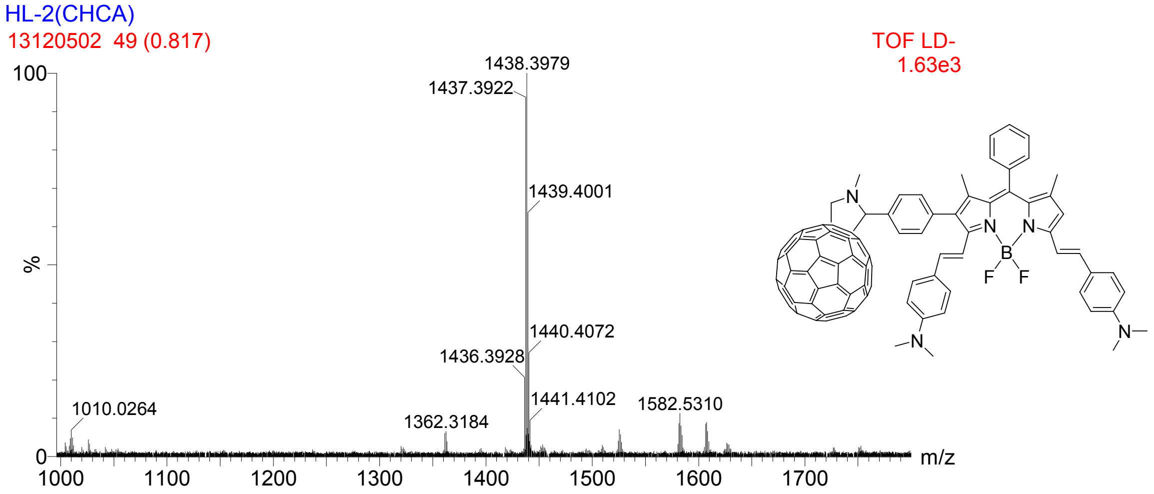

Figure S33. TOF HRMS MALDI of **B-2.**

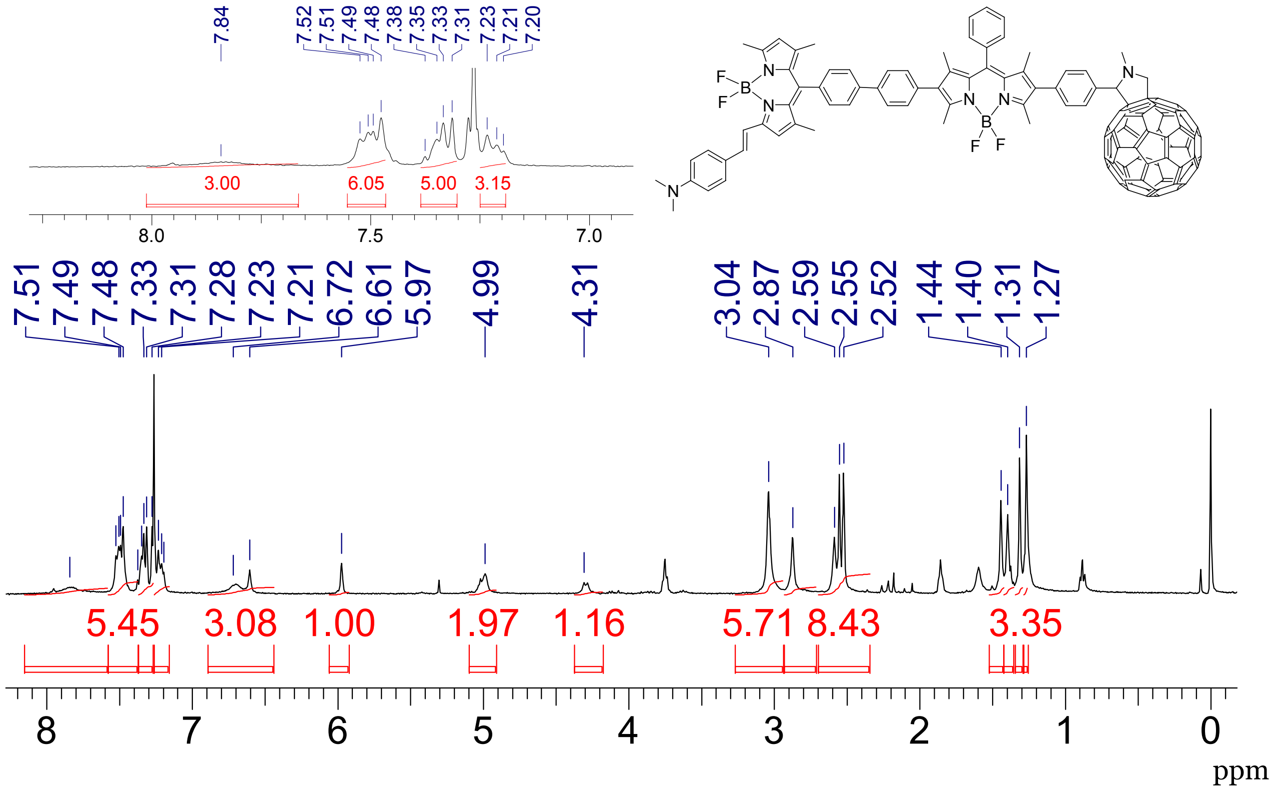

Figure S34. ^{1}H NMR of **B-3′** (400 MHz, $CDCl_3$)

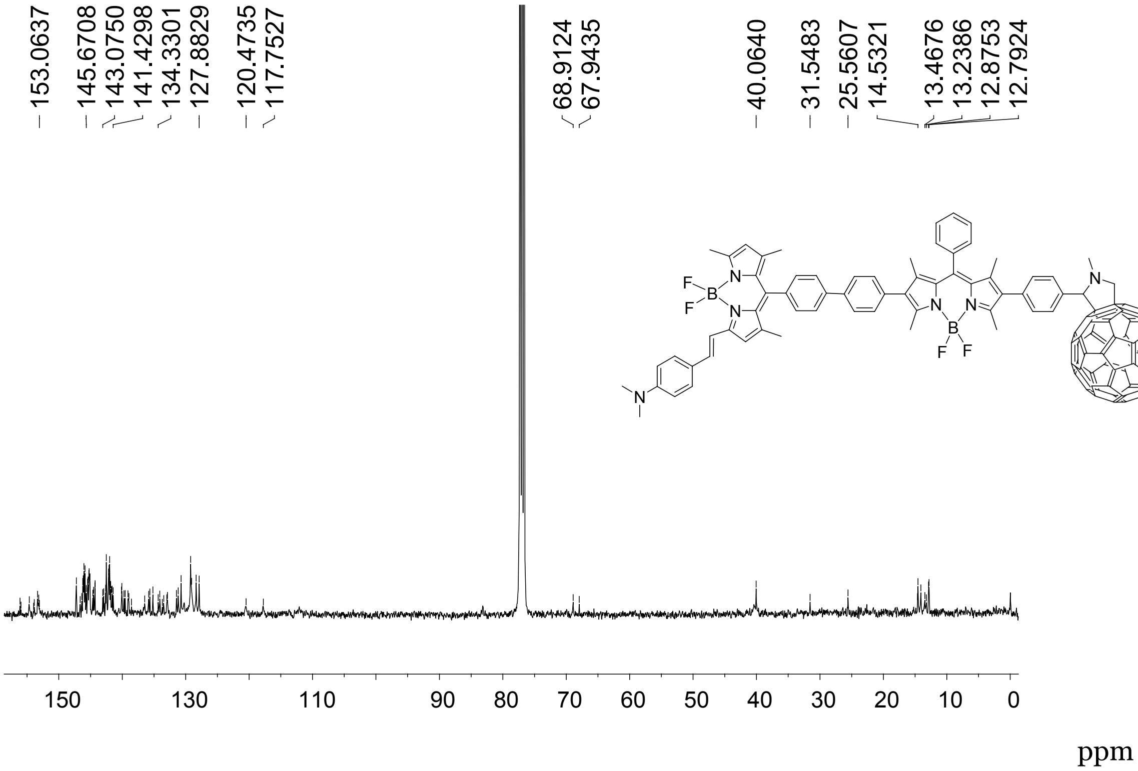

Figure S35. ^{13}C NMR of **B-3′** (100 MHz, $CDCl_3$)

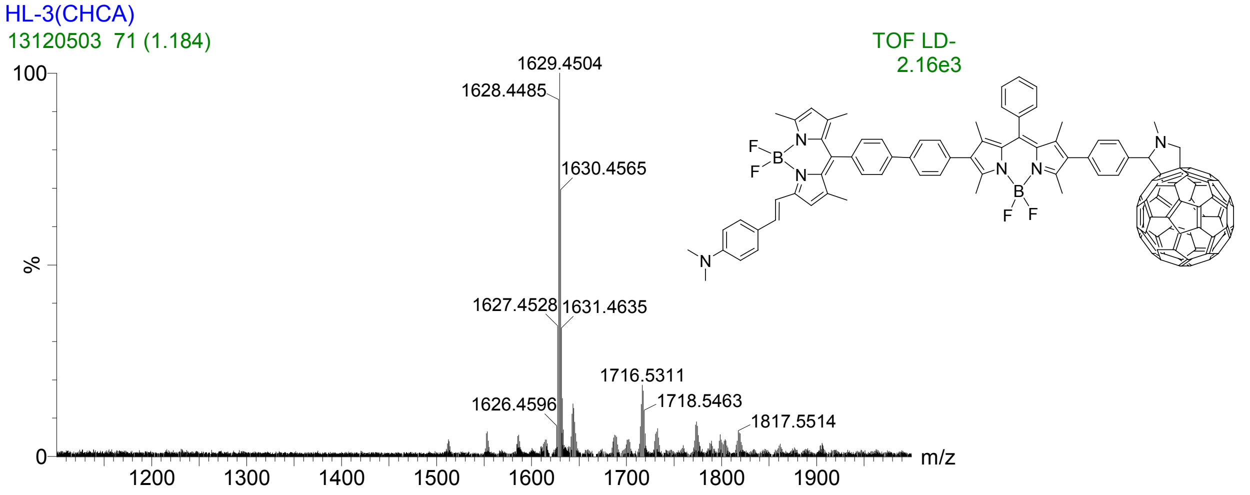

Figure S36. TOF HRMS MALDI of **B-3′**

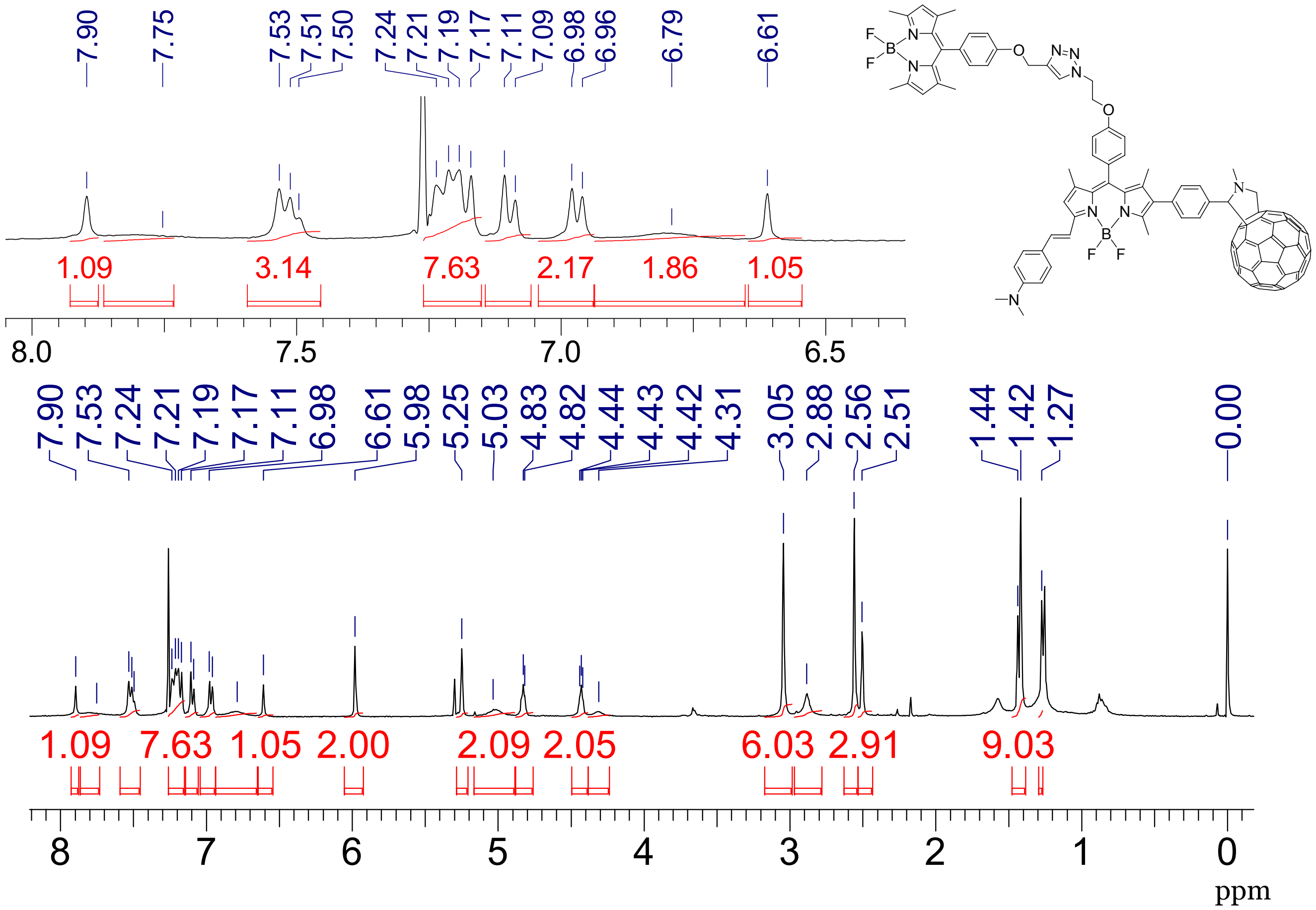

Figure S37. ^{1}H NMR of **B-3** (400 MHz, $CDCl_3$).

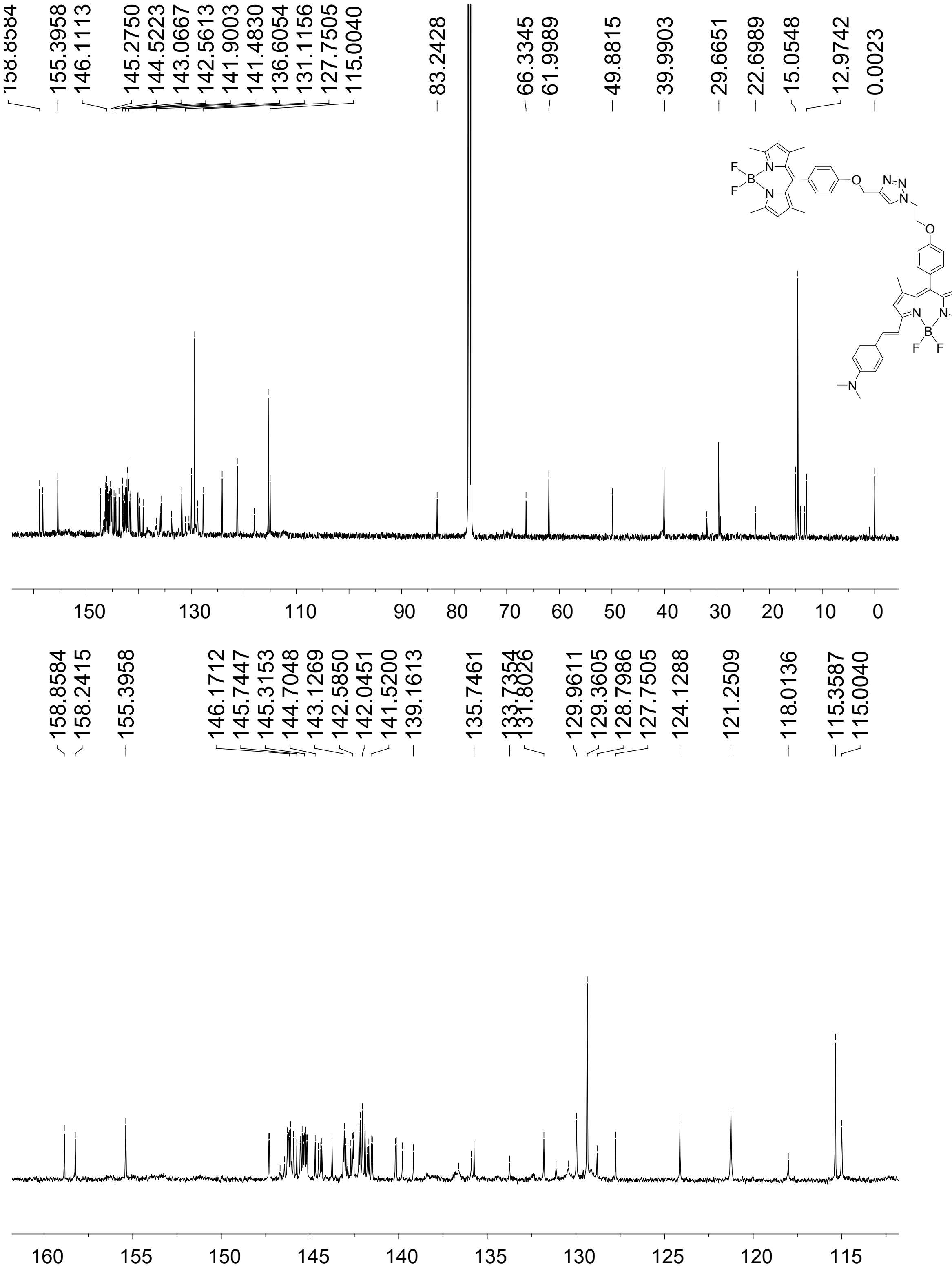

Figure S38. ^{13}C NMR of **B-3** (100 MHz, $CDCl_3$).

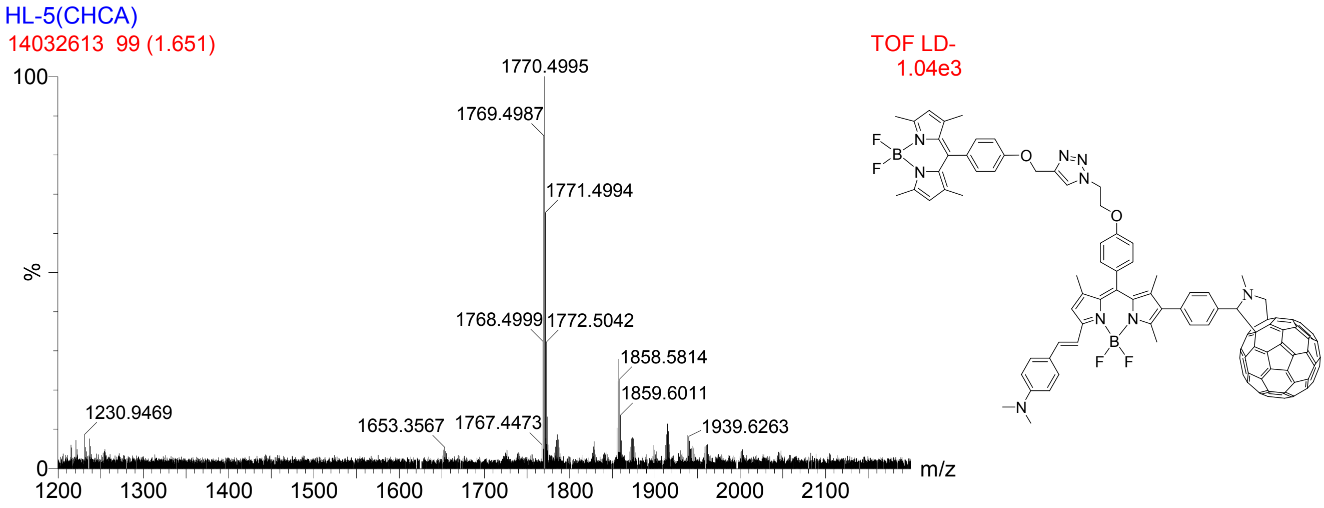

Figure S39. TOF HRMS MALDI of **B-3.**

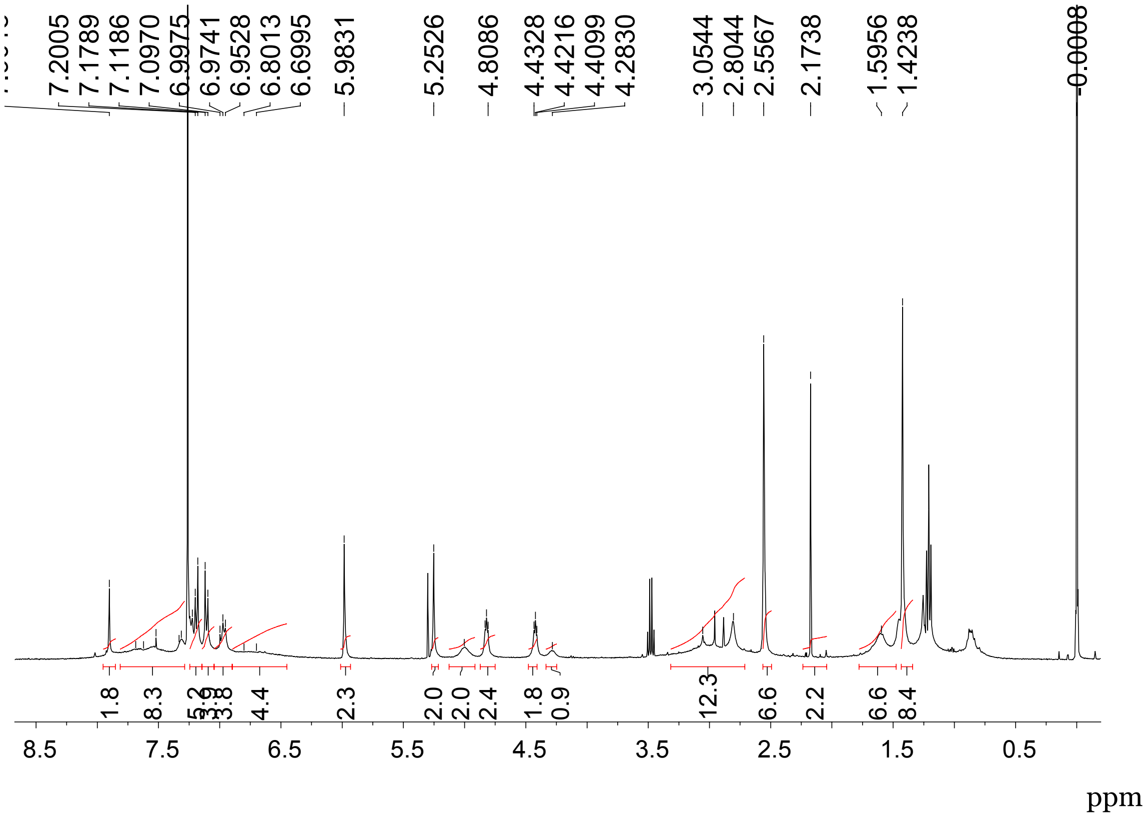

Figure S40. ^{1}H NMR of **B-4** (400 MHz, $CDCl_3$).

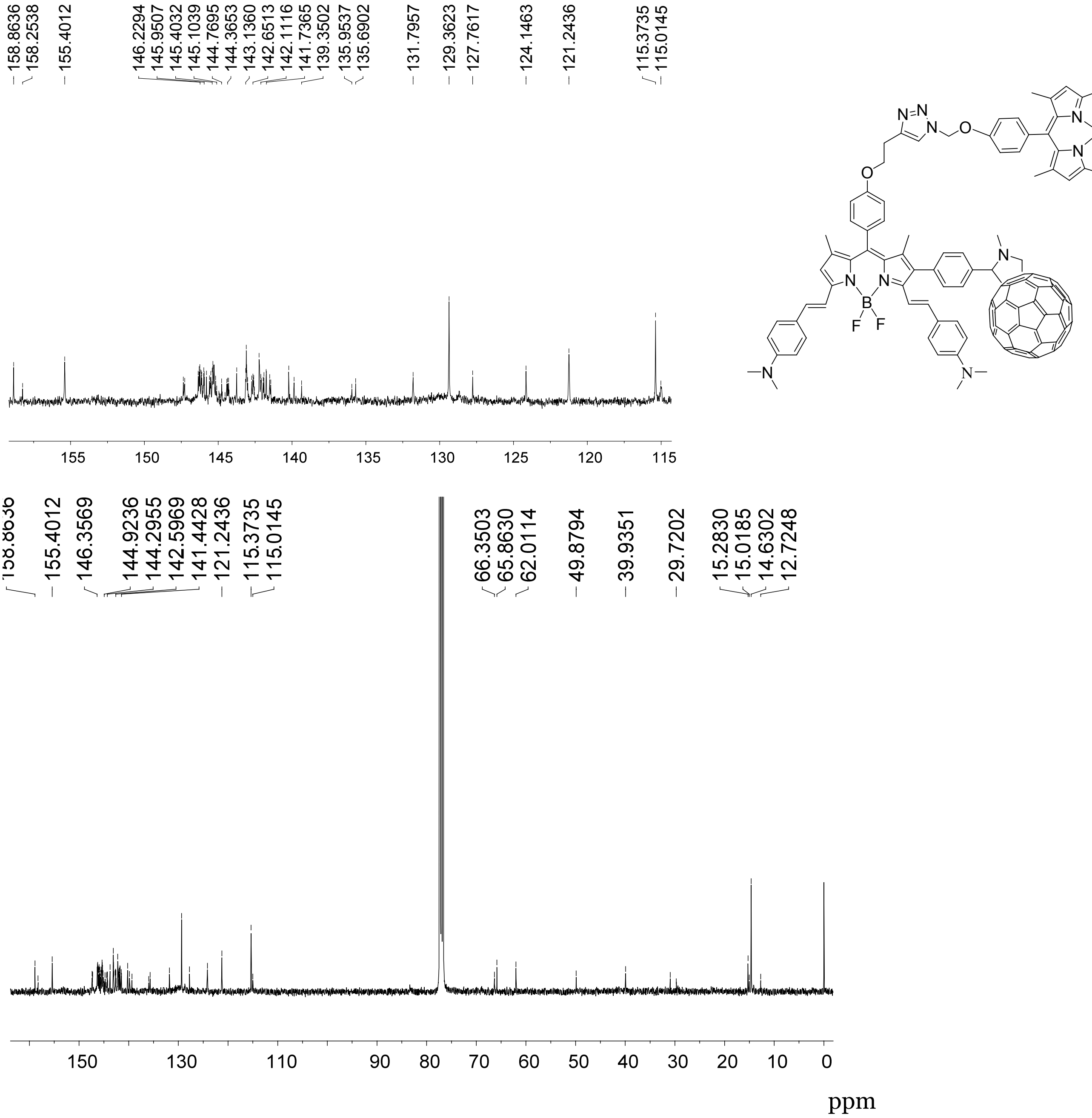

Figure S41. ^{13}C NMR of **B-4** (100 MHz, CDCl$_3$).

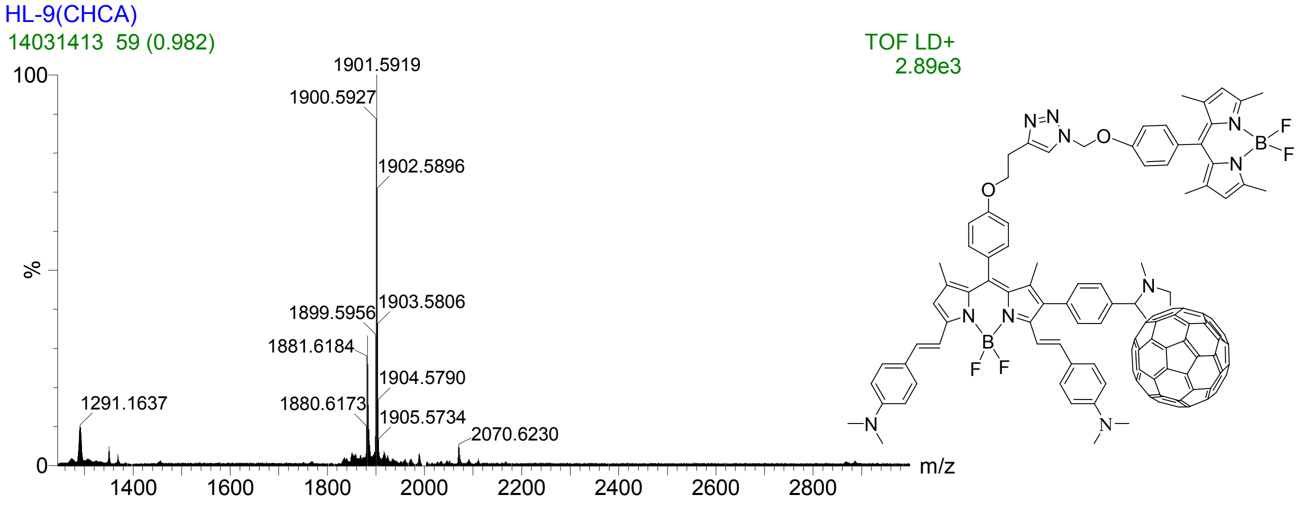

Figure S42. TOF HRMS MALDI of **B-4.**

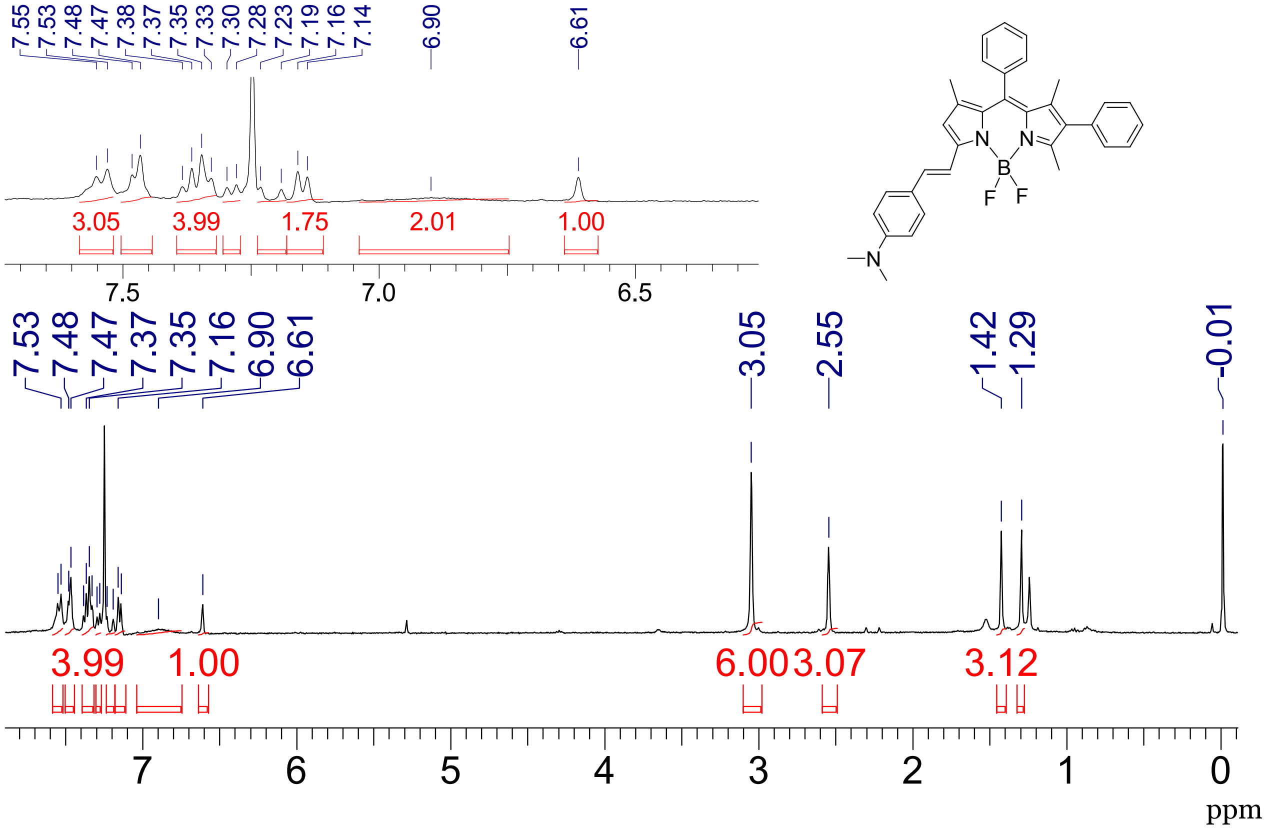

Figure S43. ^{1}H NMR of **B-5** (400 MHz, CDCl$_3$).

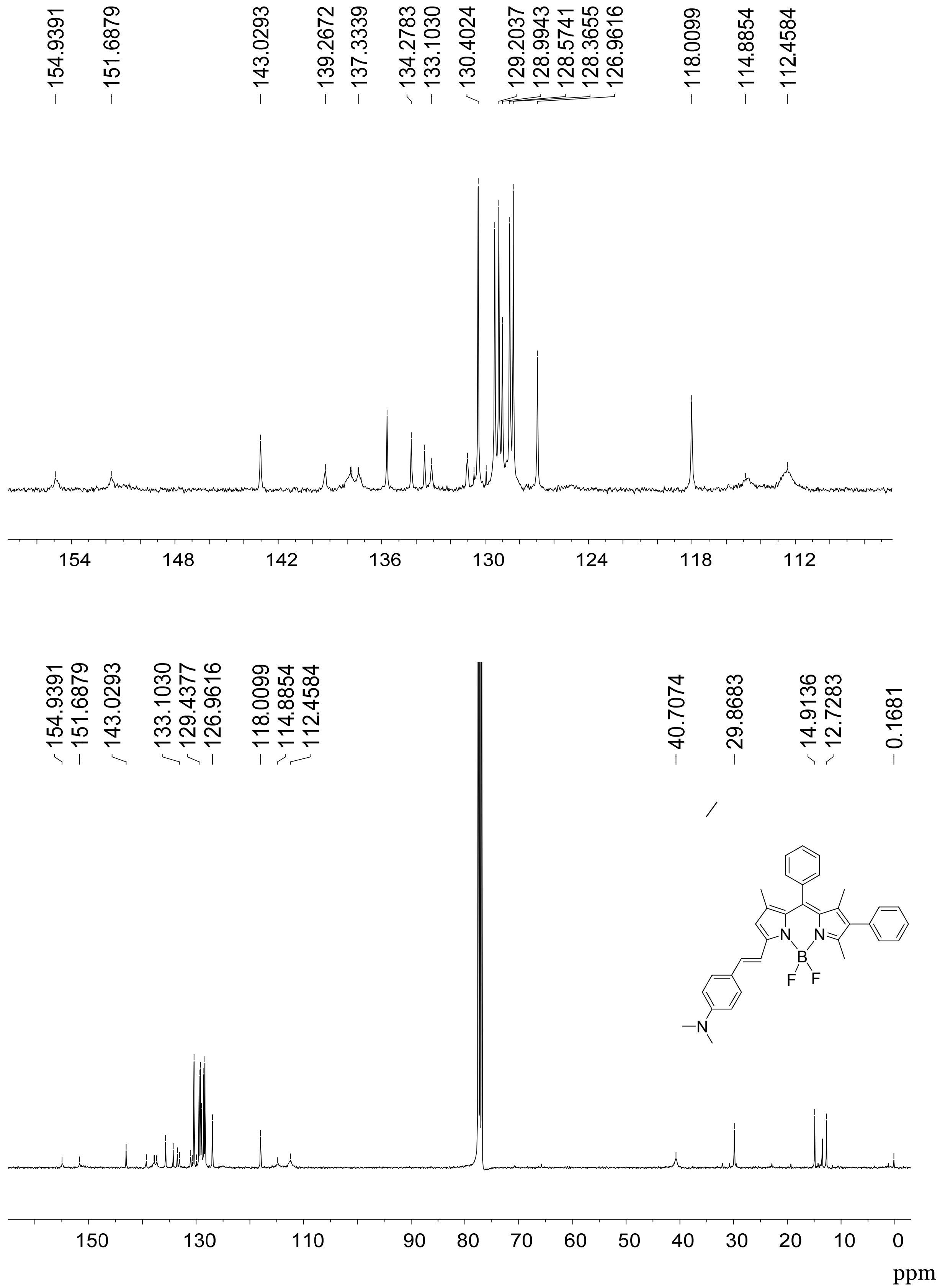

Figure S44. ^{13}C NMR of **B-5** (100 MHz, $CDCl_3$).

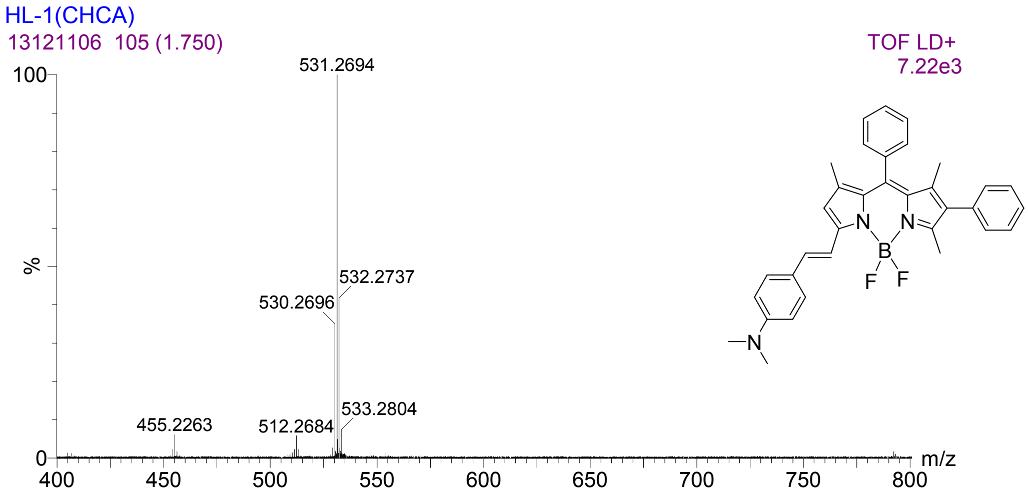

Figure S45. TOF HRMS MALDI of **B-5.**

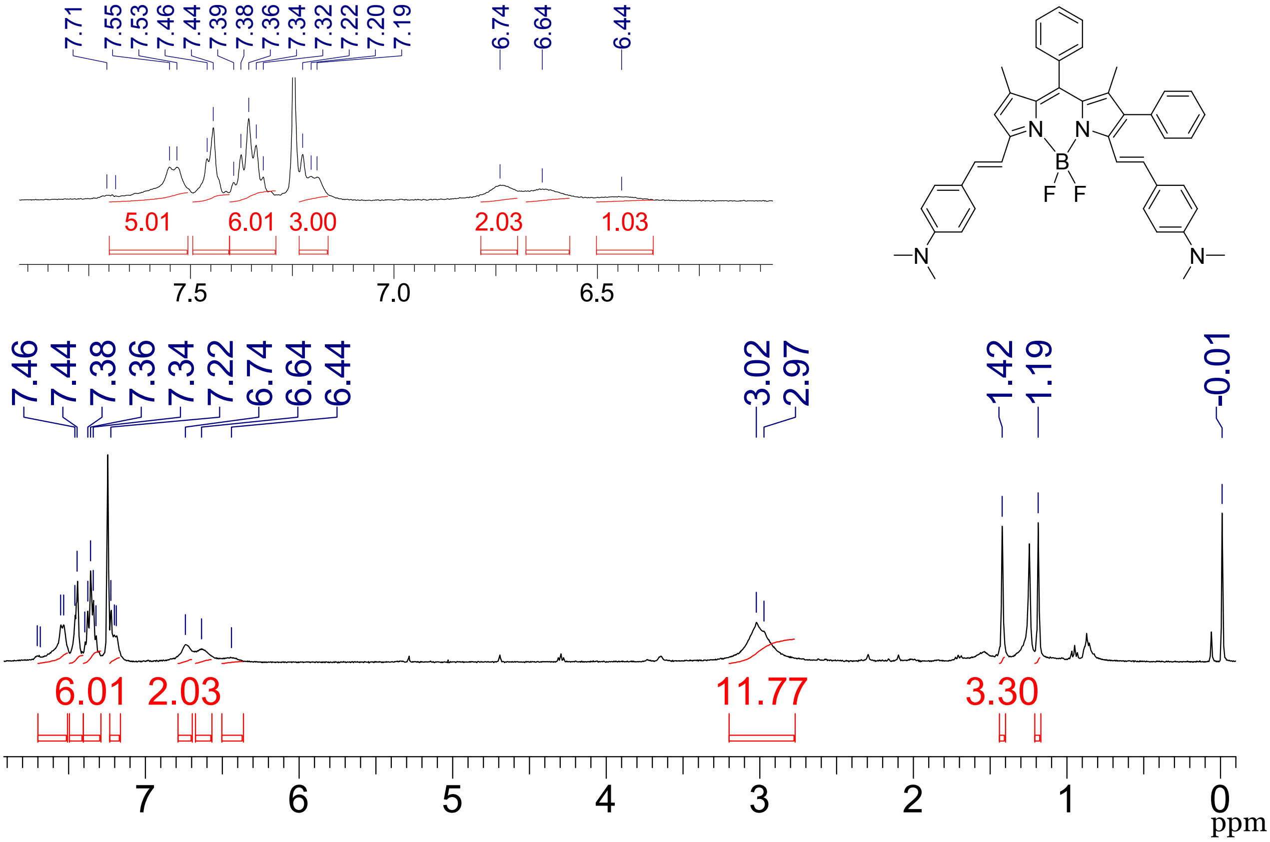

Figure S46. ^{1}H NMR of **B-6** (400 MHz, $CDCl_3$).

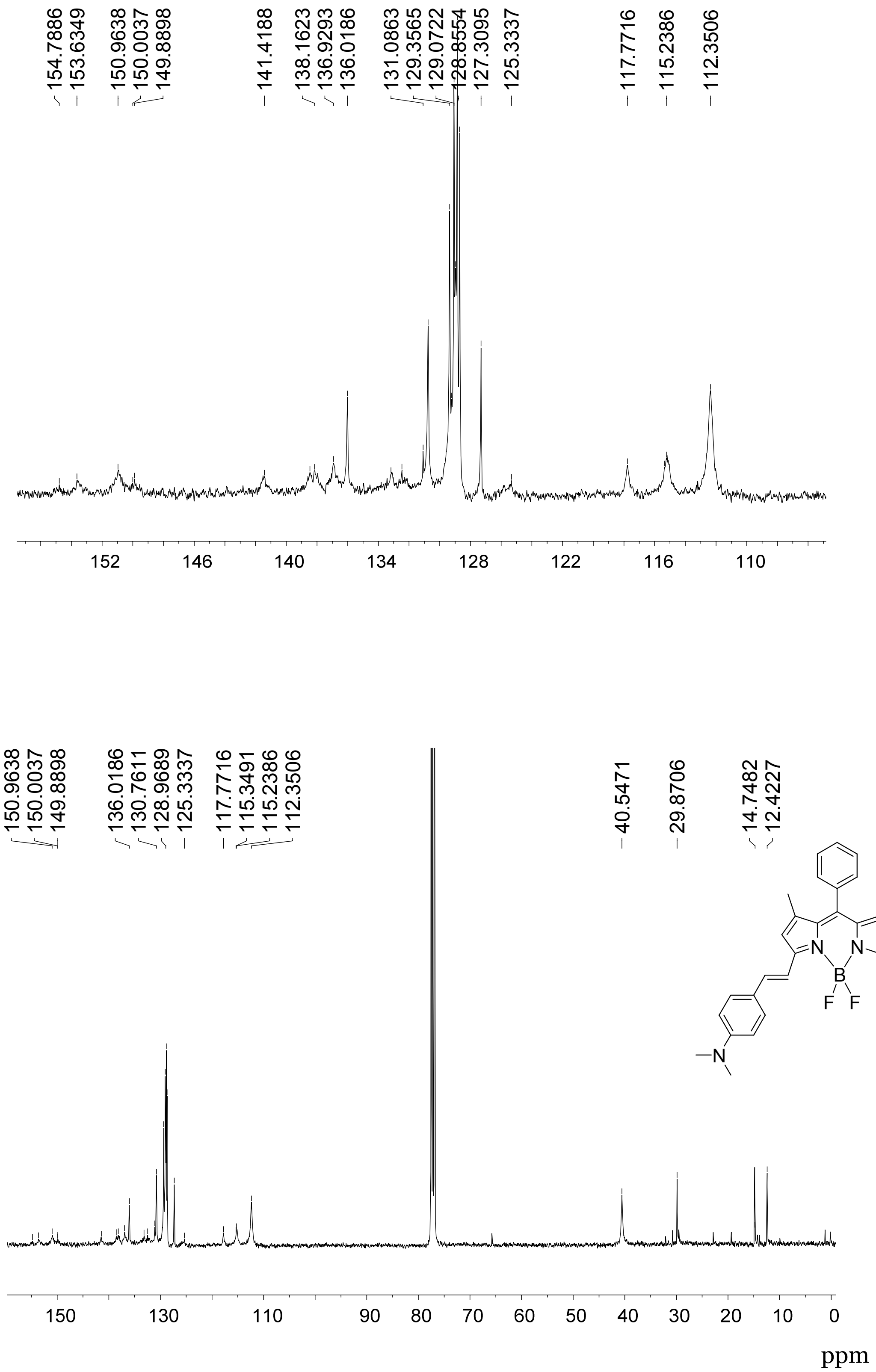

Figure S47. ^{13}C NMR of **B-6** (100 MHz, $CDCl_3$).

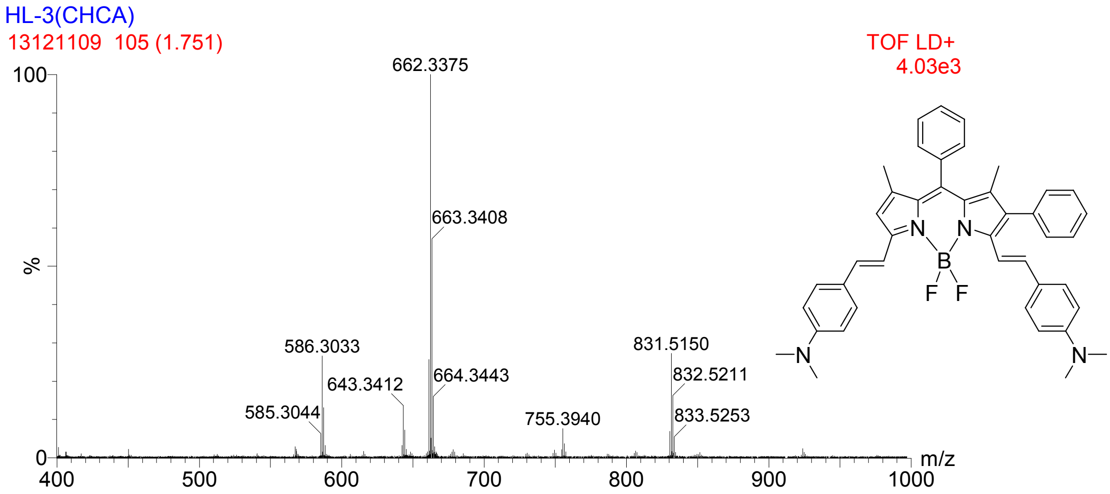

Figure S48. TOF HRMS MALDI of **B-6.**

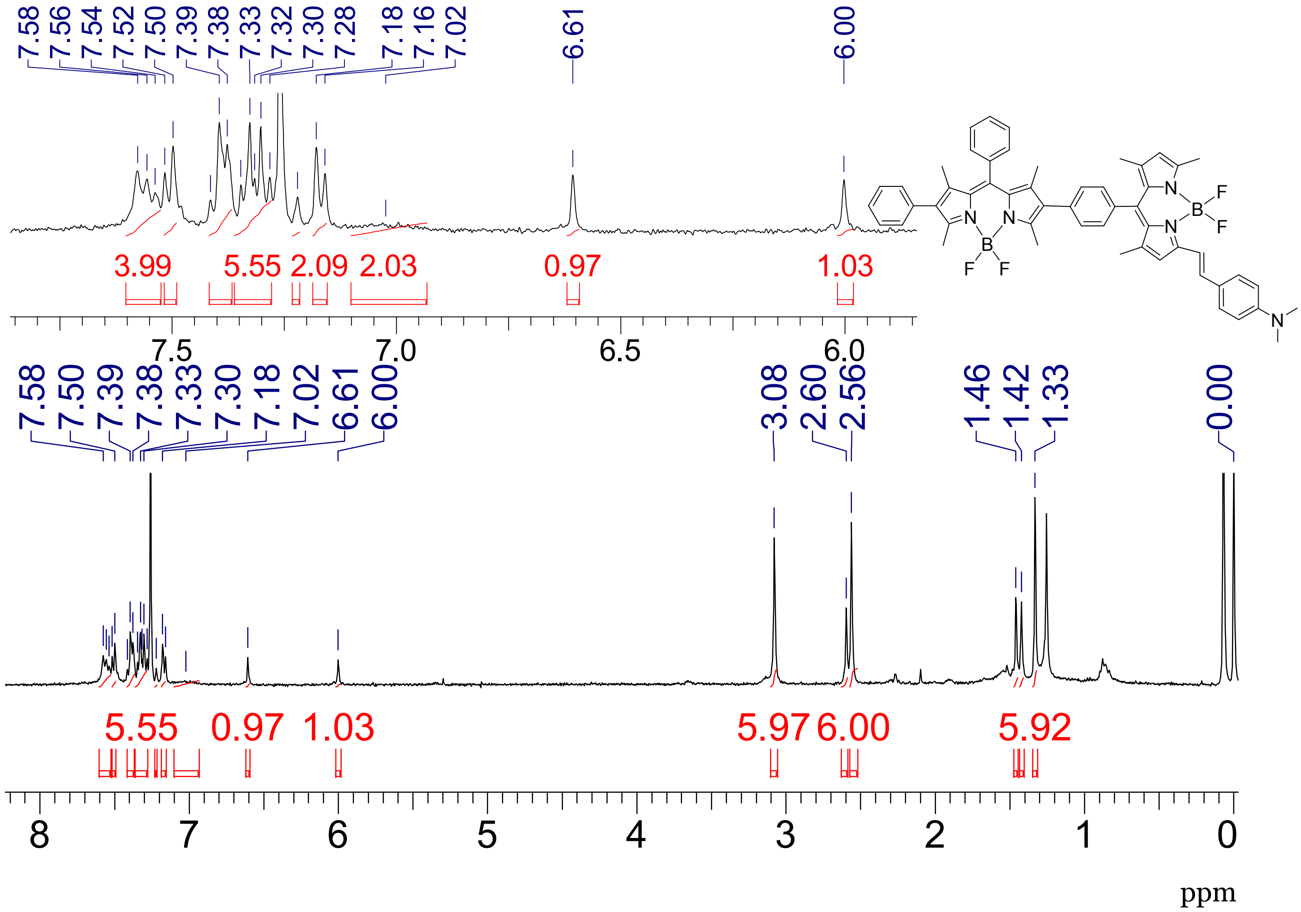

Figure S49. ^{1}H NMR of **B-7′** (400 MHz, CDCl$_3$)

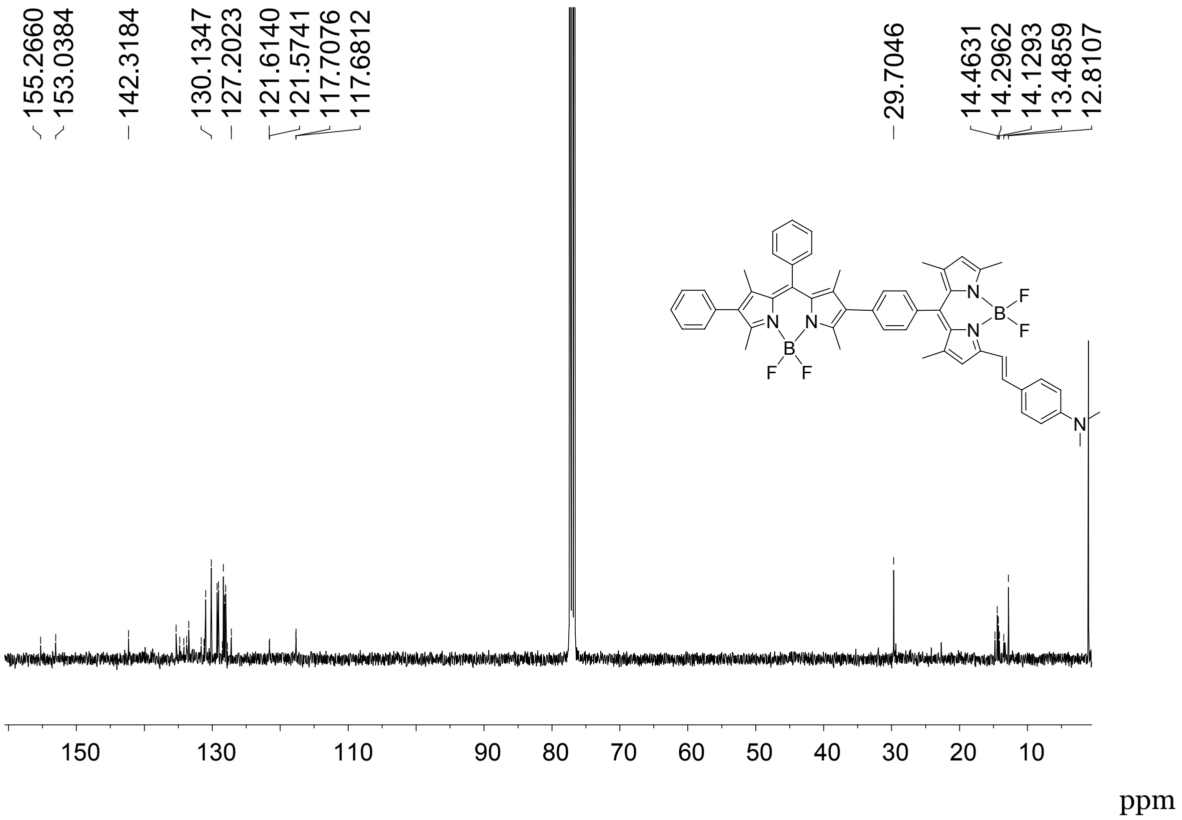

Figure S50 ^{13}C NMR of **B-7′** (100 MHz, CDCl$_3$)

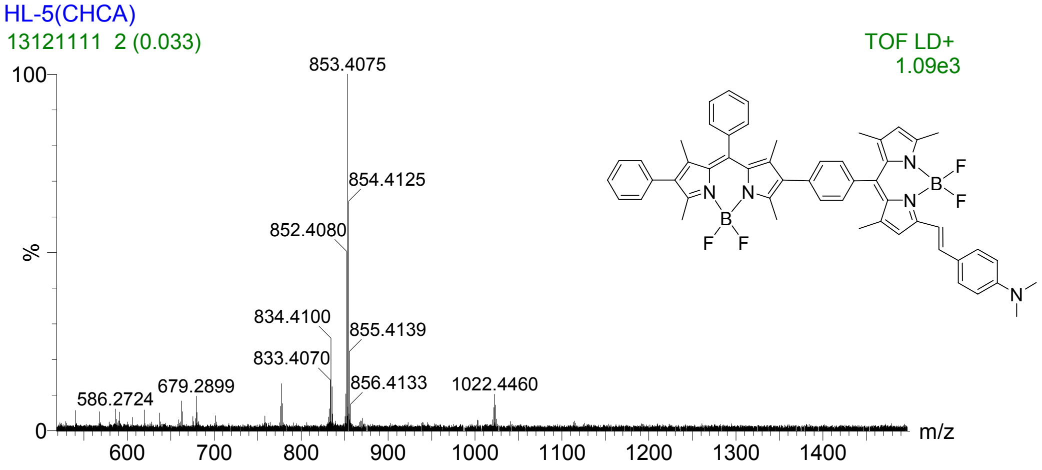

Figure S51. TOF HRMS MALDI of **B-7′**.

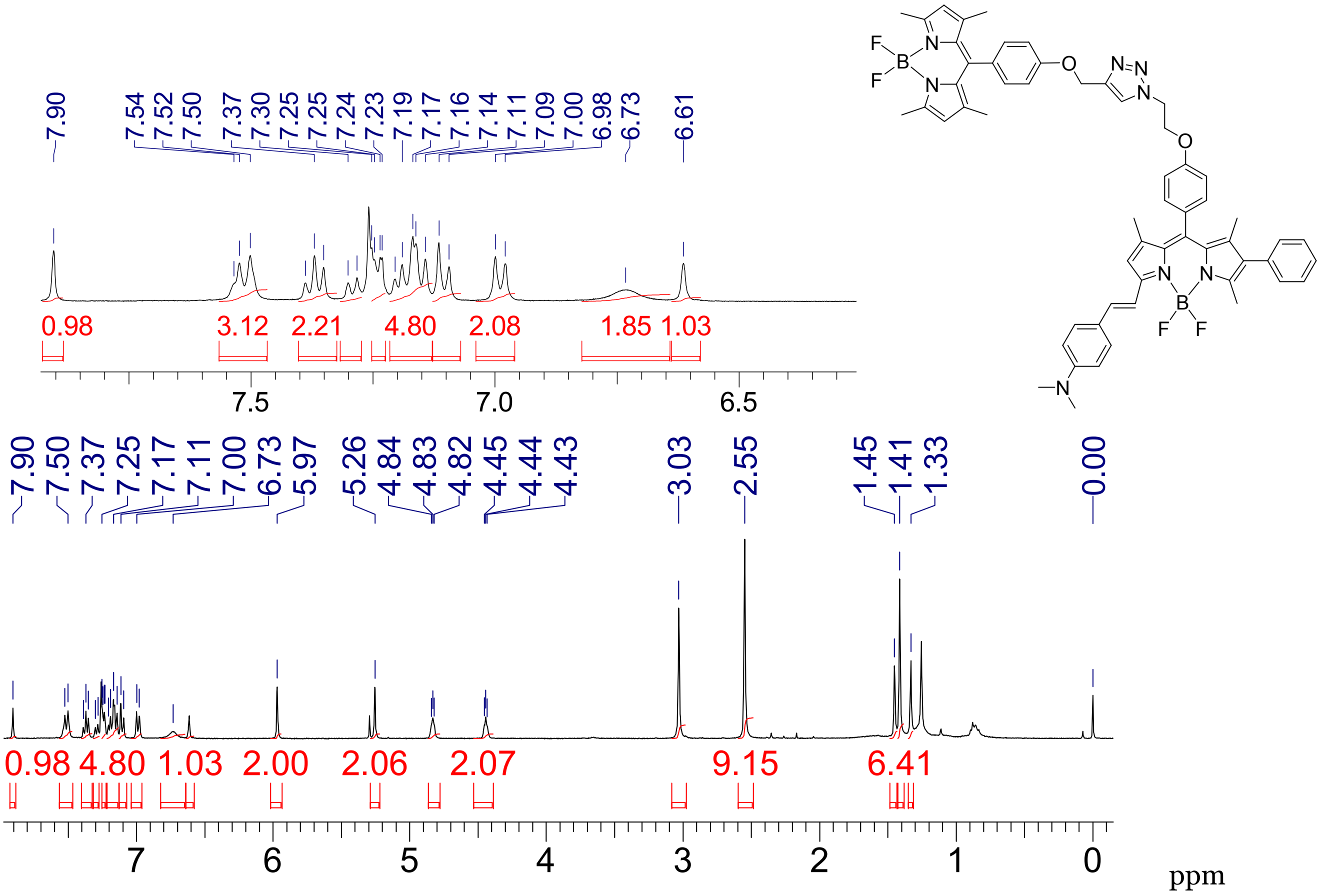

Figure S52. ^{1}H NMR of **B-7** (400 MHz, CDCl$_3$).

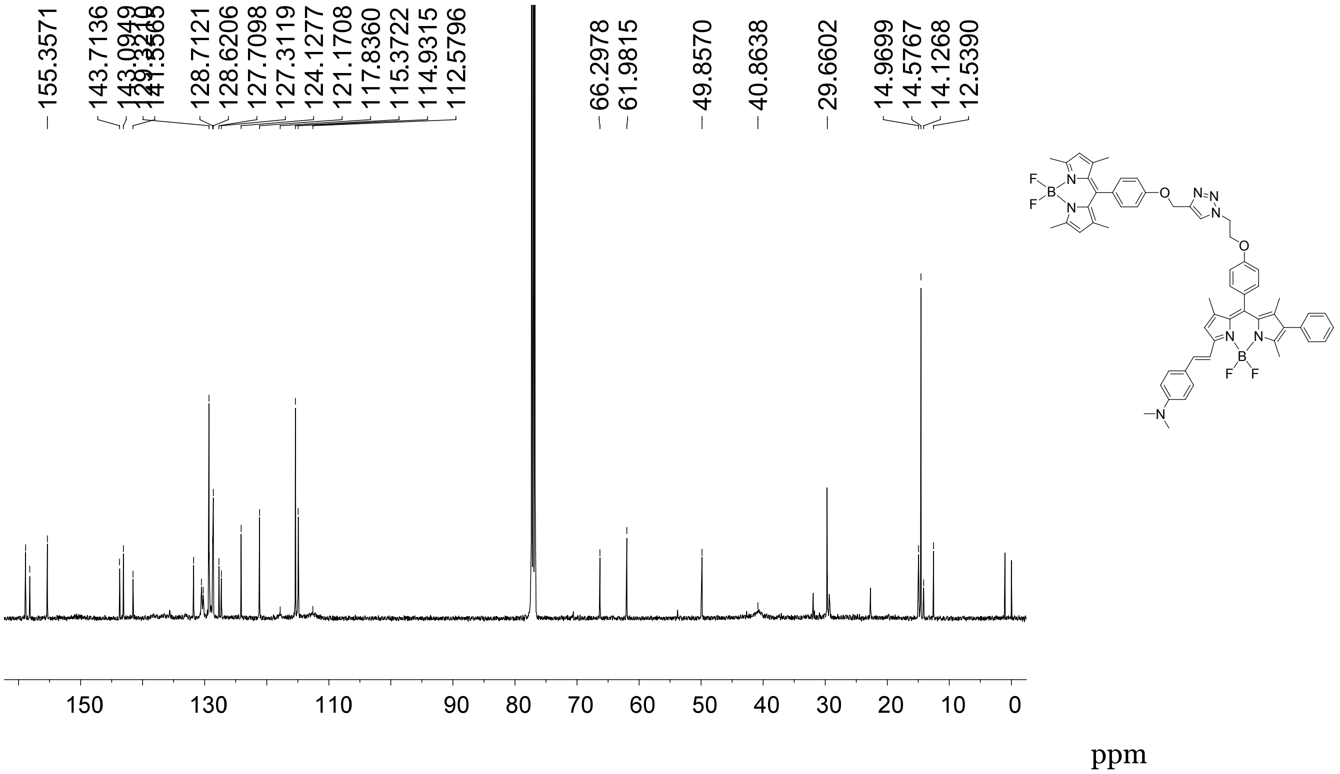

Figure S53. ^{13}C NMR of **B-7** (100 MHz, CDCl$_3$).

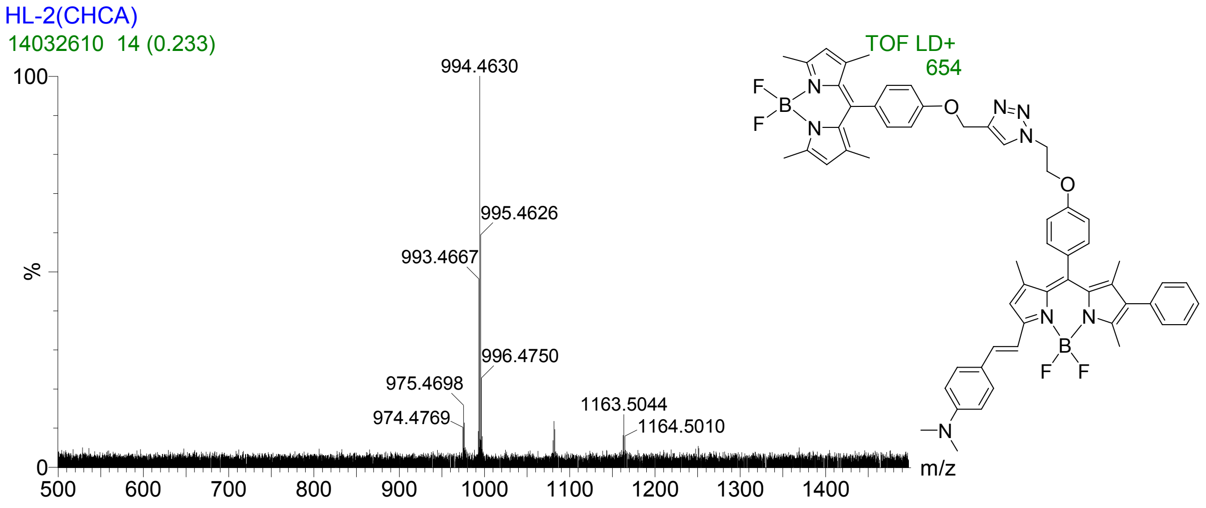

Figure 54. TOF HRMS MALDI of **B-7.**

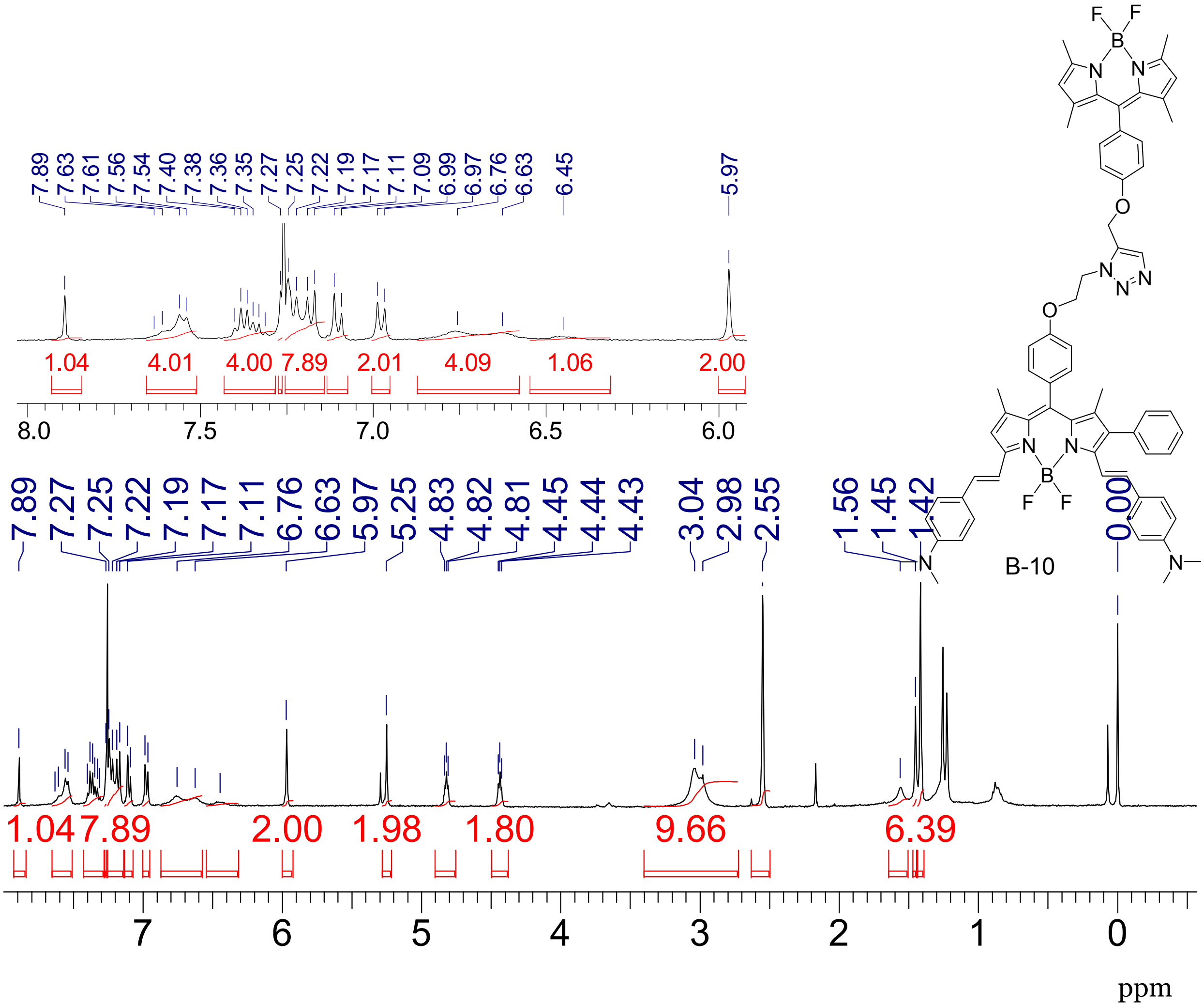

Figure S55. ^{1}H NMR of **B-8** (400 MHz, $CDCl_3$)

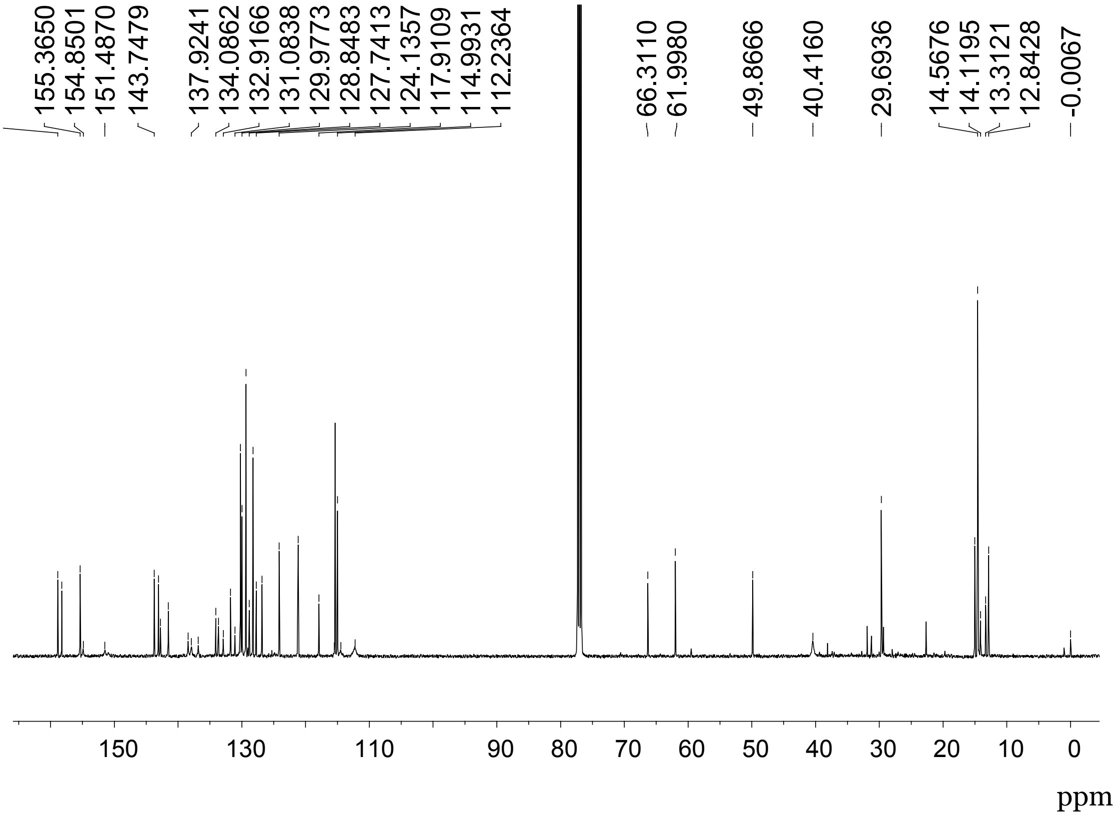

Figure S56. ^{13}C NMR of **B-8** (400 MHz, CDCl$_3$).

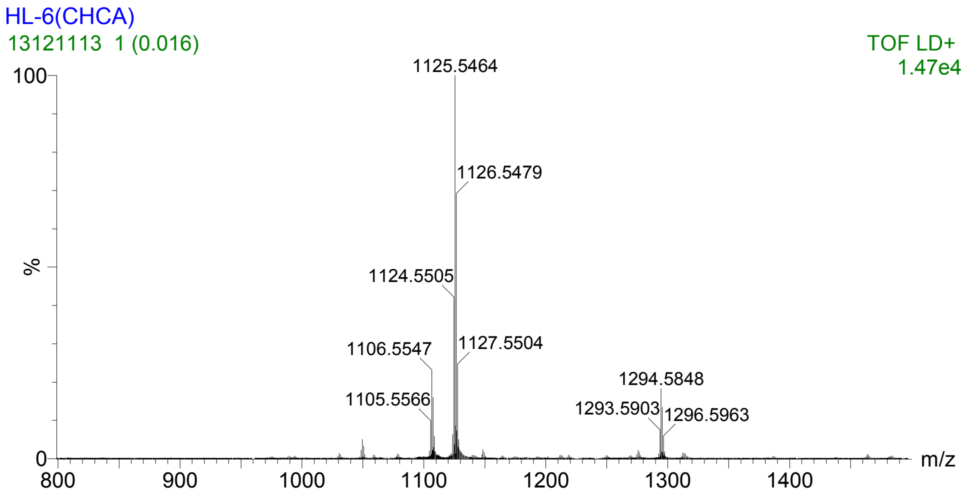

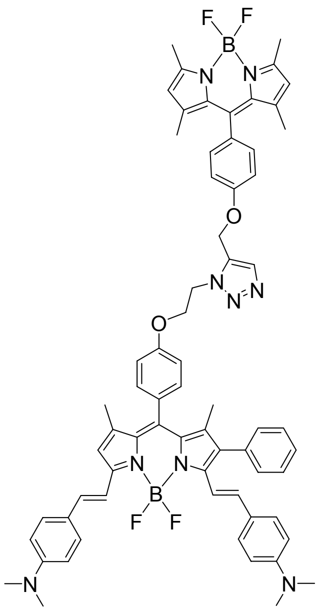

Figure 57. TOF HRMS MALDI of **B-8.**

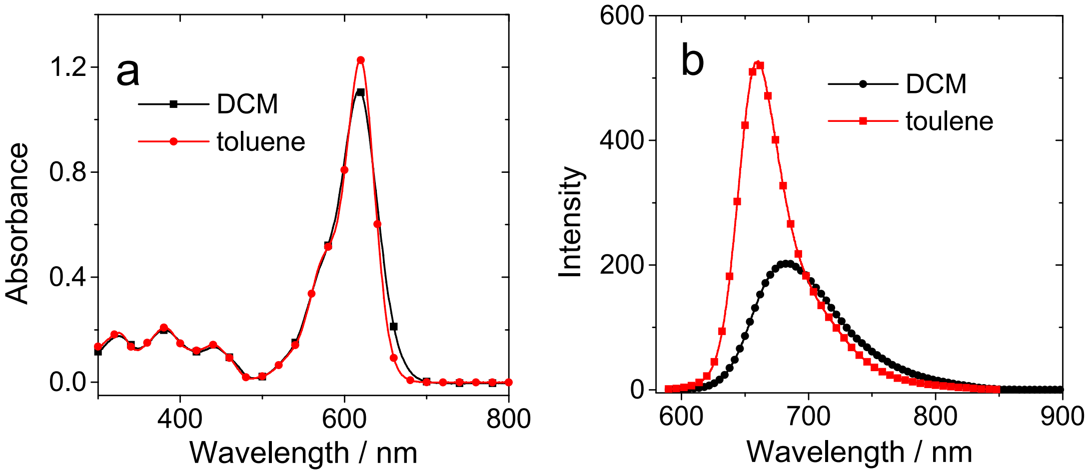

Figure S58. (a) UV-Vis absorption spectra of the **B-5** (1.0 × 10^{-5} M). (b) Fluorescence emission spectra of the **B-5**, λ_{ex} = 580 nm (A = 0.52), 20 °C.

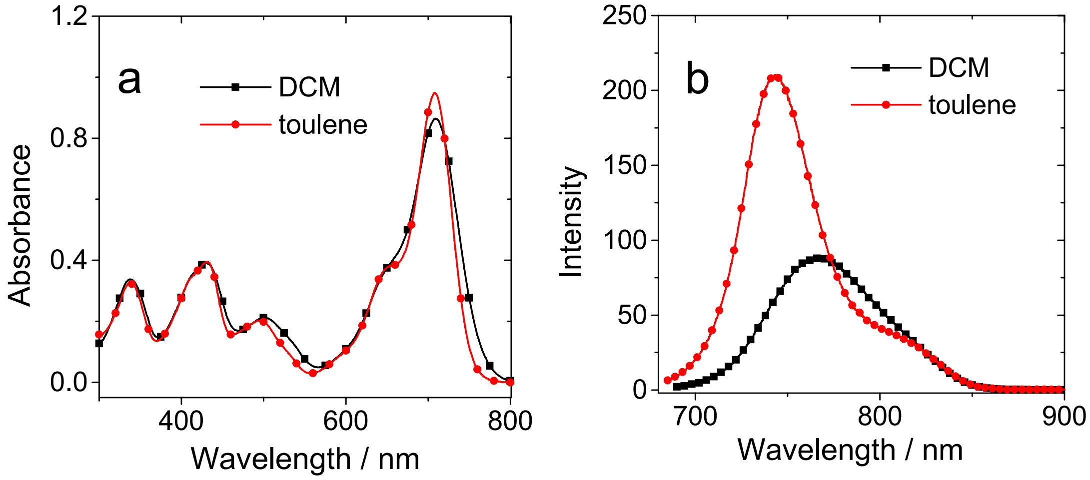

Figure S59. (a) UV-Vis absorption spectra of the **B-6**, (1.0 × 10^{-5} M; 20 °C). (b) Fluorescence emission spectra of the **B-6**, λ_{ex} = 680 nm (A=0.52), 20 °C.

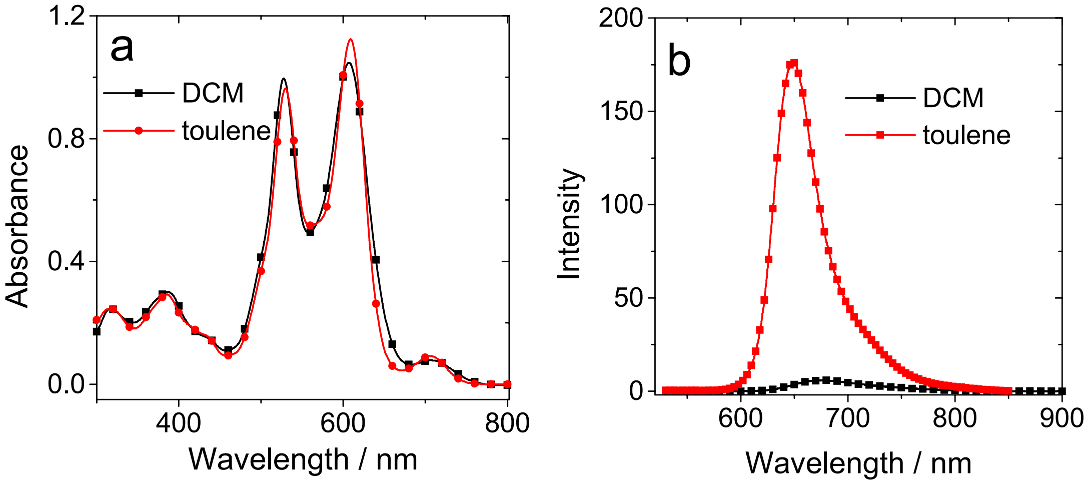

Figure S60. (a) UV-Vis absorption spectra of the **B-7′** (1.0 × 10⁻⁵ M; 20 °C). (b) Fluorescence emission spectra of the **B-7′**, λ_{ex} = 520 nm (A = 0.79), 20 °C.

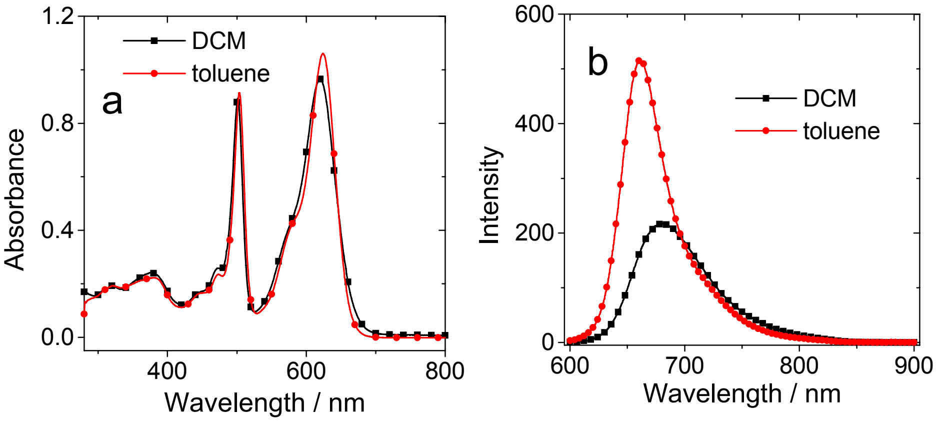

Figure S61. (a) UV-Vis absorption spectra of **B-7** (1.0 × 10⁻⁵ M; 20 °C). (b) Fluorescence emission spectra of **B-7**. λ_{ex} = 590 nm. A = 0.52, 20 °C.

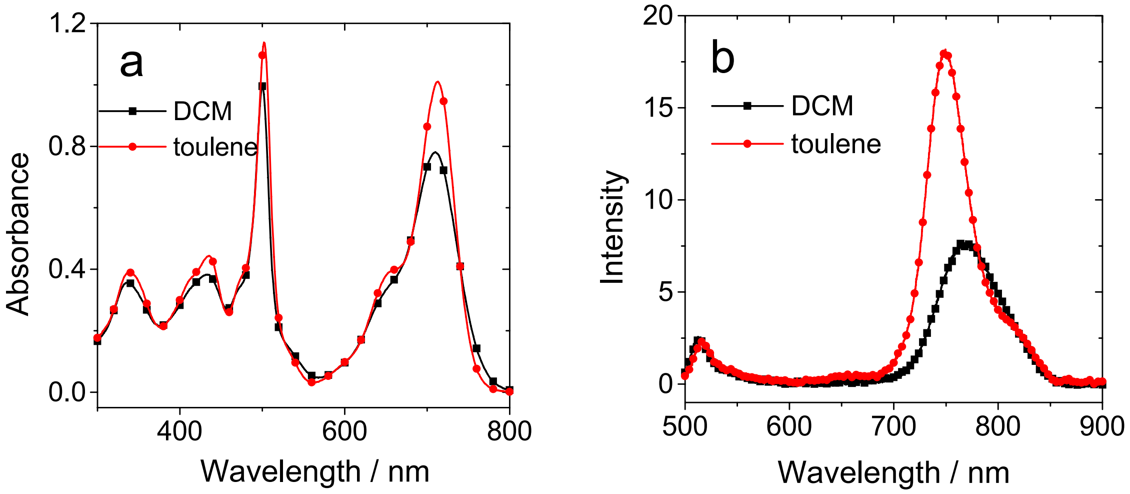

Figure S62. (a) UV/Vis absorption spectra of the **B-8**, (1.0×10^{-5} M; 20 °C). (b) Fluorescence emission spectra of the **B-8**, λ_{ex} = 486 nm (A = 0.50), 20 °C.

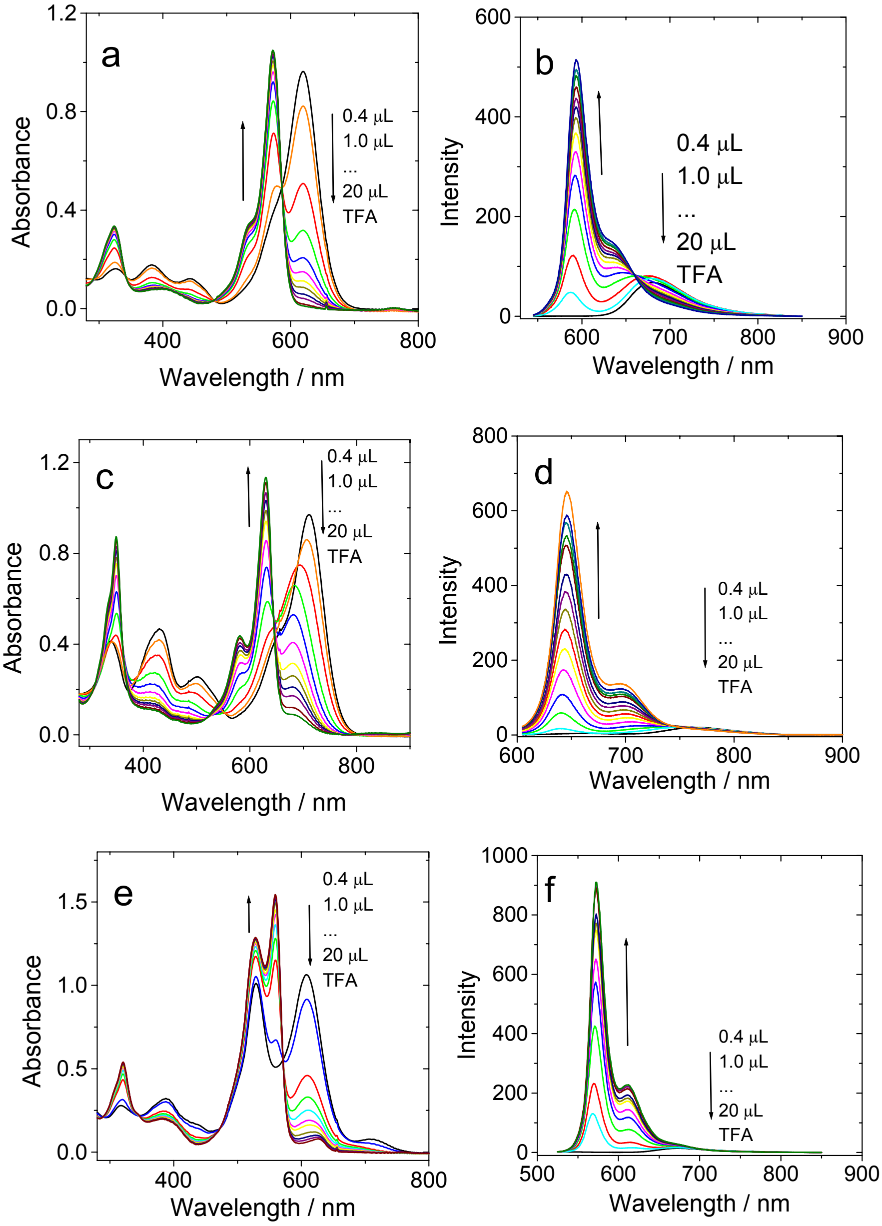

Figure S63. Variation of the UV-vis absorption spectra and the fluorescence emission spectra of **B-5**–**7′** upon protonation with TFA. (a) **B-5** with increasing TFA added and (b) the corresponding emission spectra changes of **B-1** (λ_{ex} = 540 nm) upon addition of TFA. (c) **B-6** with increasing TFA added and (d) the corresponding emission spectra changes of **B-6** (λ_{ex} = 600 nm) upon addition of TFA. (e) **B-7′** with increasing TFA added and (f) the corresponding emission spectra changes of **B-7′** (λ_{ex} = 520 nm) upon addition of TFA. The aliquots of the TFA added are 0.4 μL, 1 μL, 2 μL, 3 μL, 4 μL, 5 μL, 10 μL, 20 μL of 1 M TFA. In CH_2Cl_2 (1.0×10^{-5} M; 20 °C).

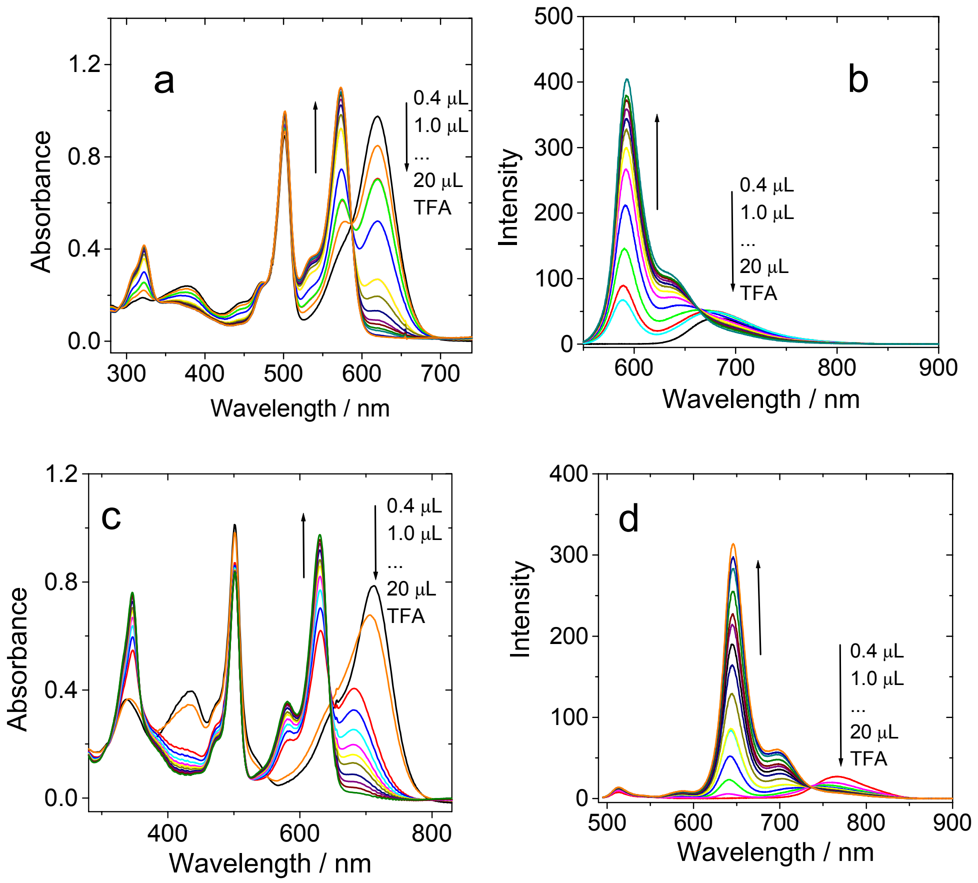

Figure S64. Variation of the UV-vis absorption spectra and the fluorescence emission spectra of **B-7–8** upon protonation with addition of TFA. (a) **B-7** with increasing TFA added and (b) the corresponding emission spectra changes of **B-7** (λ_{ex} = 540 nm) upon addition of TFA. (c) **B-8** with increasing TFA added and (d) the corresponding emission spectra changes of **B-8** (λ_{ex} = 495 nm) upon addition of TFA. The aliquot of TFA added are 0.4 μL, 1 μL, 2 μL, 3 μL, 4 μL, 5 μL, 10 μL, 20 μL of 1 M TFA. In CH_2Cl_2 (1.0×10^{-5} M; 20 °C).

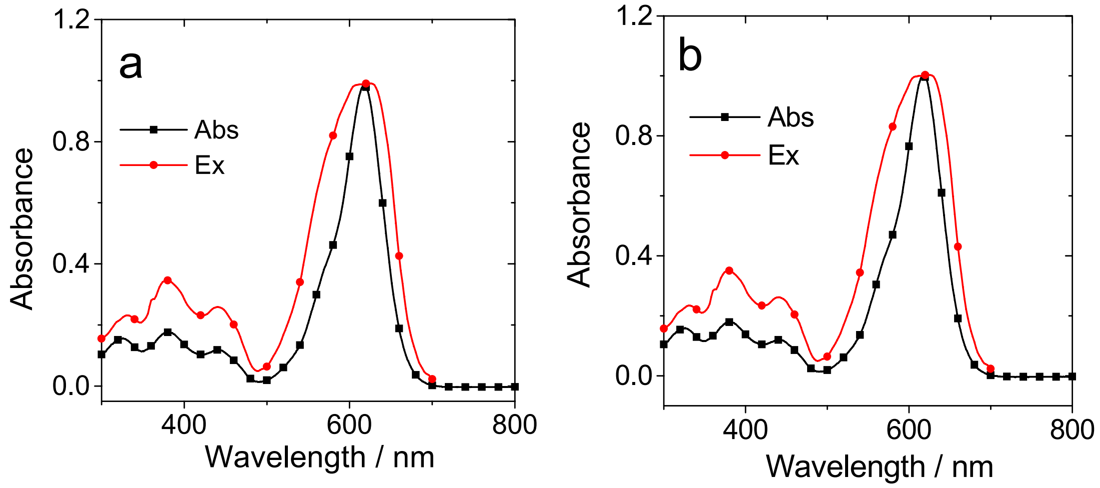

Figure S65. (a) Comparison of the fluorescence excitation (λ_{em} = 680 nm) and absorption spectra of **B-5**, in toluene. (b) Comparison of the fluorescence excitation (λ_{em} = 700 nm) and absorption spectra of **B-5**. In DCM (1.0×10^{-5} M; 20 °C).

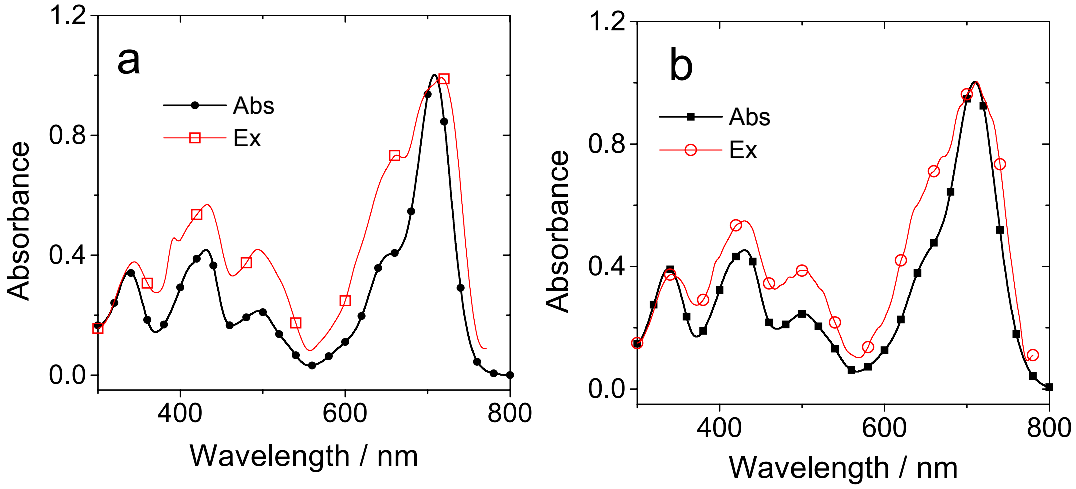

Figure S66. (a) Comparison of the fluorescence excitation (λ_{em} = 780 nm) and absorption spectra of **B-6**. In toluene. (b) Comparison of the fluorescence excitation (λ_{em} = 790 nm) and absorption spectra of **B-6**. In DCM (1.0×10^{-5} M; 20 °C).

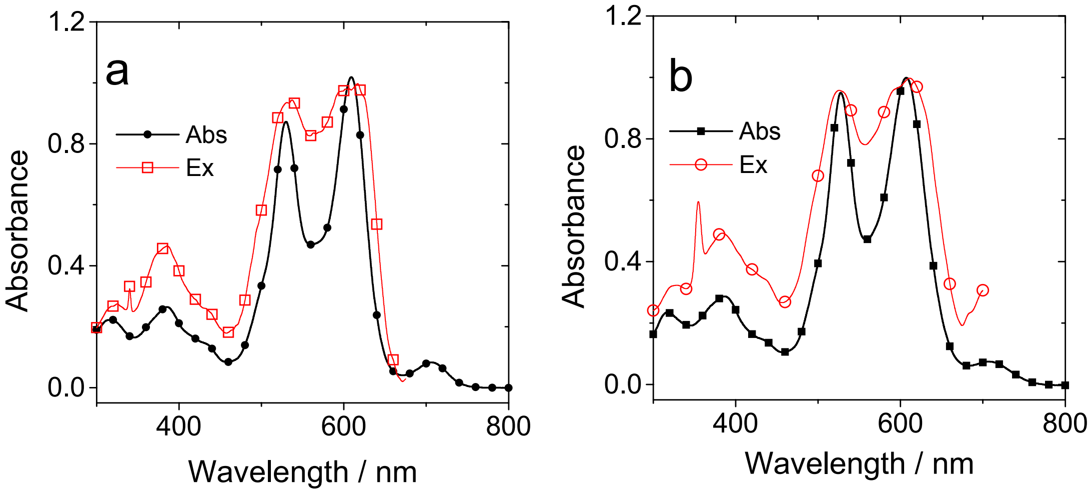

Figure S67. (a) Comparison of the fluorescence excitation (λ_{em} = 680 nm) and absorption spectra of **B-7′** in toluene. (b) Comparison of the fluorescence excitation (λ_{em} = 710 nm) and absorption spectra of **B-7′**. In DCM (1.0×10^{-5} M; 20 °C).

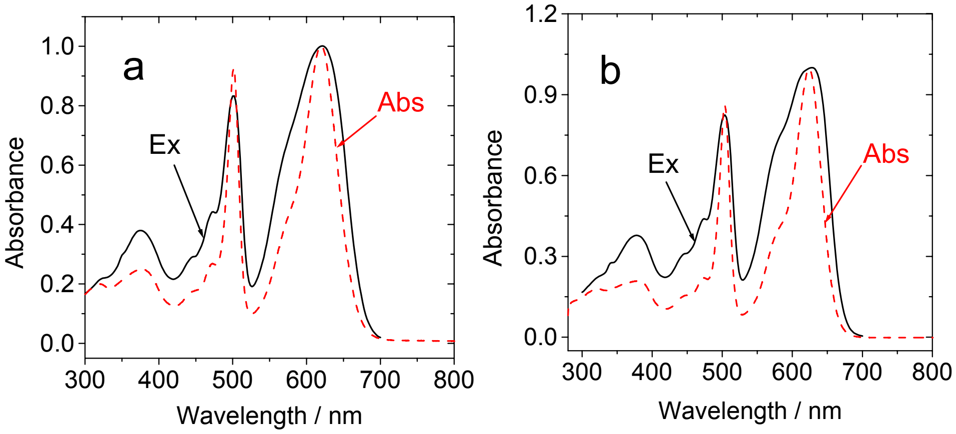

Figure S68. Comparison of the fluorescence excitation spectra (λ_{em} = 680 nm) and absorption spectra of **B-7** in different solvents. (a) In DCM. (b) In toluene ($c = 1.0 \times 10^{-5}$ M; 20 °C).

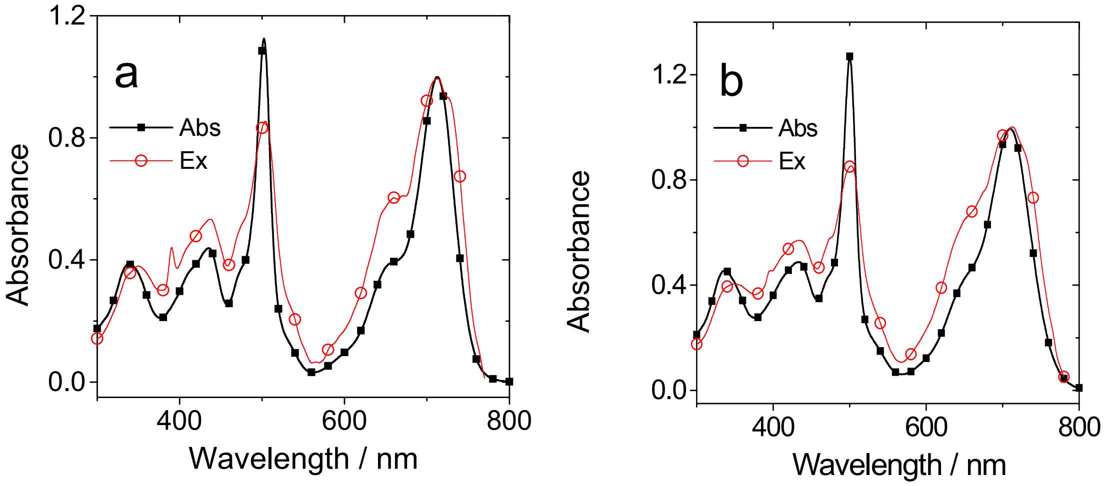

Figure S69. (a) Comparison of the fluorescence excitation spectra (λ_{em} = 780 nm) and absorption spectra of **B-8** in toluene. (b) Comparison of the fluorescence excitation (λ_{em} = 790 nm) and absorption spectra of **B-8** in DCM (1.0×10^{-5} M; 20 °C).

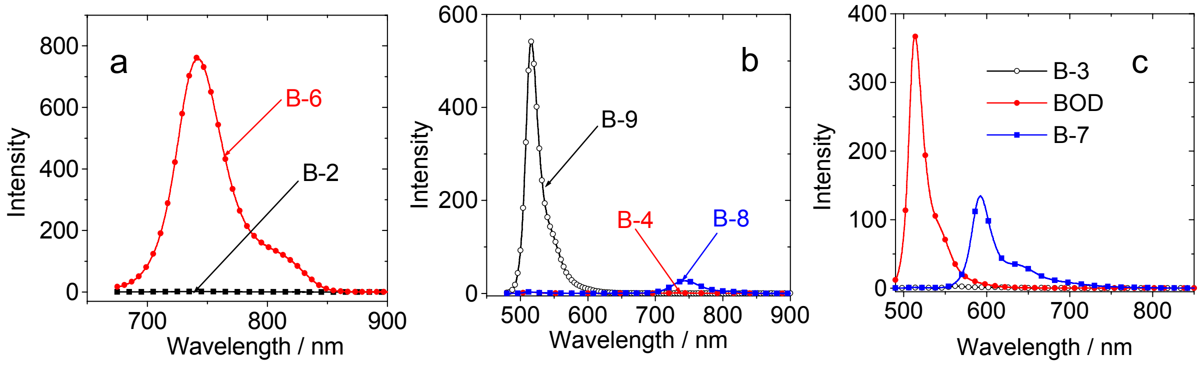

Figure S70. Fluorescence of the dyad **B-2** and triadd **B-3** and **B-4** and the reference compounds. (a) Fluorescence emission spectra of **B-2** and **B-6**. λ_{em} = 670 nm (A =0.42 for both **B-1** and **B-5**). (b) Fluorescence emission spectra of **B-4**, **B-8** and **B-9**. λ_{em} = 480 nm (A = 0.19 for all the samples). (c) Fluorescence emission spectra of **B-3**, **B-7** and **Bodipy** added TFA. λ_{em} = 480 nm (A = 0.23 for all the samples) in DCM, 20 °C.

Table S1. Photophysical parameters of **B-1—B-8** [a]

	λ_{abs} (nm)	ε / 10^5 M^{-1} cm^{-1} [b]	λ_{em} (nm)[c]	Φ_L [d]	τ_T (μs)[e]	τ_F (ns)[f]	Δ_{ST} [g]
B-1	623[h]	1.15[h]	660[h]	0.05[h]	168.6[h]	–[j]	37[h]
	622[i]	1.02[i]	674[i]		–[j]		52[i]
B-2	712[h]	1.10[h]	742[h]	0.29[h]	–[j]	–[j]	30[h]
	712[i]	0.95[i]	770[i]		–[j]		58[i]
B-3	504/627[h]	0.98/1.23[h]	659[h]	0.82[h]	333.7[h]	–[j]	155/32[h]
	504/620[i]	0.92/1.11[i]	675[i]		–[j]		171/55[i]
B-3′	533/610[h]	1.00/1.04 [h]	648[h]	2.4[h]	140.1[h]	0.55[h]	115/38[h]
	530/607[i]	0.96/0.90[i]	680[i]		100.7[i]	0.28[i]	150/83[i]
B-4	502/714[h]	1.15/1.05[h]	744[h]	1.5[h]	–[j]	2.85[h]	242/30[h]
	500/712[i]	1.15/0.99[i]	762[i]		–[j]	2.50[i]	262/50[i]
B-5	620[h]	1.23[h]	658[h]	46.5[h]	–[j]	3.61[h]	38[h]
	619[i]	1.11[i]	683[i]			3.42[i]	64[i]
B-6	708[h]	0.95[h]	743[h]	10.2[h]	–[j]	3.31[h]	35[h]
	709[i]	0.86[i]	763[i]			2.82[i]	54[i]
B-7	502/627[h]	0.91/1.06[h]	660[h]	24.2[h]	–[j]	3.02[h]	158/33[h]
	502/620[i]	0.88/0.97[i]	675[i]			3.59[i]	173/55[i]
B-7′	530/609[h]	0.96/1.12[h]	649[h]	36.9[h]	–[j]	3.48[h]	119/40[h]
	528/607[i]	1.00/1.05[i]	675[i]			0.53[i]	147/68[i]
B-8	502/714[h]	1.14/1.01[h]	748[h]	10.3[h]	–[j]	3.30[h]	246/34[h]
	502/714[i]	1.14/0.97[i]	768[i]			2.72[i]	266/54[i]

[a] Recorded at $c = 1.0 \times 10^{-5}$ M. 20 °C. [b] Molar extinction coefficient at the absorption maxima ε: 10^5 M^{-1} cm^{-1}. [c] The emission maxima. [d] Fluorescence quantum yields determined with **B-12** (Φ_F = 9.5%, in toluene) as standard. [e] Triplet excited state lifetime. [f] Fluorescence lifetime. [g] Stokes shift. [h] In toluene. [i] in 1,2-dichloromethane. [j] Not observed.

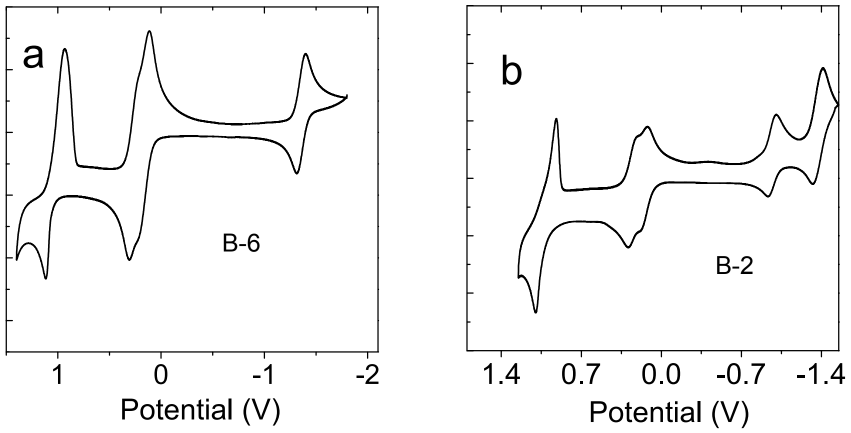

Figure S71. Cyclic voltammogram of **B-2** and **B-6**. (a) **B-6**, (b) **B-2**. In deaerated CH_2Cl_2 solutions and 0.10 M Bu_4NPF_6 as supporting electrode, Ag/$AgNO_3$ reference electrode, Scan rates: 0.1 V/s. Due to the overlap of the oxidation potential, no ferrocene was added as internal standard.

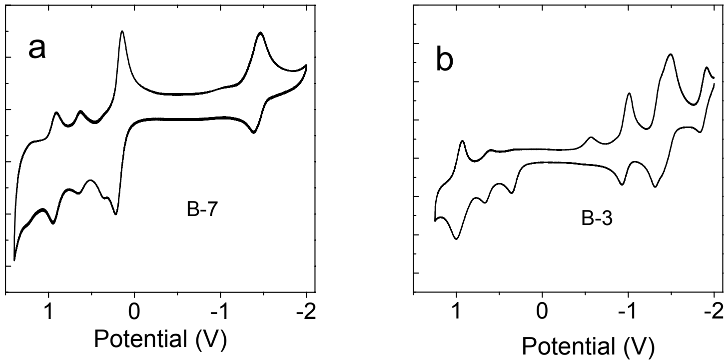

Figure S72. Cyclic voltammogram of **B-3′** and **B-7′**. (a) **B-7′**, (b) **B-3′**. In deaerated CH_2Cl_2 solutions and 0.10 M Bu_4NPF_6 as supporting electrode, Ag/$AgNO_3$ reference electrode, Scan rates: 0.1 V/s.

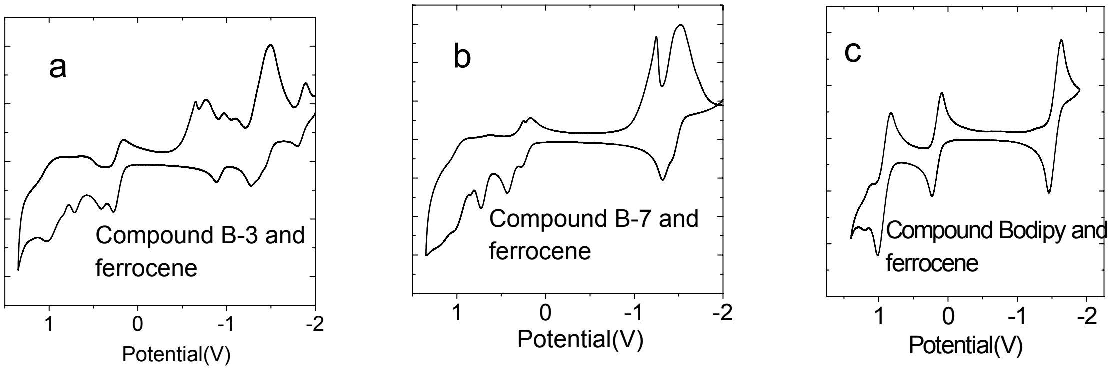

Figure S73. Cyclic voltammogram of **B-3, B-7** and **Bodipy**, respectively. (a) **B-3**, (b) **B-7,** (c) **Bodipy**. Ferrocene (Fc) was used as internal reference ($E_{1/2}$ = +0.64 V (Fc+/Fc) vs. standard hydrogen electrode). In deaerated CH_2Cl_2 with the ferrocene, 0.10 M Bu_4NPF_6 as supporting electrode, Ag/$AgNO_3$ reference electrode, Scan rates: 0.1 V/s. *c* [photosensitizers] = 5.0×10^{-4} M, 20 °C.

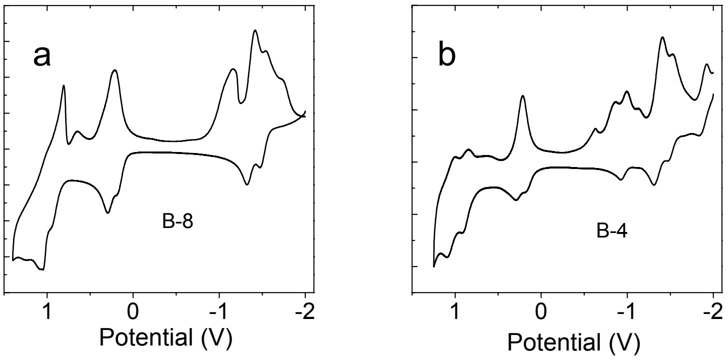

Figure S74. Cyclic voltammogram of **B-4** and **B-8**, respectively. (a) **B-8**, (b) **B-4**. In deaerated CH_2Cl_2 solutions and 0.10 M Bu_4NPF_6 as supporting electrode, Ag/$AgNO_3$ reference electrode, Scan rates: 0.1 V/s.

The free energy changes of the electron transfer process (charge separation, CS), can be calculated with the Weller equation (eq. 1 and).[7]

$$\Delta G^{0}{}_{\mathrm{CS}} = e[E_{OX} - E_{RED}] - E_{00} + \Delta G_{\mathrm{S}}$$

(Eq. 1)

$$\Delta G_{\mathrm{S}} = -\frac{e^2}{4\pi\varepsilon_{\mathrm{S}}\varepsilon_0 R_{\mathrm{CC}}} - \frac{e^2}{8\pi\varepsilon_0}\left(\frac{1}{R_D} + \frac{1}{R_{\mathrm{A}}}\right)\left(\frac{1}{\varepsilon_{REF}} - \frac{1}{\varepsilon_S}\right)$$

(Eq. 2)

Where ΔG_{S} is the static Coulombic energy, which is described by eq. 2. e = electronic charge, E_{OX} = half-wave potential for one-electron oxidation of the electron-donor unit, E_{RED} = half-wave potential for one-electron reduction of the electron-acceptor unit; note herein the anodic and cathodic peak potentials were used because in some cases the oxidation is irreversible therefore the formal potential $E_{1/2}$ cannot be derived; E_{00} = energy level approximated with the fluorescence emission wavelength (for the singlet excited state), ε_{S} = static dielectric constant of the solvent, R_{CC} = (9.0 Å) center-to-center separation distance determined by DFT optimization of the geometry, R_{D} (4.0 Å) is the radius of the BODIPY-based donor, R_{A} (5.0 Å) is the radius of the C_{60}-electron acceptor, $\varepsilon_{\mathrm{REF}}$ is the static dielectric constant of the solvent used for the electrochemical studies, ε_0 permittivity of free space. The solvents used in the calculation of free energy of the electron transfer is CH_2Cl_2 (ε = 8.9) Based on these parameters, E_{ox} is the first peak in the anodic scan, and E_{red} is the first peak in the cathodic scan, and $E_{0,0}$ is the singlet excited state energy level.

In CH_2Cl_2 : **B-1**– **B-2** and **B-4**, **B-5** – **B-6** and **B-8** ΔG_{s} = –0.18 eV, But due to donor and acceptor has long distance for **B-3** and **B-7** R_{CC} = (26.0 Å), ΔG_{s} = -0.062 eV.
In toluene: **B-1**– **B-2** and **B-4**, **B-5**– **B-6** and **B-8** ΔG_{s} = +0.32 eV, But due to donor and acceptor has long distance for **B-3** and **B-7** R_{CC} = (26.0 Å), ΔG_{s} = +0.76 eV.

In CH_2Cl_2

ΔG^o_{CS} (B-1) = e[+0.35 – (-0.97)] – 1.88 + (-0.18) = –0.74 eV

ΔG^o_{CS} (B-2) = e[+0.14 – (-0.97)] – 1.67 + (-0.18) = –0.74 eV

ΔG^o_{CS} (B-3) = e[+0.42 – (-0.96)] – 1.88 + (-0.18) = –0.68 eV

ΔG^o_{CS} (B-3′) = e[+0.36 – (–0.96)] – 1.91 + (-0.062) = –0.65 eV

ΔG^o_{CS} (B-4) = e[+0.15 – (–0.92)] – 1.66 + (-0.18) = –0.77 eV

ΔG^o_{CS} (B-7) = e[+0.35 – (-1.32)] – 1.88 + (-0.18) = –0.39 eV

ΔG^o_{CS} (B-7′) = e[+0.37 – (–1.42)] –1.91 + (-0.062) = –0.18 eV

ΔG^o_{CS} (B-8) = e[+0.17 – (–1.32)] –1.65 + (-0.18) = –0.34 eV

In toluene

ΔG^o_{CS} (B-1) = e[+0.35 – (-0.97)] – 1.88 + 0.32= –0.24 eV

ΔG^o_{CS} (B-2) = e[+0.14 – (-0.97)] – 1.67 + 0.32= –0.24 eV

ΔG^o_{CS} (B-3) = e[+0.42 – (-0.96)] – 1.88 + 0.32= –0.18 eV

$\Delta G^o{}_{\mathrm{CS}}$ (B-3′) = e[+0.36 – (−0.96)] – 1.91 + 0.76 = +0.17 eV

$\Delta G^o{}_{\mathrm{CS}}$ (B-4) = e[+0.15 – (−0.92)] – 1.66 + 0.32 = −0.27 eV

$\Delta G^o{}_{\mathrm{CS}}$ (B-7) = e[+0.35 – (−1.32)] −1.88 + 0.32 = + 0.11 eV

$\Delta G^o{}_{\mathrm{CS}}$ (B-7′) = e[+0.37 – (−1.42)] −1.91 + 0.76 = + 0.64 eV

$\Delta G^o{}_{\mathrm{CS}}$ (B-8) = e[+0.17 – (−1.32)] −1.65 + 0.32 = + 0.16 eV

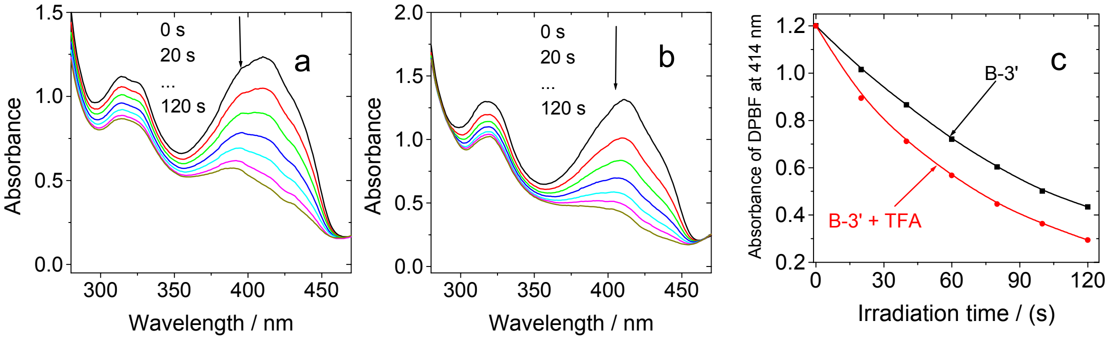

Figure S75. Switching of the singlet oxygen ($^1O_2$) photosensitizing ability of the compounds in the absence and in the presence of TFA. The decreasing of the absorption of $^1O_2$ scavenger 1,3-diphenylisobenzofuran (DPBF) at 414 nm was monitored upon the monochromic light irradiation. UV–Vis absorption spectral changes for the singlet oxygen was captured by DPBF, **B-3′** as photosensitizer (a) in the absence of acid, (b) in the presence of acid. (c) Comparative the absorbance of DPBF in 414 nm for DPBF (λ_{ex} = 515 nm). c [photosensitizers] = 1.0 × 10^{-5} M in CH_2Cl_2; 20 °C.

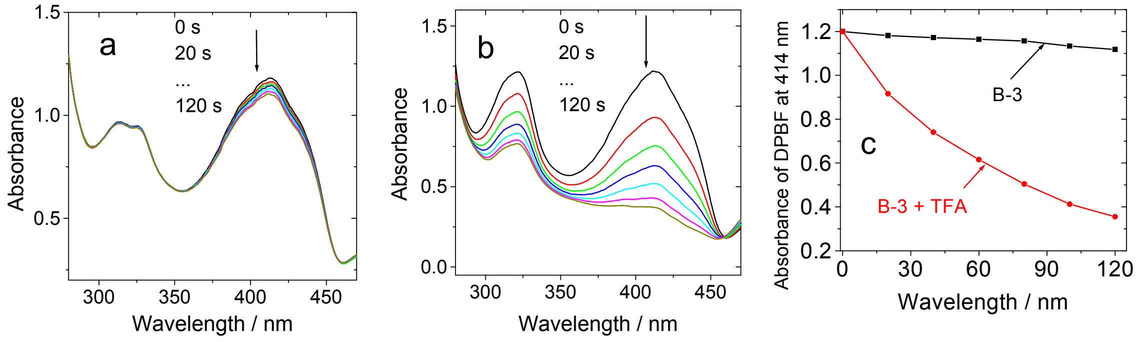

Figure S76. Switching of the singlet oxygen ($^1O_2$) photosensitizing ability of the compounds in the absence and the presence of TFA. The decreasing of the absorption of $^1O_2$ scavenger 1,3-diphenylisobenzofuran (DPBF) at 414 nm was monitored upon the monochromic light irradiation. UV/Vis absorption spectral changes **B-3** as photosensitizer. (a) In the absence of TFA acid and (b) in the presence of TFA; (c) absorbance of DPBF at 414 nm (in mixture with **B-3**) changes in the absence and in the presence of TFA (λ_{ex} =497 nm). *c* [photosensitizers] = 1.0 × 10^{-5} M in CH_2Cl_2; 20 °C.

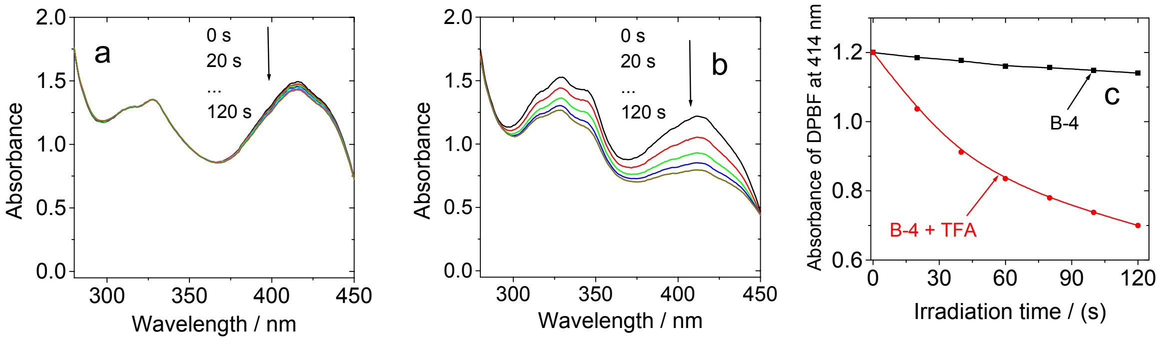

Figure S77. Switching of the singlet oxygen ($^1O_2$) photosensitizing ability of the compounds in the absence and the presence of TFA. The decreasing of the absorption of $^1O_2$ scavenger 1,3-diphenylisobenzofuran (DPBF) was monitored upon the monochromic light irradiation. (a) and (b) UV/Vis absorption spectral changes, with the singlet oxygen captured by DPBF, **B-4** as photosensitizer, (a) in the absence of acid, (b) in the presence of acid, (c) Comparative the absorbance of DPBF in 414 nm for DPBF (λ_{ex} =495 nm). *c* [photosensitizers] = 1.0 × 10^{-5} M in CH_2Cl_2; 20 °C.

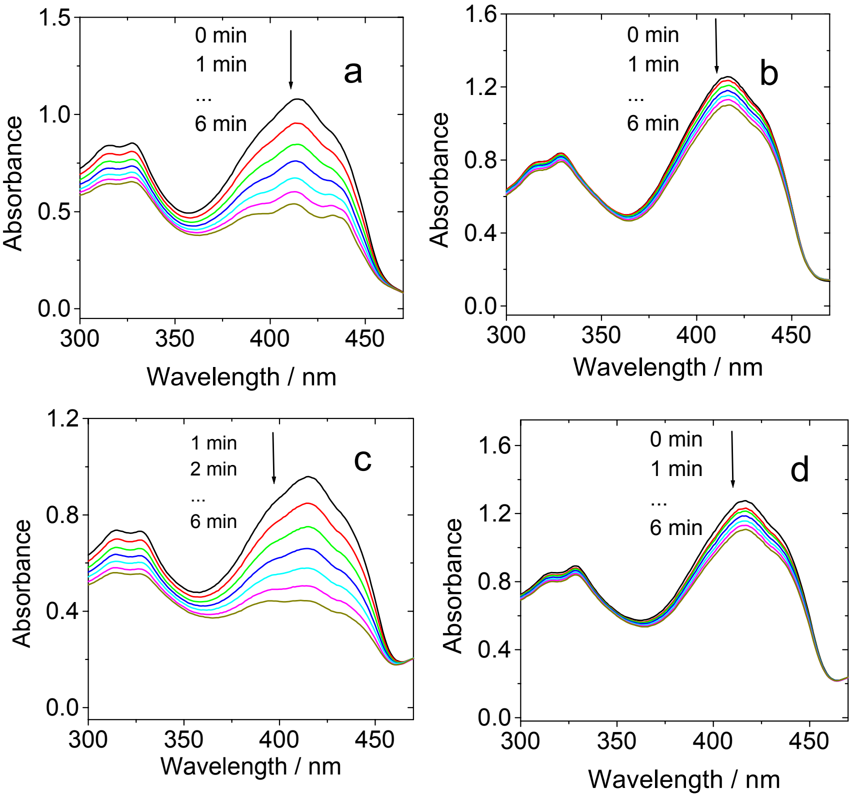

Figure S78. The decreasing of the absorption of $^1O_2$ scavenger 1,3-diphenylisobenzofuran (DPBF) at 414 nm was monitored upon the monochromic light irradiation. UV/Vis absorption spectral changes **B-1**–**B-4** as photosensitizer in toluene. (a) **B-1**, (b) **B-2**, (c) **B-3**, (d) **B-4**. λ_{ex} =654 nm, A = 0.29. 20 °C.

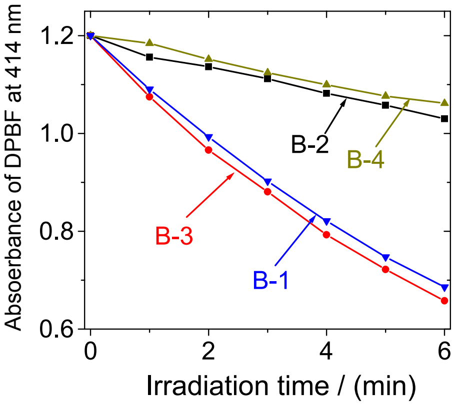

Figure S79. Comparison of the ability of photosensitizing of singlet oxygen ($^1O_2$) in toluene. **B-1**–**B-4**, λ_{ex} =654 nm, A = 0.29. 20 °C.

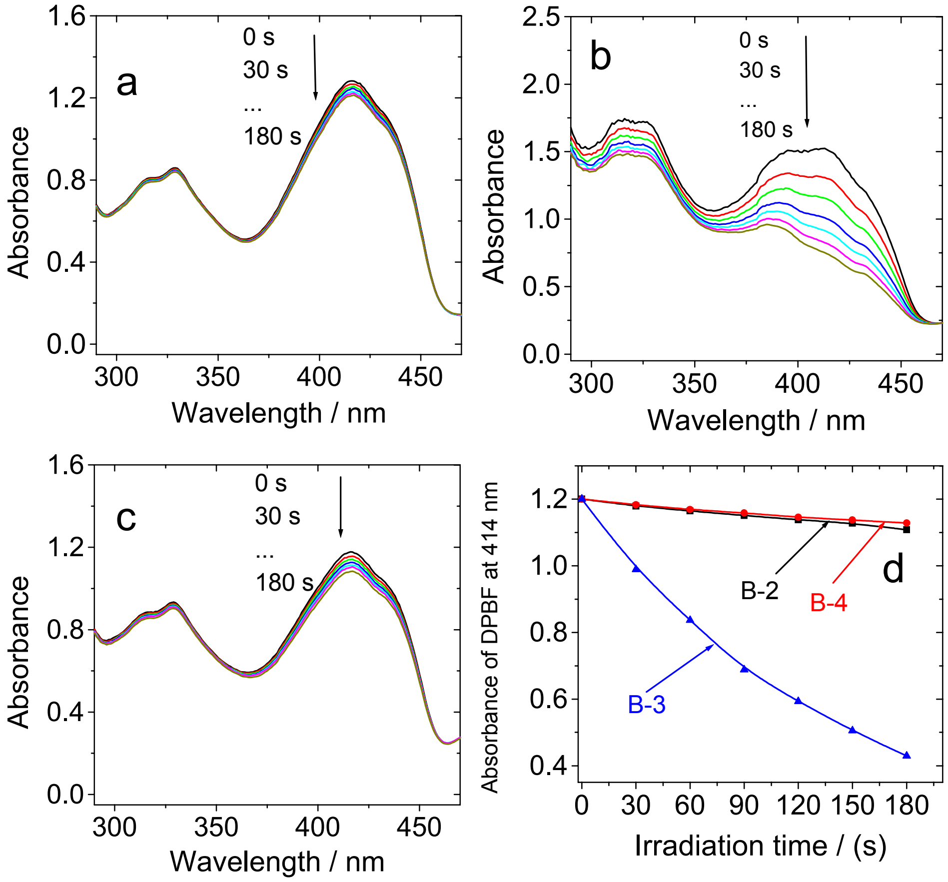

Figure S80. UV-Vis absorption spectral changes for the mixtures of **B-2, B-3′, B-4** photosensitizers with the singlet oxygen ($^1O_2$) scavenger DPBF upon photoexcitation. (a) **B-2** as photosensitizer, (b) **B-3′** as photosensitizer, (c) **B-4** as photosensitizer, (d) Comparison of the absorbance of DPBF at 414 nm in the presence of different photosensitizers upon photoexcitation. λ_{ex} = 648 nm, A = 0.30. c [photosensitizers] = 1.0×10^{-5} M in toluene; 20 °C.

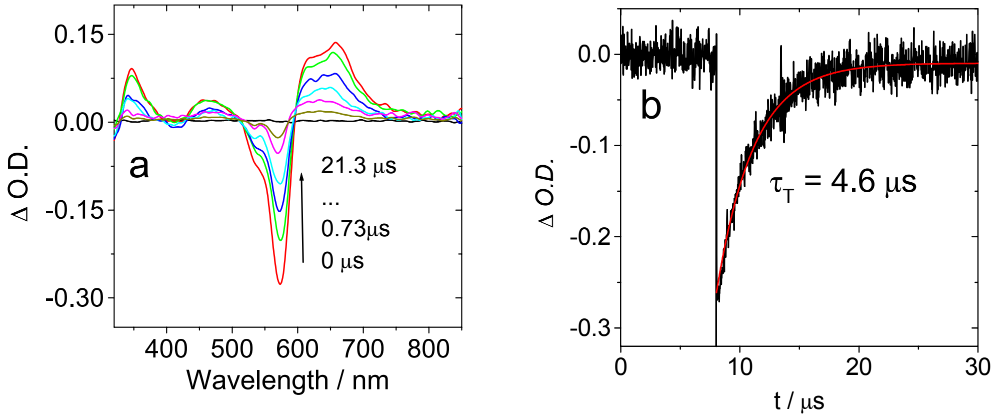

Figure S81. Nanosecond time–resolved transient difference absorption spectra of **B-12**. (a) Transient absorption difference spectra and (b) decay trace at 580 nm. 20 μL of 1 M TFA was added. λ_{ex} = 532 nm, $c = 1.0 \times 10^{-5}$ M in DCM; 20 °C.

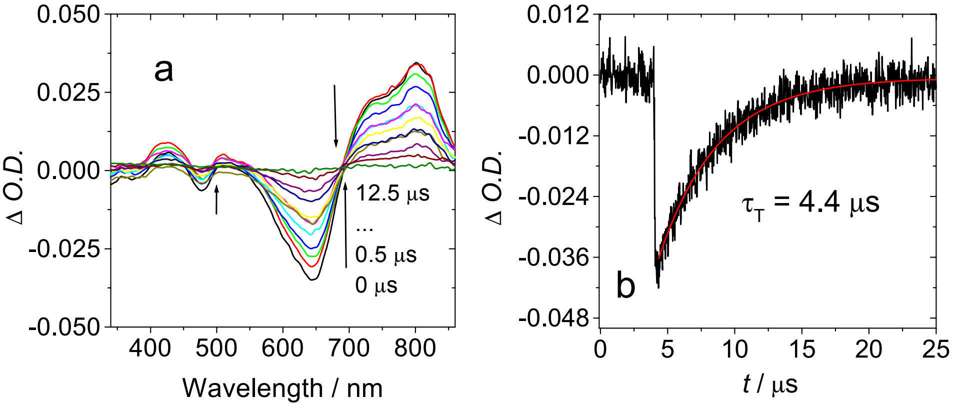

Figure S82. Nanosecond time–resolved transient difference absorption spectra of **B-12**. (a) Transient difference absorption spectra and (b) decay trace at 620 nm. λ_{ex} = 532 nm, $c = 1.0 \times 10^{-5}$ M in deaerated toluene. 20 °C.

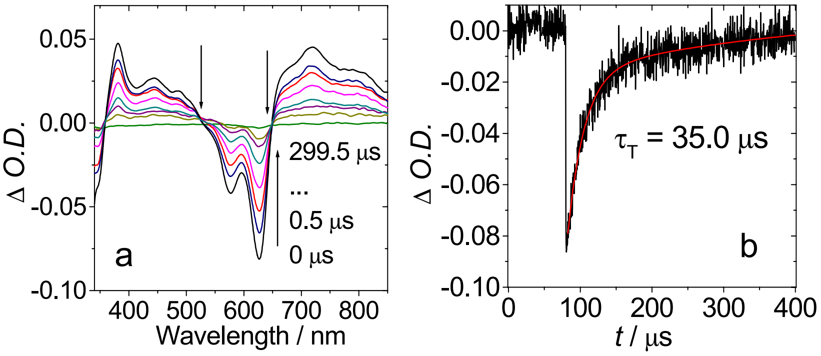

Figure S83. Nanosecond time-resolved transient difference absorption spectra of **B-4**. (a) Transient difference absorption spectra and (b) the decay trace at 630 nm. In deaerated DCM with 20 μL of 1 M TFA added. λ_{ex} = 532 nm (c = 1.0×10^{-5} M, 20 °C).

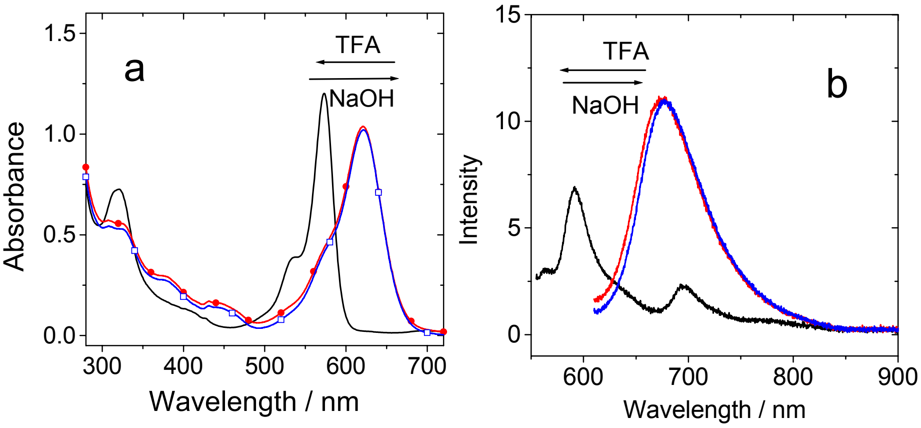

Figure S84. Switching of the UV-Vis absorption and emission spectra of **B-1** with acid/base. (a) UV–Vis absorption spectral of **B-1**, without acid (TFA), and with acid (TFA) added and with base (NaOH) added to neutralize the acid. (b) The fluorescence emission spectra **B-1**, includes the spectrum measured without acid, λ_{ex} = 600 nm; with acid (TFA) added, λ_{ex} =545 nm; and with base added to neutralize acid, λ_{ex} = 600 nm. c = 1.0 × 10^{-5} M; 20 °C.

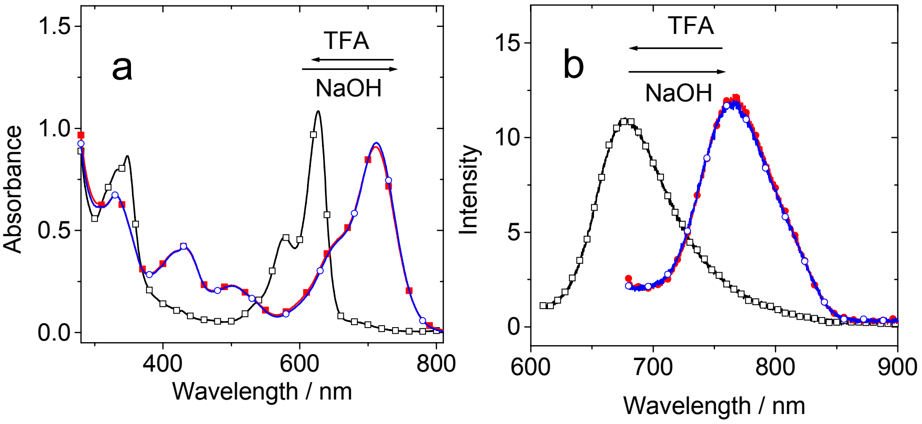

Figure S85. Switching of the UV-Vis absorption and emission of **B-2** with acid/base. (a) UV/Vis absorption spectral of **B-2**, without acid and with added acid, and with base added to neutralize the acid. (b) The fluorescence emission spectra **B-2**, include the spectrum measured in the absence of acid, λ_{ex} = 670 nm; with acid (TFA) added, λ_{ex} =600 nm and with base (NaOH) added to neutralize the acid, λ_{ex} = 670 nm. $c = 1.0 \times 10^{-5}$ M; 20 °C.

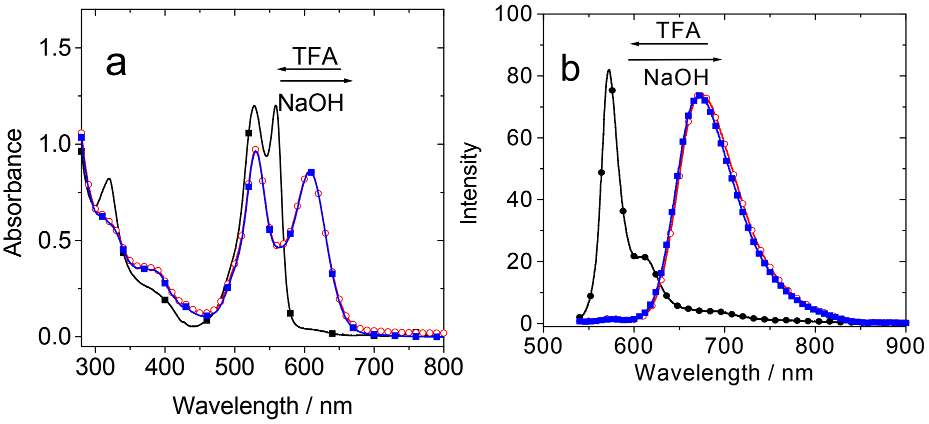

Figure S86. Switching of the UV-Vis absorption and emission of **B-3’** with acid/base. (a) UV/Vis absorption spectral of **B-3′**, without acid and with acid (TFA) added, and with based (NaOH) added to neutralize the acid. (b) The fluorescence emission spectra **B-3′**, included the spectra measured without acid, λ_{ex} = 530 nm; with acid (TFA) added, λ_{ex} =530 nm and with based (NaOH) added to neutralize the acid, λ_{ex} = 530 nm. $c = 1.0 \times 10^{-5}$ M; 20 °C.

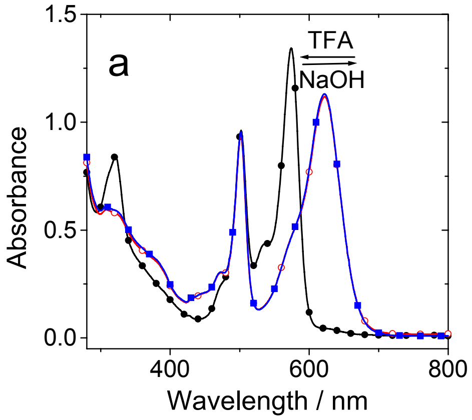

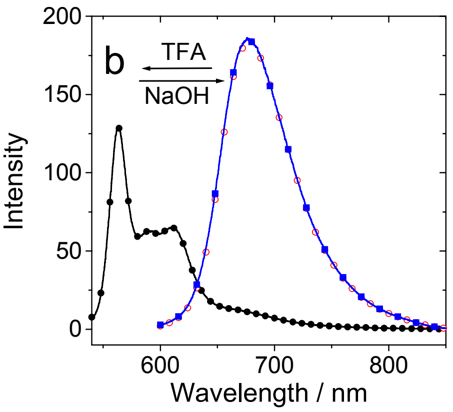

Figure S87. Switching of the UV-Vis absorption and emission of **B-3** with acid/base. (a) UV/Vis absorption spectral **B-3;** (b) The fluorescence emission spectra **B-3**, without acid, λ_{ex} = 600 nm, and with acid added, λ_{ex} =540 nm, and with base added to neutralize the acid, *c* [photosensitizers] = 1.0 × 10^{-5} M in CH_2Cl_2; 20 °C

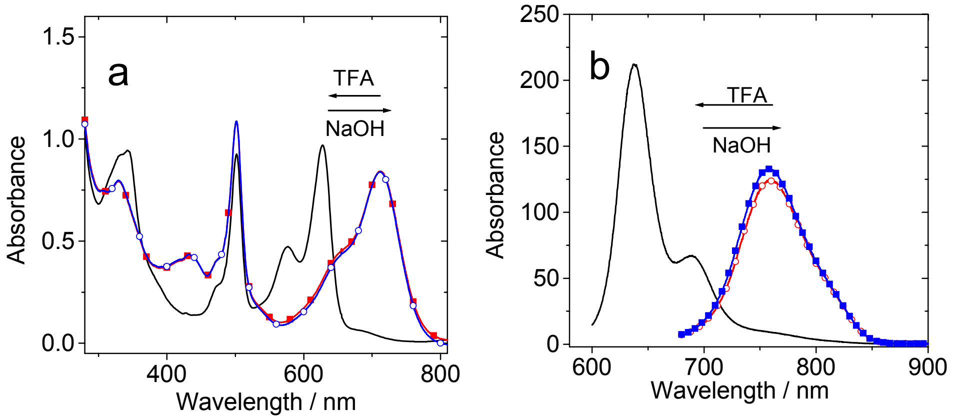

Figure S88. Switching of the UV-Vis absorption and emission of **B-4** with acid/base. (a) UV/Vis absorption spectral of **B-4**, included the spectra measured without acid, with acid (TFA) added and with base (NaOH) added to neutralize acid. (b) The fluorescence emission spectra **B-4**, included the spectra measured without acid, λ_{ex} = 670 nm, with acid added, λ_{ex} =600 nm, and with base (NaOH) added to neutralize the acid, λ_{ex} = 670 nm. (1.0 × 10^{-5} M; 20 °C).

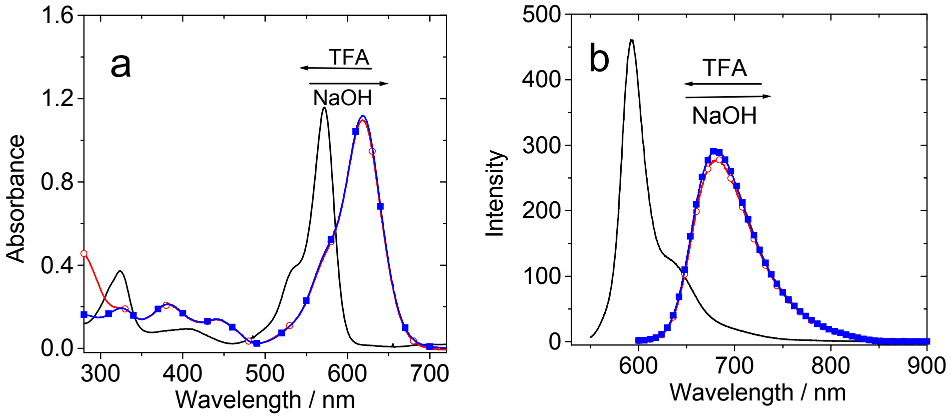

Figure S89. Switching of the UV-Vis absorption and emission of **B-5** with acid/base. (a) UV/Vis absorption spectral of **B-5**, included the spectra measured without acid, with acid (TFA) added and with based (NaOH) added to neutralize the acid. (b) The fluorescence emission spectra **B-5**, included the spectra measured without acid, λ_{ex} = 590 nm; with acid (TFA) added, λ_{ex} = 535 nm and with base (NAOH) added to neutralize the acid, λ_{ex} = 590 nm. $c = 1.0 \times 10^{-5}$ M; 20 °C.

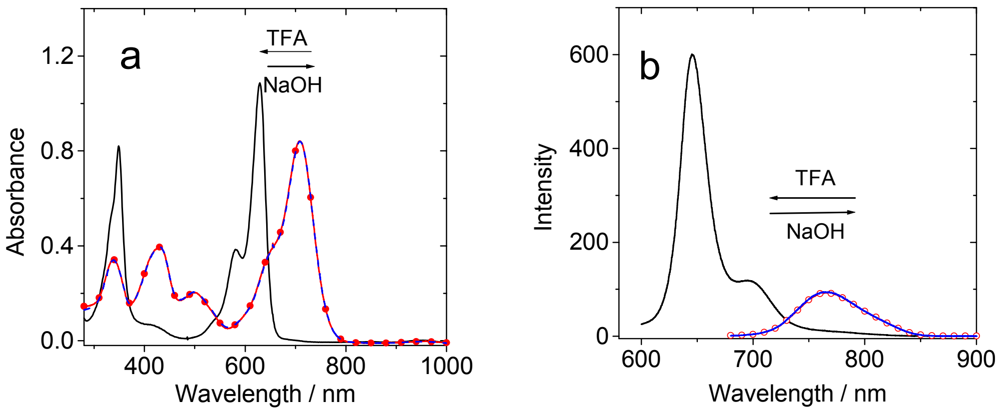

Figure S90. Switching of the UV-Vis absorption and emission of **B-6** with acid/base. (a) UV/Vis absorption spectral of **B-6**, included the spectra measured without acid, with acid added, and with base added to neutralize the acid. (b) The fluorescence emission spectra **B-6**, included the spectra measured without acid, λ_{ex} = 670 nm, with acid added, λ_{ex} =590 nm and with based added to neutralize the acid, λ_{ex} = 670 nm. $c = 1.0 \times 10^{-5}$ M; 20 °C.

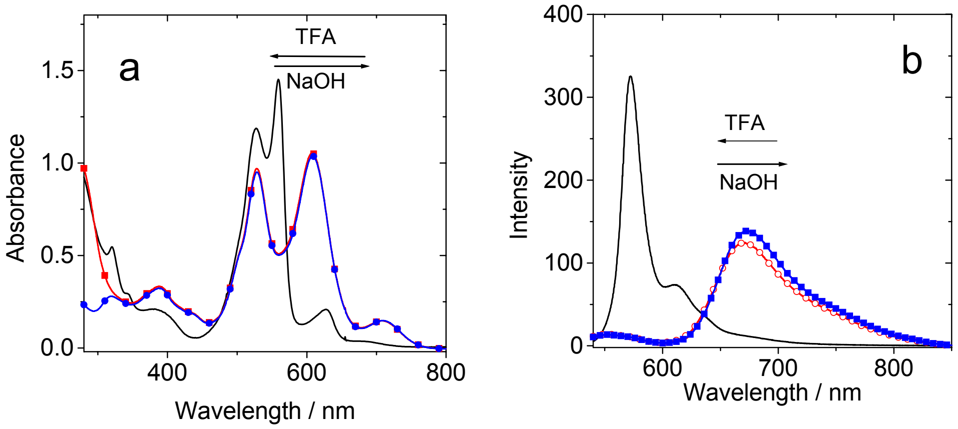

Figure S91. Switching of the UV-Vis absorption and emission of **B-7'** with acid/base. (a) UV/Vis absorption spectral of **B-7′**, include the spectra measured in the absence of acid, and with acid (TFA) added, with with base (NaOH) added to neutralize the acid. (b) The fluorescence emission spectra **B-7′**, include the spectrum determined without acid, λ_{ex} = 530 nm, with acid (TFA) added, λ_{ex} =530 nm and with base (NaOH) added to neutralize acid, λ_{ex} = 530 nm. $c = 1.0 \times 10^{-5}$ M; 20 °C.

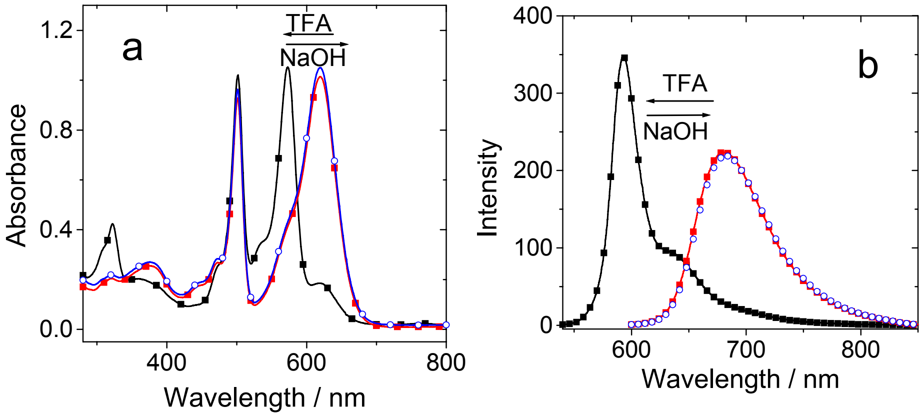

Figure S92. Switching of the UV-Vis absorption and emission of **B-7** with acid/base. (a) UV/Vis absorption spectral **B-7**, (b) The fluorescence emission spectra of **B-7**. Both figures include spectra measured without acid, λ_{ex} = 600 nm; with acid (TFA) added, λ_{ex} =540 nm and with base (NaOH) added to neutralize the acid. c [photosensitizers] = 1.0×10^{-5} M in CH_2Cl_2; 20 °C.

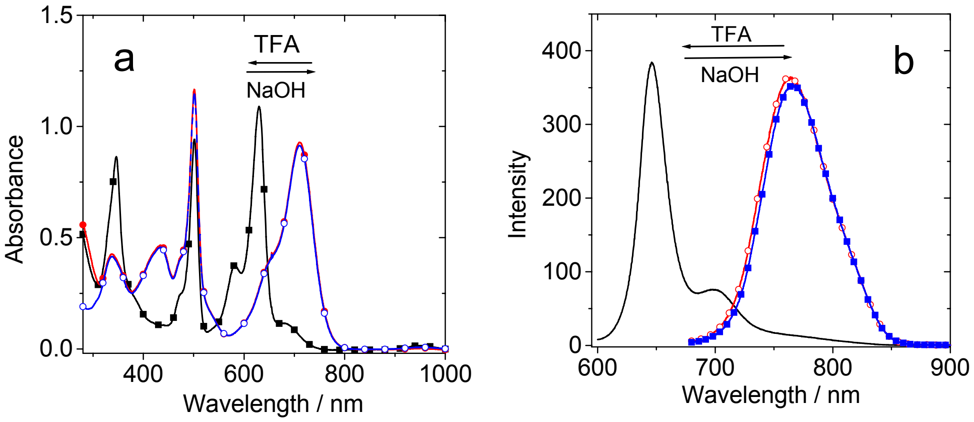

Figure S93. Switching of the UV-Vis absorption and emission of **B-8** with acid/base. (a) UV/Vis absorption spectral of **B-8**, include the spectra measured without acid, with acid (TFA) added acid and with base (NaOH) added to neutralize the acid. (b) The fluorescence emission spectra of **B-8**, include the spectrum measured without acid, λ_{ex} = 670 nm; the spectrum measured with acid (TFA) added, λ_{ex} =590 nm; and with base (NaOH) added to neutralize the acid, λ_{ex} = 670 nm. $c = 1.0 \times 10^{-5}$ M; 20 °C.

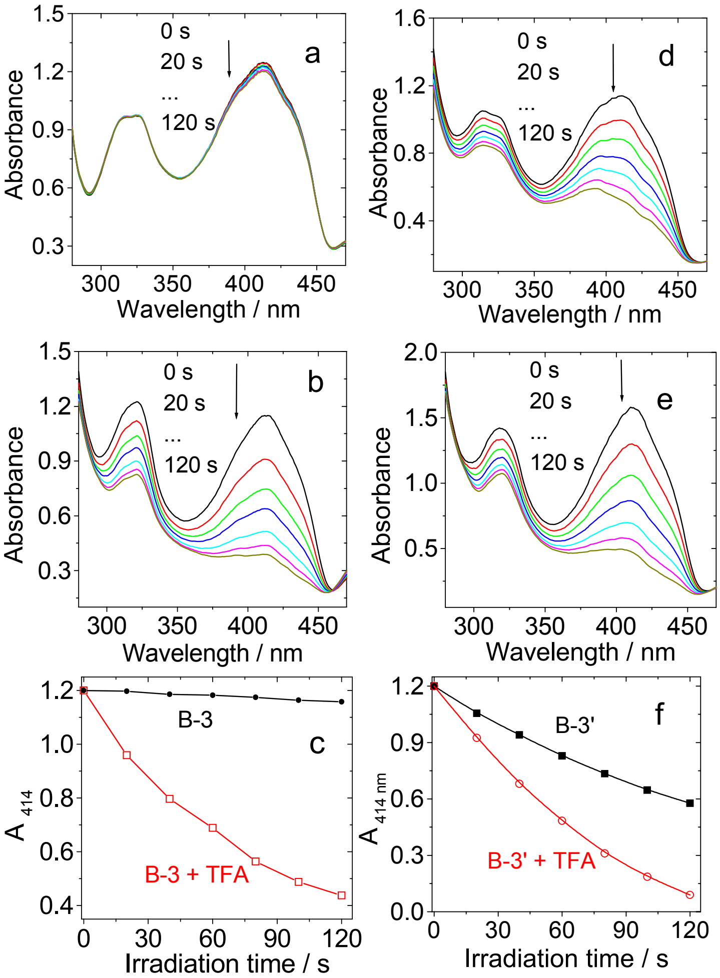

Figure S94. Switching of the singlet oxygen ($^1O_2$) photosensitizing ability of the compounds in the absence and in the presence of TFA. The decreasing of the absorption of $^1O_2$ scavenger 1,3-diphenylisobenzofuran (DPBF) at 414 nm was monitored upon the monochromic light irradiation. UV/vis absorption spectral changes **B-3** as photosensitizer. (a) In the absence of TFA acid and (b) in the presence of TFA . (c) Absorbance changes of DPBF at 414 nm in the absence and in the presence of TFA (λ_{ex} = 588 nm). UV/vis absorption spectral changes with **B-3′** as photosensitizer (d) in the absence of TFA and (e) in the presence of acid, (f) in the absorbance of DPBF at 414 nm changes in the absence and in the presence of TFA (λ_{ex} =571 nm). *c* [photosensitizers] = 1.0 × 10^{-5} M in CH_2Cl_2, 20 °C.

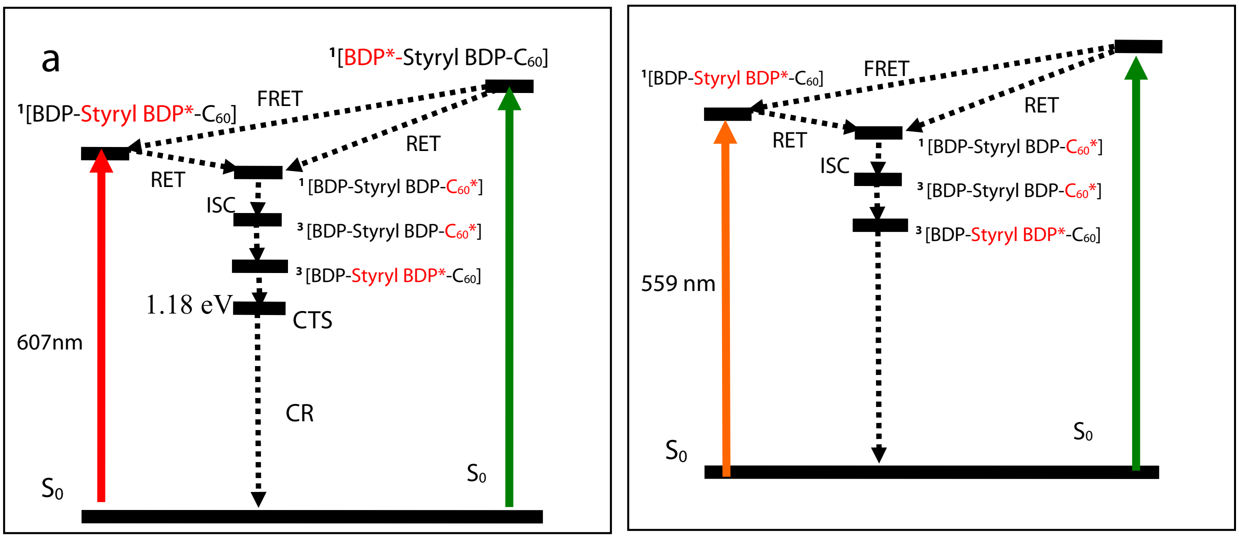

Scheme S5. Simplified Jablonski diagram illustrating the photophysical processes involved in (a) **B-3′** in the absence of acid and (b) **B-3′** in the presence of acid. [BDP-Styryl BDP-C_{60}] stands for **B-3**. The localization of the excited state in the triad was designated with red color and an asterisk. The number of the superscript designated the spin multiplicity of the excited state. The triplet state of **B-3′** were switched by the presence and the absence of the charge transfer state (CTS). Note in the absence of acid, the singlet state and the triplet state of **B-3′** were efficiently quenched by the charge transfer state. In the presence of acid, this CTS either disappear or be elevated to much higher energy level, as a result the triplet state on the [BDP-Styryl BDP-C_{60}] was observed.

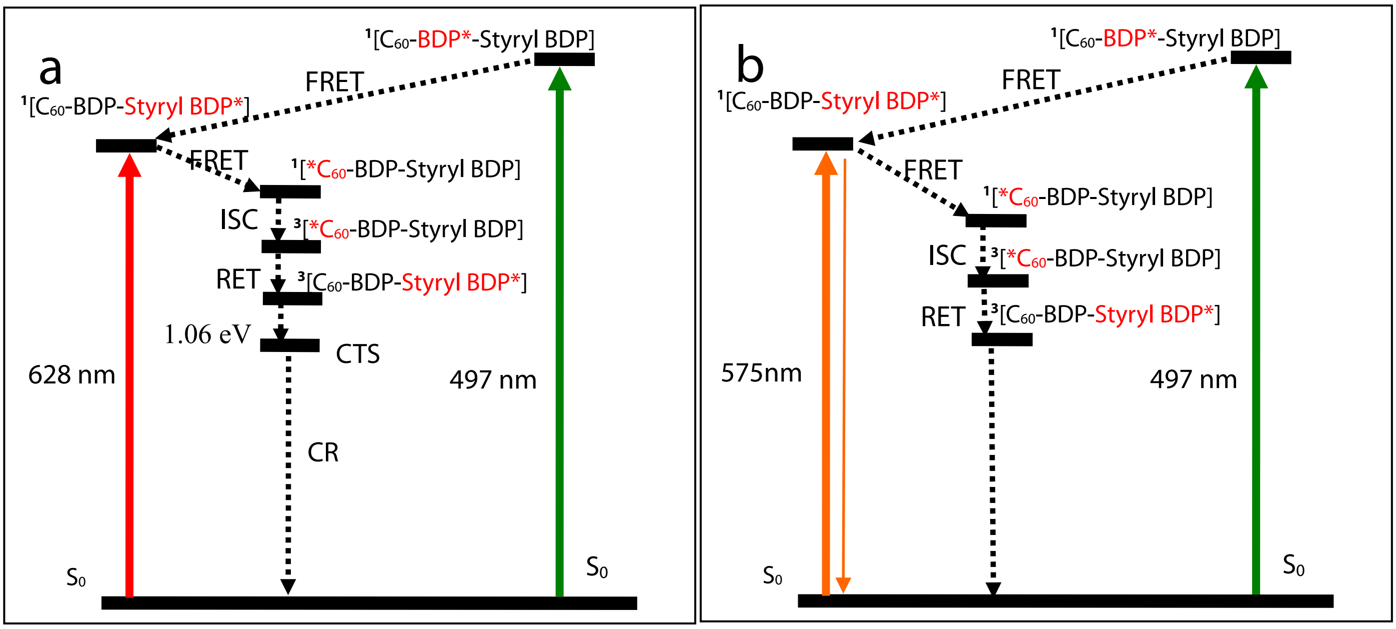

Scheme S6. Simplified Jablonski diagram illustrating the photophysical processes involved in (a) **B-3** in the absence of acid and (b) **B-3** in the presence of acid. [C_{60}-BDP-Styryl BDP] stands for **B-3**. The localization of the excited state in the triad was designated with red color and a asterisk. The number of the superscript designated the spin multiplicity of the excited state. The fluorescence and the triplet state of **B-3** were switched by the presence and the absence of the charge transfer state (CTS). Note in the absence of acid, the singlet state and the triplet state of **B-3** were efficiently quenched by the charge transfer state. In the presence of acid, this CTS either disappeared or be elevated to much higher energy level, as a result the fluorescence and the triplet state on the C_{60}-styryl Bodipy were observed.

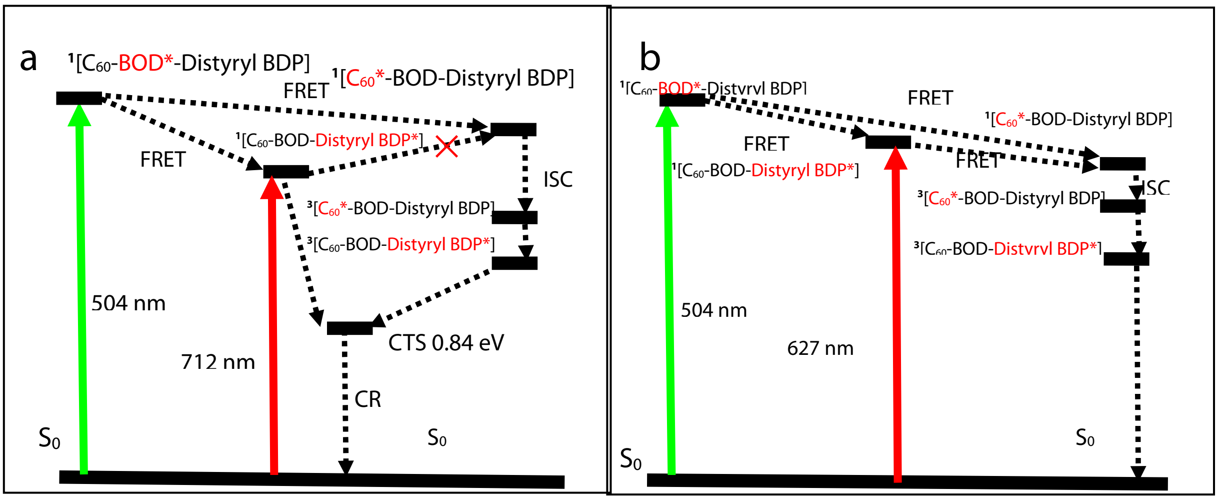

Scheme S7. Simplified Jablonski diagram illustrating the photophysical processes involved in (a) **B-4** in the absence of acid and (b) **B-4** in the presence of acid. [C_{60}-BOD-Distyryl BDP] stands for **B-4**. The localization of the excited state in the triad was designated with red color and a asterisk. The number of the superscript designated the spin multiplicity of the excited state. The triplet state of **B-4** was switched by the presence and the absence of the charge transfer state (CTS). Note in the absence of acid, the singlet state and the triplet state of **B-4** were efficiently quenched by the charge transfer state. In the presence of acid, this CTS either disappear or be elevated to much higher energy level, as a result the triplet state on the [C_{60}-BOD-Distyryl BDP] were observed.